JOURNAL OF PETROLOGY | VOLUME 55 | NUMBER 1 | PAGES 133–180 | 2014 | doi:10.1093/petrology/egt063

Sr, Nd, Pb and Os Isotope Systematics of CAMP Tholeiites from Eastern North America (ENA): Evidence of a Subduction-enriched Mantle Source

RENAUD MERLE[1]*, ANDREA MARZOLI[1], LAURIE REISBERG[2], HERVÉ BERTRAND[3], ALEXANDER NEMCHIN[4], MASSIMO CHIARADIA[5], SARA CALLEGARO[1], FRED JOURDAN[4], GIULIANO BELLIENI[1], DAN KONTAK[6], JOHN PUFFER[7] AND J. GREGORY McHONE[8]

[1]DIPARTIMENTO DI GEOSCIENZE, UNIVERSITÀ DI PADOVA, IGG-CNR PADOVA, VIA GRADENIGO 6, 35100 PADOVA, ITALY

[2]CENTRE DE RECHERCHES PETROGRAPHIQUES ET GEOCHIMIQUES (CRPG/CNRS), BP 20, 54501 VANDOEUVRE-LES-NANCY CEDEX, FRANCE

[3]LABORATOIRE DE GEOLOGIE DE LYON, UMR-CNRS 5276, UNIVERSITE DE LYON 1 AND ENS LYON, 46 ALLEE D'ITALIE, 69364 LYON CEDEX 07, FRANCE

[4]DEPARTMENT OF APPLIED GEOLOGY, CURTIN UNIVERSITY, GPO BOX U1987, PERTH, WA 6845, AUSTRALIA

[5]SECTION DES SCIENCES DE LA TERRE, UNIVERSITÉ DE GENÈVE, 13 RUE DES MARAÎCHERS, 12011 GENÈVE, SWITZERLAND

[6]DEPARTMENT OF EARTH SCIENCES, LAURENTIAN UNIVERSITY, 935 RAMSEY LAKE ROAD, SUDBURY, ON, CANADA

[7]DEPARTMENT OF EARTH AND ENVIRONMENTAL SCIENCES, RUTGERS UNIVERSITY, SMITH HALL, NEWARK, NJ 07102, USA

[8]9 DEXTERS LANE, GRAND MANAN, NB E5G 3A6, CANADA

RECEIVED JUNE 4, 2012; ACCEPTED SEPTEMBER 30, 2013
ADVANCE ACCESS PUBLICATION NOVEMBER 21, 2013

The Central Atlantic Magmatic Province (CAMP) is one of the largest igneous provinces on Earth, with an areal extent exceeding 10^7 km^2. Here we document the geochemical characteristics of CAMP basalts from Triassic–Jurassic basins in northeastern USA and Nova Scotia (Canada). The CAMP rocks occur as lava flows, sills and dykes. All of our analysed samples show chemical characteristics typical of CAMP basalts with low titanium content, which include enrichment in the most incompatible elements and negative Nb anomalies. All the basalts also show enriched Sr–Nd–Pb initial (t = 201 Ma) isotopic compositions ($^{206}Pb/^{204}Pb_{ini.} = 18{\cdot}155$–$18{\cdot}691$, $^{207}Pb/^{204}Pb_{ini.} = 15{\cdot}616$–$15{\cdot}668$, $^{208}Pb/^{204}Pb_{ini.} = 38{\cdot}160$–$38{\cdot}616$, $^{143}Nd/^{144}Nd_{ini.} = 0{\cdot}512169$–$0{\cdot}512499$). On the basis of stratigraphy, rare earth element (REE) chemistry and Sr–Nd–Pb isotope composition, three chemical groups are defined. The Hook Mountain group, with the lowest La/Yb ratios, initial $^{206}Pb/^{204}Pb_{ini.} > 18{\cdot}5$ and $^{143}Nd/^{144}Nd_{ini.} > 0{\cdot}51238$, comprises all the lastest and upper stratigraphic units. The Preakness group, with intermediate La/Yb ratios, $^{206}Pb/^{204}Pb_{ini.} > 18{\cdot}5$ and

*Corresponding author. Present address: Department of Applied Geology, Curtin University, GPO Box U1987, Perth, WA 6845, Australia. E-mail: r.merle@curtin.edu.au

0·51233>$^{143}Nd/^{144}Nd_{ini.}$>0·51225, comprises the intermediate units. The Orange Mountain group has the highest La/Yb ratios and $^{143}Nd/^{144}Nd_{ini.}$<0·51235 and involves all the earliest and stratigraphically lowest units, including the entire North Mountain basalts from Nova Scotia. In this last group, three sub-groups may be distinguished: the Rapidan sill, which has $^{206}Pb/^{204}Pb_{ini.}$ higher than 18·5, the Shelburne sub-group, which has $^{143}Nd/^{144}Nd_{ini.}$<0·51225, and the remaining Orange Mt samples. With the exception of one sample, the Eastern North America (ENA) CAMP basalts display initial $^{187}Os/^{188}Os$ ratios in the range of mantle-derived magmas (<0·15). Simple modelling shows that the composition of the ENA CAMP basalts cannot plausibly be explained solely by crustal contamination of oceanic island basalt (OIB), mid-ocean ridge basalt (MORB) or oceanic plateau basalt (OPB) magmas. Mixing of such magma compositions with sub-continental lithospheric mantle (SCLM)-derived melts followed by crustal contamination, by either assimilation–fractional crystallization (AFC) or assimilation through turbulent ascent (ATA) processes is somewhat more successful. However, this latter scenario does not reproduce the REE and isotopic composition of the ENA CAMP in a fully satisfactory manner. Alternatively, we propose a model in which asthenospheric mantle overlying a subducted slab (i.e. mantle wedge) was enriched during Cambrian to Devonian subduction by sedimentary material, isotopically equivalent to Proterozoic–Lower Paleozoic crustal rocks. Subsequently, after subduction ceased, the isotopic composition of this mantle evolved by radioactive decay for another 170 Myr until the CAMP magmatic event. Varying amounts and compositions of the incorporated sedimentary component coupled with radiogenic ingrowth over time can account for the main geochemical characteristics of the ENA CAMP (enriched incompatible element patterns, negative Nb anomalies, enriched Sr–Nd–Pb isotopic composition) and the differences between the three chemical groups.

KEY WORDS: *flood basalt; subcontinental lithospheric mantle; Re–Os isotopes*

INTRODUCTION

The Central Atlantic Magmatic Province (CAMP, Marzoli *et al.*, 1999) is one of the largest continental flood basalt (CFB) provinces on Earth. The CAMP extends for more than 7500 km from north to south, exceeds 10^7 km^2 and is distributed over four continents on both sides of the central Atlantic Ocean (Fig. 1; Marzoli *et al.*, 1999; McHone, 2003). The CAMP is dominated by low-titanium (low-Ti, with TiO_2 contents lower than 2%), and rare high-titanium (high-Ti), basaltic dykes, sills and remnants of more extensive lava flows that are now preserved in Triassic–Jurassic basins (Olsen *et al.*, 2003). This magmatic event mainly occurred at the Triassic–Jurassic boundary at ~201 Ma, as constrained mostly by $^{40}Ar/^{39}Ar$ ages [recalibrated using the decay constants proposed by Renne *et al.* (2010); see Marzoli *et al.* (2011)]. However, magmatism may also have occurred in distinct pulses spaced over a few million years, with the latest volcanic activity lasting until ~190 Ma (Sebai *et al.*, 1991; Deckart *et al.*, 1997; Marzoli *et al.*, 1999, 2004, 2011; Knight *et al.*, 2004; Nomade *et al.*, 2007; Verati *et al.*, 2007; Jourdan *et al.*, 2009). The CAMP event is linked to the break-up of Pangaea, which resulted in incipient opening of the Central Atlantic Ocean in the Florida–Guyana–Guinea area, pre-dating by *c.* 10 Myr the opening of the ocean between the Morocco–Mauritania and Nova Scotia–northern USA conjugate margins (Sahabi *et al.*, 2004).

The genesis of CAMP magmatism remains controversial (e.g. Bertrand *et al.*, 1982; Alibert, 1985; Dupuy *et al.*, 1988; Pegram, 1990; Bertrand, 1991; Sebai *et al.*, 1991; Deckart *et al.*, 1997; Marzoli *et al.*, 1999; Hames *et al.*, 2000; McHone, 2000; Cebria *et al.*, 2003; De Min *et al.*, 2003; Jourdan *et al.*, 2003; Verati *et al.*, 2005; Nomade *et al.*, 2007) as is true for many other CFB provinces. It has been proposed that CAMP magmatism may have been induced either by a plume head under the continental lithosphere (May, 1971; Morgan, 1983; White & McKenzie, 1989; Hill, 1991; Wilson, 1997; Courtillot *et al.*, 1999; Ernst & Buchan, 2002; Cebria *et al.*, 2003) or by heat incubation under thick continental lithosphere, possibly coupled with edge-driven convection generated by the thickness contrast of different lithospheric domains (McHone, 2000; De Min *et al.*, 2003; Puffer, 2003; McHone *et al.*, 2005; Verati *et al.*, 2005; Coltice *et al.*, 2007).

Understanding the genetic relationship of the CAMP magmatism with continental rifting and possibly with mantle plume impingement requires identification of its source(s), notably through the use of isotopic tracers. A recent Sr–Nd–Pb–Os isotopic study of Brazilian CAMP basalts from the western part of the Maranhão basin failed to identify a clear plume source component, but instead suggested that the low-Ti basaltic melts were derived mainly from a shallow mantle source with the geochemical characteristics of subduction-metasomatized sub-continental lithospheric mantle (SCLM; Merle *et al.*, 2011). This study raises the question of whether the specific geological setting of the Maranhão basin, in which small volumes of magma erupted over 700 km from the Atlantic margin and 2000 km from the first Pangaea break-up site, promoted the local melting of the most fusible portions of the SCLM or whether a shallow SCLM-like source can be identified on a large (supercontinent) scale.

To further evaluate the mechanism of basalt magma generation and its source, in particular where the volume is substantial, we selected CAMP basalts occurring in the Triassic–Jurassic Eastern North American (ENA) basins. They are situated along 1000 km of the Atlantic margin. This sampling represents a transect across a large area of the CAMP providing a large range of chemical types. The study area includes Connecticut, Massachusetts, New

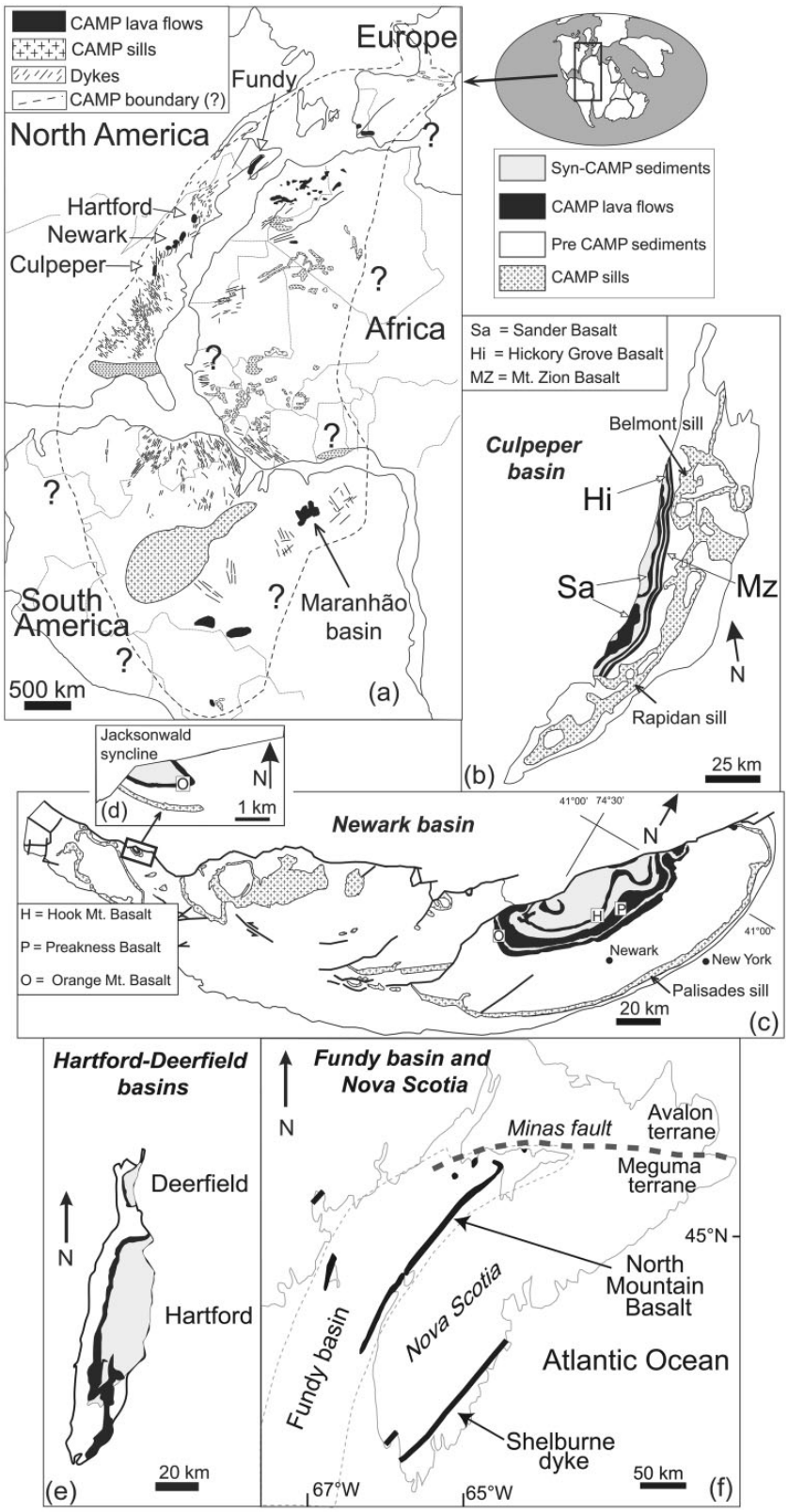

Fig. 1. (a) General map of the circum-Atlantic region at the time of CAMP emplacement and Pangea break-up [~200 Ma; modified after Deckart *et al.* (2005)]. Schematic maps of the Culpeper (b), Newark (c), and Hartford–Deerfield (e) basins of the eastern USA. Inset (d) shows the Jacksonwald syncline where Orange Mountain basalt (NEW133) was sampled. (f) Schematic map of the Fundy basin of Nova Scotia showing extent of the North Mountain Basalt and dykes (e.g. Shelburne).

Jersey and Virginia in the eastern USA and Nova Scotia in eastern Canada. In these areas, the basalts occur as three successive lava flow units with associated sills and feeder dykes, separated by thick layers of sedimentary rocks of latest Triassic to earliest Jurassic age (e.g. Webster *et al.*, 2006; Kontak, 2008; Cirilli *et al.*, 2009; Marzoli *et al.*, 2011). The few Sr–Nd–Pb isotopic studies on the ENA CAMP basalts have suggested derivation from an SCLM-type source (Pegram, 1990; Puffer, 1992; Heatherington & Mueller, 1999; Murphy *et al.*, 2011). However, these studies were provincial in extent and, therefore, did not provide an assessment of the possibility of chemical variation along the entire ENA. Moreover, these studies did not investigate the time-related isotopic variations between the various flow units and their potential sources [SCLM-like source, asthenosphere, ocean island basalt (OIB)-type mantle].

This study presents a comprehensive Sr–Nd–Pb–Os isotopic investigation of the entire ENA CAMP sub-province, which includes the first Pb isotopic data for the Nova Scotian CAMP basalts and the first Os isotopic data for any basalts in the North American CAMP.

Geological setting and previous results

The ENA CAMP basaltic rocks sampled occur onshore in Triassic–Jurassic rifted basins from Nova Scotia (Canada) to Virginia (USA). They include, from south to north, the Culpeper, Newark and Hartford basins in the USA, and the Fundy basin in Nova Scotia (Figs 1 and 2). These basins formed during the early stages of extensional activity preceding the breakup of Pangaea during the late Triassic–early Jurassic and are filled with fluvial–lacustrine sedimentary rocks of Late Triassic to Early Jurassic age (e.g. Olsen *et al.*, 2003).

The local continental crust

The Triassic–Jurassic rifting event affected a very complex continental crust that was assembled during the Grenvillian (~1300–1000 Ma) and Appalachian–Ouachita orogenies (~500–270 Ma). This crust was formed by the successive accretion of parallel slivers during the Late Precambrian to the Palaeozoic (e.g. Thomas, 2004, for an overview). The most landward terranes, of Grenvillian age, formed the Laurentia margin during the Appalachian–Ouachita orogeny. This orogeny involved successive, diachronous Taconic (~485–420 Ma), Acadian (~420–320 Ma) and Alleghanian (~320–270 Ma) phases culminating in closure of the Iapetus and Rheic Oceans and Pangaea assembly (e.g. Drake *et al.*, 1989; Hatcher *et al.*, 1989; Osberg *et al.*, 1989; Van Staal *et al.*, 1998; Hibbard *et al.*, 2002). These phases are related to the accretion of peri-Laurentian and peri-Gondwanan ribbon-shaped micro-continental masses (including magmatic arcs) to the Laurentian margin, which are now found from Cape Breton Island and Newfoundland to Alabama (e.g. Murphy & Nance, 2002; Hibbard *et al.*, 2007; Van Staal *et al.*, 2009). All of these terranes are formed of highly diverse Mesoproterozoic to Late Palaeozoic lithologies, which include reworked Grenvillian meta-igneous and metasedimentary rocks. They are intruded by several generations of mafic and calc-alkaline felsic magmatic suites formed during Palaeozoic extensional and subduction-related magmatic phases (e.g. Ayuso & Bevier, 1991; Barr & Hegner, 1992; Whalen *et al.*, 1994; Samson *et al.*, 1995; Murphy & Keppie, 1998; Pe-Piper & Piper, 1998; Pe-Piper & Jansa, 1999; Moench & Aleinikoff, 2002; Tomascak *et al.*, 2005). In Nova Scotia, and the northeastern USA, the CAMP basalts occur within the peri-Gondwanan Meguma, Avalonia, Gander and Carolina terranes and several segments of the Laurentian margin or peri-Laurentian terranes (Piedmont and Blue Ridge terranes; e.g. Hibbard *et al.*, 2007). The Meguma, Avalonia and Carolina terranes were the last to be accreted to the Laurentia margin in Canada and the northern USA during the Appalachian orogenesis (e.g. Pollock *et al.*, 2012). Gander, Avalonia and Carolina were once located together along the northern margin of Gondwana and share a Neoproterozoic magmatic arc-related basement (e.g. Nance & Murphy, 1996; Murphy *et al.*, 2004; Hibbard *et al.*, 2007; Schultz *et al.*, 2008; Pollock & Hibbard, 2010).

Previous geological, geochronological and chemical data for the CAMP in eastern North America

The CAMP basalts occur as lava flow sequences up to 450 m thick, and also as dykes and sills. In the Triassic–Jurassic basins, the lava piles consist of a maximum of three main units, each unit comprising multiple flows. In the USA basins, the ENA basalt units are interlayered with latest Triassic and possibly earliest Jurassic sedimentary rocks. In the Culpeper basin (Virginia, USA; Fig. 2), the CAMP lava flows comprise three main units, which, from bottom to top, are the Mt Zion Church, the Hickory Grove and the Sander basalts. In the Newark basin (New Jersey and Pennsylvania, USA; Fig. 2), the CAMP lava flow units are the Orange Mountain, Preakness and Hook Mountain basalts (e.g. Puffer & Student, 1992). In the Hartford basin and its northernmost extension (Connecticut and Massachusetts, USA), the units, which are up to 400 m thick, include, from bottom to top, the Talcott, Holyoke (named Deerfield basalt in the Deerfield basin) and Hampden units. These units are fed by the Higganum or Fairhaven, Buttress and Bridgeport dykes, respectively (Philpotts & Martello, 1986; Philpotts *et al.*, 1996; Philpotts, 1998). In the Fundy basin, located on the western side of Nova Scotia and ~500 km north of the Hartford basin, the CAMP basaltic flows occur as the North Mountain Basalt (NMB) and comprise three units (from bottom to top: East Ferry, Margaretsville and Brier Island members; Kontak, 2008), which we will refer to, respectively, as the lower, intermediate and upper NMB. These units have an aggregate thickness of up to 500 m.

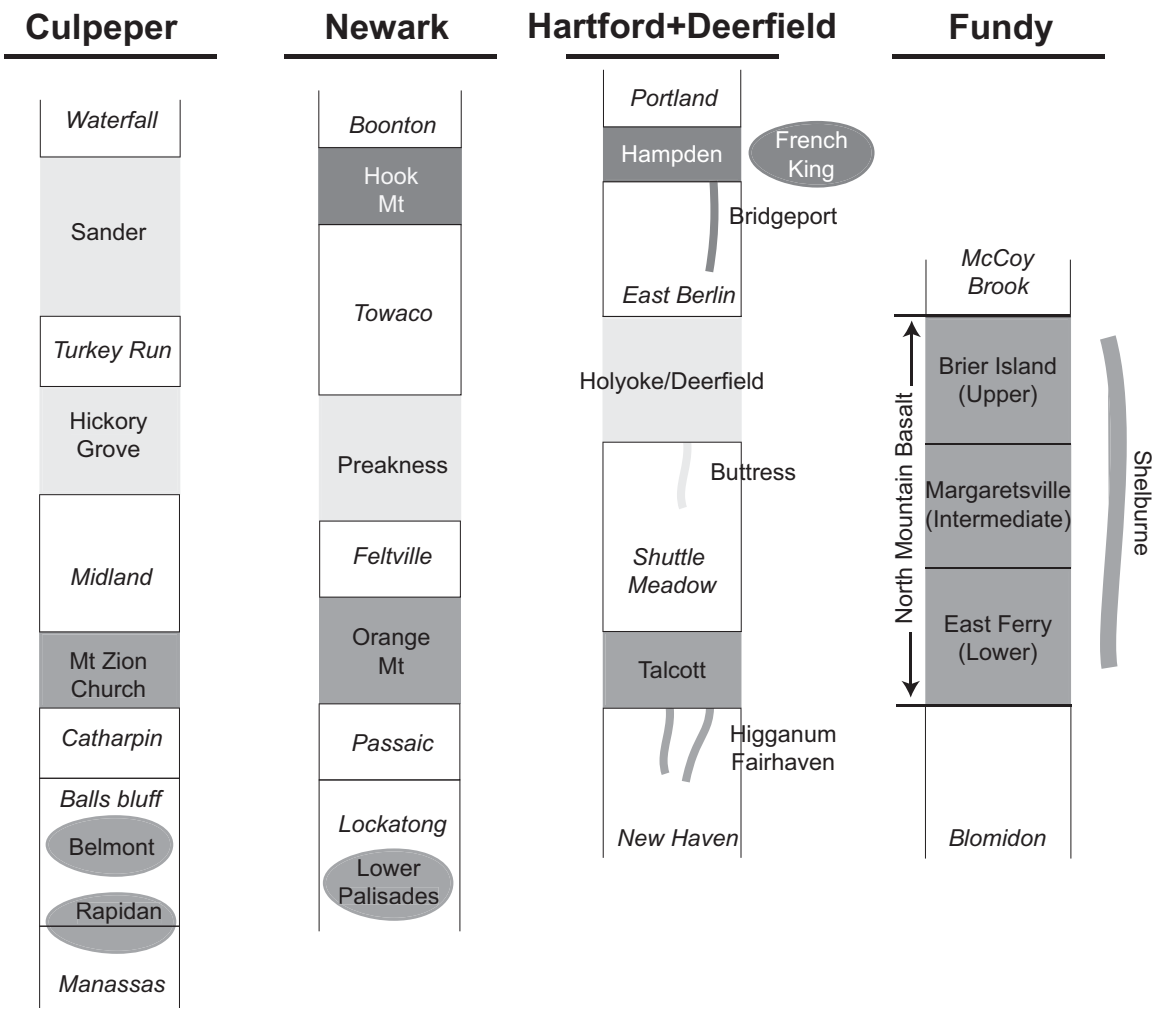

Fig. 2. Stratigraphic correlations between the CAMP units (sills, flows and dykes) within the Culpeper, Newark, Hartford, and Fundy basins and adjacent areas. Thick lines, dykes; grey rectangles, flows; ovals, sills. The stratigraphic (for the flows) and chemical correlations between the CAMP units are represented by similar shades of grey. Units located within the basins are represented in the schematic stratigraphic logs. Sedimentary formations are represented as white rectangles. Not to scale.

Shallow intrusive mafic rocks also occur in the ENA basins as thick sills and dykes, such as the Rapidan and Belmont sills in the Culpeper basin (Woodruff *et al.*, 1995), the Palisades sill in the Newark basin, the French King sill in the Hartford basin, and the Shelburne dyke in Nova Scotia. The Palisades and Rapidan sills reach a thickness of up to 350 m.

Reliable, high-quality $^{40}Ar/^{39}Ar$ plateau ages (selection criteria discussed by Nomade *et al.*, 2007) for the Culpeper and Newark sills and flows give a weighted mean age of $201{\cdot}8 \pm 0{\cdot}7$ Ma (2σ; Marzoli *et al.*, 2011), which is similar within error to the age of the basalts from the nearby Hartford basin in the USA and the NMB ($201{\cdot}6 \pm 1{\cdot}1$ Ma) in Nova Scotia (Jourdan *et al.*, 2009; recalculated by Marzoli *et al.*, 2011). By combining the ages of the USA and Nova Scotia basins, the peak activity of the CAMP event in ENA occurred at $201{\cdot}5 \pm 0{\cdot}9$ Ma. This age is similar to those obtained by thermal ionization mass spectrometry (TIMS) U–Pb dating for the NMB and for the Triassic–Jurassic boundary ($201{\cdot}4 \pm 0{\cdot}4$ Ma and $201{\cdot}3 \pm 0{\cdot}4$ Ma, respectively; Schoene *et al.*, 2010). It should be noted that the Hook Mt basalt (uppermost flows) yielded a slightly younger, but statistically indistinguishable age of $200{\cdot}3 \pm 0{\cdot}9$ Ma (Marzoli *et al.*, 2011).

The ENA CAMP basalts are quartz- and olivine-normative, low-Ti tholeiites ($TiO_2 < 2$ wt %) (Weigand & Ragland, 1970; McHone, 2000; Heatherington & Mueller, 2003). To differentiate the high-Mg, olivine normative tholeiites with very low Ti contents found in the southeastern USA, some researchers divide the low-Ti group into low-Ti basalts ($TiO_2 < 1$ wt %) and intermediate-Ti basalts ($TiO_2 \approx 1$ wt %; McHone, 2000; Salters *et al.*, 2003) The ENA CAMP basalts contain calcic plagioclase, augitic and pigeonitic clinopyroxene and occasional

orthopyroxene (mainly in the intrusive rocks). Olivine microphenocrysts are rare, but can be locally abundant in cumulus layers of the thick Rapidan and Palisades sills (Hush, 1990; Philpotts *et al.*, 1996). The major element and compatible trace element trends for the lava flows and sills can be related to fractional crystallization, mineral accumulation, and post-emplacement differentiation processes such as compaction and gas-filter pressing (Woodruff *et al.*, 1995; Philpotts *et al.*, 1996; Kontak, 2008). These latter processes are thought to generate differentiated pegmatitic or granophyric layers, which are commonly observed in the thick ENA flows and sills (Puffer & Horter, 1993; Philpotts, 1998; Kontak, 2008). The most significant geochemical trends occurring from base to top within each sill are a decrease of MgO and Cr (e.g. Walker, 1969; Shirley, 1987; Gorring & Naslund, 1995; Woodruff *et al.*, 1995; Puffer *et al.*, 2009). Re-injection of variably differentiated magmas has been also suggested to explain the observed geochemical trends (Hush, 1990; Marzoli *et al.*, 2011). Nevertheless, overall geochemical similarities exist between the lower part of the Palisades sill and the Orange Mountain basalt, and between the upper half of the sill and the Preakness basalt (Puffer *et al.*, 2009). As is also true for CAMP basalts from other locations, there are no picrites or other primitive rocks in the ENA in contrast to what is observed in other continental or oceanic large igneous provinces (LIPs).

Based on detailed field observations, biostratigraphic data, and major- (TiO_2) and trace-element chemistry (e.g. La/Yb ratios), and despite the large variety of petrogenetic processes that may have influenced the generation of the ENA CAMP basalts (polybaric fractional crystallization, post-magmatic differentiation, melting rate variation, upper crust assimilation and alteration), correlations can be established between the various units within the US basins (Fig. 2; Weigand & Ragland, 1970; Tollo & Gottfried, 1992; Fowell & Olsen, 1993; Olsen *et al.*, 2003; Puffer *et al.*, 2009; Marzoli *et al.*, 2011). The Mt Zion Church unit is equivalent to the Orange Mountain and Talcott basalts (lower units), and the Hickory Grove and Sander units of the Culpeper basin (separated locally by more than 100 m of sediments of the Turkey Run formation) are equivalent to the Preakness and Holyoke basalts (e.g. Tollo & Gottfried, 1992; Marzoli *et al.*, 2011). The Hook Mountain basalt from the Newark basin is equivalent to the Hampden basalt from the Hartford basin (upper units), whereas a geochemically and stratigraphically equivalent basaltic flow does not occur in the Culpeper basin. The NMB from Nova Scotia show the same biostratigraphic markers and paleomagnetic intervals as the Orange Mt basalt group flows (Kent & Olsen, 2000; Cirilli *et al.*, 2009), yet until now no clear geochemical correlation has been established between the flows in the USA and Nova Scotia basins.

Compared with normal mid-ocean ridge basalts (N-MORB, basalts from mid-ocean ridges derived from the depleted asthenosphere), the ENA CAMP basalts show moderate enrichment in large ion lithophile elements (LILE; e.g. Rb, Cs, Ba), systematic negative Nb anomalies, and slightly sloped to flat heavy rare earth element (HREE) patterns (Dostal & Dupuy, 1984; Pegram, 1990; Dostal & Greenough, 1992; Heatherington & Mueller, 1999; Murphy *et al.*, 2011).

The few existing Sr–Nd–Pb isotope data available for the CAMP tholeiites from Connecticut to Florida ($^{87}Sr/^{86}Sr = 0{\cdot}70583–0{\cdot}71083$, $^{143}Nd/^{144}Nd = 0{\cdot}51207–0{\cdot}51247$, $^{206}Pb/^{204}Pb = 18{\cdot}26–18{\cdot}63$, $^{207}Pb/^{204}Pb = 15{\cdot}57–15{\cdot}65$, $^{208}Pb/^{204}Pb = 38{\cdot}16–38{\cdot}31$: initial ratios recalculated at 201 Ma), have been interpreted as arguing against significant involvement of MORB or OIB mantle components, but may indicate derivation from (or substantial contamination by) the SCLM and/or variable contamination by the upper crust (Pegram, 1990; Puffer, 1992, 2001; Heatherington & Mueller, 1999). Based on Pb–Pb mantle isochrons and Nd model ages, it has been proposed that this SCLM might be derived from a ~1 Ga, sediment-contaminated, sub-arc mantle related to the Carolina and Suwannee (Avalonian) terranes that was later incorporated into the Laurentian lithosphere (Pegram, 1990; Heatherington & Mueller, 1999).

In Nova Scotia, only a few initial Sr and Nd isotopic ratios ($^{87}Sr/^{86}Sr = 0{\cdot}70443–0{\cdot}71285$, $^{143}Nd/^{144}Nd = 0{\cdot}51203–0{\cdot}51256$) are available for the CAMP tholeiites (Greenough *et al*, 1989; Dostal & Durning, 1998; Murphy *et al.*, 2011). As for the USA CAMP basalts, the Nd model ages argue for derivation from an SCLM source underneath the Avalonia–Meguma terranes that was enriched by Neoproterozoic subduction (Murphy & Dostal, 2007; Murphy *et al.*, 2011). The CAMP magmas derived from this source were eventually contaminated by the Meguma terrane crust (Murphy *et al.*, 2011). Prior to the formation of the CAMP, the Avalonia and Meguma terranes experienced successive rift-related, tholeiitic magmatic episodes of Neoproterozoic to Devonian age. It has been suggested that all of these magmatic episodes, including CAMP, were derived from the same Avalonia–Meguma SCLM (Murphy & Dostal, 2007; Murphy *et al.*, 2011). Whereas this might be expected to lead to progressive SCLM depletion, the initial εNd values of these basalts indicate progressive enrichment of their source (see Murphy *et al.*, 2011). We note, however, that contamination by the continental crust might invalidate the Nd model ages (e.g. Arndt & Goldstein, 1987) and thus weaken this argument favouring an SCLM origin for the ENA CAMP basalts.

SAMPLE SELECTION

After discarding the rocks that show obvious evidence of alteration in thin section (large amounts of sericite and chlorite replacing plagioclase and pyroxene, and clay

minerals replacing the microcrystalline matrix), 132 samples of flows, sills, and dykes were selected for major and compatible trace element analysis by X-ray fluorescence (XRF). This set includes, from south to north, 22 samples from the Culpeper basin, 30 samples from the Newark basin, 29 samples from the Hartford–Deerfield basin, and 51 samples from the Fundy basin (Nova Scotia). The Nova Scotia samples include four Shelburne dyke samples and 25 drill-hole samples (hole GAV-77-3; Kent & Olsen, 2000) from the North Mountain Basalt.

A subset of samples with low loss on ignition (LOI < 3·5 wt %) and negligible optical alteration was selected for REE and incompatible trace element analysis by inductively coupled plasma mass spectrometry (ICP-MS; 55 samples) and Sr–Nd–Pb isotopic analysis (43 samples). A subset of 20 of the least differentiated samples was also selected for Re–Os analysis.

The detailed analytical procedures, major and trace element analyses, and the geographic coordinates of the samples are given in Supplementary Data Tables A1 and A2 (supplementary data are available for downloading at http://www.petrology.oxfordjournals.org). The Sr–Nd–Pb isotope data are reported in Table 1 and the Re–Os data in Table 2. All the isotopic ratios discussed in the following sections are back-calculated to 201 Ma (Jourdan *et al.*, 2009; Marzoli *et al.*, 2011) using the incompatible element contents measured by ICP-MS for the Sr–Nd–Pb isotopic ratios and the Re and Os contents measured by isotopic dilution for the Os isotope ratios.

RESULTS

Major and trace elements

All the samples analysed for major and compatible and incompatible trace elements are fairly fresh or slightly altered and have LOI values lower than 3·5 wt %. Samples with LOI higher than 3·5% are not considered further.

The primary mineralogy of the ENA rocks consists of augite, plagioclase, and Fe–Ti oxides, and, in some samples, olivine and/or pigeonite. Orthopyroxene is common in the Rapidan and Palisades Sills.

Bulk-rock compositions, recast to anhydrous values, range from basalt to basaltic andesite (Fig. 3a) and all samples can be classified as low-Ti with $TiO_2 < 2$ wt % (Fig. 3b). The four samples with TiO_2 close to or higher than 2 wt % are evolved pyroxene-rich rocks with MgO contents lower than 4 wt % (NS19, NS23, NS24 and CUL67A). Most samples are moderately evolved with MgO contents between 5 and 8 wt %. Sixteen samples are less evolved with more than 8 wt % MgO, but have Ni and Co contents lower than 234 ppm and 57 ppm, respectively, thus indicating early olivine fractionation (Fig. 3c and d). Four samples from the Palisades Sills have MgO between 15 and 19 wt %, together with high Ni, Cr and Co contents, owing to olivine and pyroxene accumulation, as confirmed from thin-section observations.

As discussed above, field observations and geochemical considerations allow units from the various basins to be correlated. Three groups of effusive and intrusive samples can be defined based on both stratigraphic position (Fig. 2) and incompatible element composition, as best illustrated by the La/Yb vs TiO_2 plot (Fig. 4). The stratigraphically uppermost group has the highest TiO_2 (~1·3–1·5 wt%) and the lowest La/Yb (~2), and encompasses the Hampden and Hook Mt flow units, their feeder dyke (Bridgeport dyke), and the French King sill. This group is referred to hereafter as the Hook Mt group. The group with $TiO_2 \sim 0{\cdot}7$–$1{\cdot}1$ wt % and La/Yb ~ 2·5–3·5 encompasses the Holyoke, Preakness, Sander and Hickory Grove flow units and their feeder dyke (Buttress dyke) and is referred to as the Preakness group in the following sections. The stratigraphically lowest group, with the largest TiO_2 variation (0·5–1·3 wt %) and the highest La/Yb (~4–6), includes the Talcott, Orange Mountain and Mt Zion Church flow units and their feeder dyke (Higganum–Fairhaven dyke) and all Nova Scotian samples, both the NMB and Shelburne dyke. In addition, the lower part of the Palisades sill and the Culpeper basin sills (including the Rapidan sill) belong to this group. This group is referred to as the Orange Mt group.

In primitive mantle-normalized multi-element diagrams all the samples display moderate enrichment of the most incompatible elements with respect to the least incompatible ones, as well as prominent positive Pb and negative Nb anomalies (Fig. 5). The samples are all enriched in LILE and light REE (LREE) with $La/Sm_N = 1{\cdot}38$–$2{\cdot}71$. It should be noted that the most enriched samples, which have $La/Sm_N > 2{\cdot}5$, are evolved rocks (NS19 and NS23). The parallel chondrite-normalized REE patterns (Fig. 6) observed within a given flow unit are probably related to fractional crystallization (e.g. the Sander unit in the Culpeper basin).

The REE patterns of the Hook Mt group are similar to those of the Preakness group, but distinct from those of the Orange Mt group. Whereas the Hook Mt group shows the least LREE enrichment ($La/Sm_N = 1{\cdot}38$–$1{\cdot}46$) and flat HREE patterns ($Dy/Yb_N = 1{\cdot}05$–$1{\cdot}10$), the Preakness group shows slightly more enriched LREE patterns ($La/Sm_N = 1{\cdot}66$–$1{\cdot}88$), but similar flat HREE patterns ($Dy/Yb_N = 1{\cdot}04$–$1{\cdot}11$). The Orange Mt group shows the most LREE-enriched patterns ($La/Sm_N = 1{\cdot}76$–$2{\cdot}45$; excluding the differentiated samples) and sloped HREE patterns ($Dy/Yb_N = 1{\cdot}15$–$1{\cdot}36$). It should be noted that among these samples, the NMB upper and intermediate flow units and the Shelburne dyke (hereafter the Shelburne sub-group) show slightly lower Dy/Yb_N (1·15–1·30), but slightly higher La/Sm_N (1·90–2·45) values than the remaining samples of the Orange Mt group

Table 1: Sr–Nd–Pb isotope data for the ENA CAMP basalts

Unit	Sample	$(^{87}Sr/^{86}Sr)_{meas.}$	±1σ	$^{87}Rb/^{86}Sr$	$(^{87}Sr/^{86}Sr)_{ini.}$	±1σ	$(^{143}Nd/^{144}Nd)_{meas.}$	±1σ	$^{147}Sm/^{144}Nd$	$(^{143}Nd/^{144}Nd)_{ini.}$	±1σ	$\varepsilon Nd_{ini.}$
Talcott flow	HB64	0·706744	0·000002	0·151	0·706311	0·000031	0·512532	0·000004	0·153	0·512330	0·000009	−0·95
Higganum Dike	HB87	0·706627	0·000003	0·243	0·705933	0·000041	0·512537	0·000005	0·155	0·512333	0·000010	−0·91
Holyoke flow	HB56	0·707274	0·000004	0·353	0·706266	0·000060	0·512509	0·000017	0·164	0·512293	0·000019	−1·68
Buttress dike	HB102	0·706690	0·000002	0·185	0·706160	0·000031	0·512545	0·000004	0·169	0·512323	0·000010	−1·11
Hampden flow	HB29	0·710390	0·000006	0·307	0·709511	0·000052	0·512630	0·000012	0·184	0·512388	0·000016	0·16
Bridgeport Dike	HB98	0·707298	0·000002	0·406	0·706137	0·000069	0·512740	0·000016	0·183	0·512499	0·000019	2·33
NMB lower flow	NS1	0·707118	0·000007	0·425	0·705801	0·000072	0·512522	0·000007	0·161	0·512309	0·000011	−1·36
NMB lower flow	NS6	0·707418	0·000009	0·348	0·706342	0·000060	0·512495	0·000004	0·159	0·512296	0·000010	−1·62
NMB lower flow	NS19	0·707148	0·000003	0·494	0·705000	0·000084	n.d.	n.d.	n.d.	n.d.	n.d.	n.d.
NMB lower flow	NS23	0·706436	0·000005	0·388	0·705007	0·000066	0·512540	0·000005	0·158	0·512343	0·000010	−0·70
NMB Middle flow	NS7	0·708609	0·000008	0·146	0·708224	0·000026	0·512412	0·000005	0·154	0·512207	0·000010	−3·36
NMB Middle flow	NS12	0·708407	0·000006	0·318	0·707631	0·000054	0·512413	0·000007	0·153	0·512202	0·000011	−3·45
NMB Upper flow	NS8	0·707241	0·000002	0·079	0·707014	0·000014	0·512378	0·000004	0·157	0·512169	0·000010	−4·10
NMB Upper flow	NS9	0·707416	0·000002	0·116	0·707085	0·000020	0·512395	0·000004	0·153	0·512203	0·000009	−3·45
NMB Upper flow	NS13	0·707417	0·000003	0·243	0·706783	0·000041	0·512392	0·000005	0·156	0·512192	0·000010	−3·66
NMB Upper flow	NS15	0·707415	0·000002	0·181	0·706924	0·000031	0·512362	0·000005	0·155	0·512169	0·000010	−4·10
NMB Upper flow	NS21	0·707414	0·000003	0·275	0·706739	0·000047	0·512393	0·000003	0·152	0·512197	0·000009	−3·56
GAV Middle flow	GAV81	0·706575	0·000008	0·302	0·705726	0·000052	0·512522	0·000006	0·149	0·512325	0·000010	−1·05
GAV Lower flow	GAV162	0·706743	0·000009	0·223	0·706104	0·000039	0·512490	0·000004	0·150	0·512293	0·000009	−1·68
GAV Lower flow	GAV174	0·706778	0·000007	0·149	0·706353	0·000026	0·512512	0·000003	0·145	0·512322	0·000009	−1·13
GAV Lower flow	GAV181	0·706561	0·000008	0·163	0·706095	0·000029	0·512500	0·000005	0·151	0·512301	0·000010	−1·52
GAV Lower flow	GAV193	0·706504	0·000002	0·175	0·706004	0·000030	0·512536	0·000007	0·148	0·512341	0·000011	−0·75
Shelburne dyke	NS27	0·707357	0·000003	0·221	0·706724	0·000038	0·512414	0·000006	0·154	0·512211	0·000010	−3·28
Shelburne dyke	NS28	0·708018	0·000002	0·359	0·706991	0·000061	0·512392	0·000003	0·155	0·512189	0·000009	−3·72
Palisades sill	NEW3	0·707903	0·000009	0·395	0·706773	0·000068	0·512535	0·000006	0·152	0·512335	0·000010	−0·87
Palisades sill	NEW136C	0·706674	0·000012	0·219	0·706047	0·000039	0·512516	0·000013	0·161	0·512305	0·000016	−1·46
Palisades sill	NEW16	0·707911	0·000003	0·338	0·706962	0·000057	0·512520	0·000004	0·156	0·512318	0·000010	−1·28
Palisades sill	NEW17	0·706829	0·000007	0·338	0·705880	0·000058	0·512530	0·000006	0·156	0·512328	0·000011	−1·08
Palisades sill	NEW18	0·706879	0·000008	0·322	0·705986	0·000055	0·512517	0·000004	0·156	0·512318	0·000010	−1·34
Orange Mt	NEW69	0·706695	0·000004	0·135	0·706309	0·000023	0·512526	0·000007	0·158	0·512318	0·000011	−1·20
Orange Mt	NEW133	0·708305	0·000002	0·029	0·708221	0·000005	0·512552	0·000007	0·156	0·512347	0·000011	−0·63
Preakness	NEW52	0·707285	0·000004	0·294	0·706445	0·000050	0·512486	0·000005	0·163	0·512271	0·000010	−2·11
Preakness	NEW68	0·706377	0·000002	0·230	0·705719	0·000039	0·512531	0·000007	0·170	0·512307	0·000012	−1·41
Hook Mt	NEW73	0·708134	0·000002	0·466	0·706802	0·000079	0·512649	0·000003	0·184	0·512407	0·000011	0·54
Hook Mt	NEW74	0·707088	0·000002	0·513	0·705621	0·000087	0·512681	0·000002	0·183	0·512440	0·000010	1·19
Hook Mt	NEW134	0·706881	0·000004	0·513	0·705414	0·000087	0·512677	0·000001	0·183	0·512436	0·000010	1·11
Mt Zion Church	CUL6	0·707413	0·000002	0·041	0·707296	0·000007	0·512539	0·000003	0·156	0·512333	0·000009	−0·90
Hickory Grove	CUL13	0·706630	0·000015	0·178	0·706122	0·000034	0·512551	0·000017	0·170	0·512327	0·000019	−1·02
Sander	CUL25	0·707872	0·000009	0·225	0·707228	0·000039	0·512471	0·000003	0·161	0·512260	0·000009	−2·33
Sander	CUL28	0·707514	0·000003	0·316	0·706612	0·000054	0·512534	0·000007	0·165	0·512317	0·000012	−1·21
Rapidan sill	CUL8	0·706617	0·000006	0·309	0·705735	0·000053	0·512491	0·000003	0·159	0·512282	0·000009	−1·90
Rapidan sill	CUL9	0·706459	0·000003	0·135	0·706073	0·000023	0·512516	0·000005	0·164	0·512300	0·000010	−1·55
Belmont Sill	CUL67	0·707107	0·000002	0·357	0·706086	0·000061	0·512478	0·000003	0·155	0·512274	0·000009	−2·05

(continued)

Table 1: Continued

Sample	$(^{206}Pb/^{204}Pb)_{meas.}$	±1σ	$^{238}U/^{204}Pb$	$(^{207}Pb/^{204}Pb)_{meas.}$	±1σ	$^{235}U/^{204}Pb$	$(^{208}Pb/^{204}Pb)_{meas.}$	±1σ	$^{232}Th/^{204}Pb$	$(^{206}Pb/^{204}Pb)_{ini.}$	±1σ	$(^{207}Pb/^{204}Pb)_{ini.}$	±1σ	$(^{208}Pb/^{204}Pb)_{ini}$	±1σ
HB64	18·650	0·001	6·6	15·648	0·000	0·049	38·668	0·001	24·24	18·440	0·025	15·637	0·001	38·424	0·028
HB87	18·586	0·001	7·6	15·656	0·001	0·056	38·726	0·001	30·17	18·346	0·029	15·644	0·002	38·422	0·035
HB56	18·849	0·001	9·2	15·644	0·000	0·068	38·741	0·001	31·72	18·557	0·035	15·629	0·002	38·421	0·037
HB102	18·880	0·001	7·2	15·669	0·001	0·053	38·850	0·001	23·21	18·652	0·027	15·658	0·001	38·616	0·027
HB29	n.d.	n.d.	n.d.	n.d.	n.d.	n.d.	n.d.	n.d.	n.d.	n.d.	n.d.	n.d.	n.d.	n.d.	n.d.
HB98	18·719	0·000	4·9	15·640	0·000	0·036	38·611	0·001	12·03	18·562	0·019	15·632	0·001	38·490	0·014
NS1	18·541	0·001	7·1	15·628	0·001	0·052	38·642	0·002	31·97	18·315	0·027	15·616	0·002	38·320	0·037
NS6	18·651	0·001	9·9	15·640	0·001	0·073	38·760	0·003	42·08	18·337	0·037	15·624	0·002	38·336	0·049
NS19	18·676	0·001	10·0	15·656	0·001	0·073	38·823	0·002	44·35	18·359	0·038	15·640	0·002	38·376	0·052
NS23	18·594	0·002	9·4	15·633	0·002	0·069	38·688	0·005	41·76	18·295	0·036	15·618	0·003	38·267	0·049
NS7	18·681	0·001	11·4	15·642	0·001	0·084	38·808	0·003	45·08	18·318	0·043	15·624	0·002	38·353	0·053
NS12	18·442	0·001	7·8	15·629	0·001	0·058	38·556	0·001	35·31	18·193	0·030	15·616	0·002	38·200	0·041
NS8	18·490	0·001	7·2	15·640	0·001	0·053	38·648	0·002	34·73	18·263	0·027	15·628	0·002	38·298	0·041
NS9	18·490	0·005	8·9	15·631	0·004	0·066	38·639	0·010	40·80	18·206	0·034	15·617	0·005	38·228	0·049
NS13	18·500	0·002	7·5	15·641	0·001	0·055	38·672	0·003	30·67	18·262	0·028	15·629	0·002	38·363	0·036
NS15	18·446	0·007	7·5	n.d.	n.d.	0·055	38·528	0·014	36·47	18·206	0·029	n.d.	n.d.	38·160	0·045
NS21	n.d.	n.d.	n.d.	n.d.	n.d.	n.d.	n.d.	n.d.	n.d.	n.d.	n.d.	n.d.	n.d.	n.d.	n.d.
GAV81	18·661	0·005	9·0	15·646	0·004	0·066	38·808	0·010	38·67	18·376	0·034	15·632	0·004	38·418	0·046
GAV162	18·613	0·001	6·8	15·635	0·001	0·050	38·711	0·002	29·19	18·396	0·026	15·624	0·001	38·417	0·034
GAV174	18·640	0·002	9·0	15·639	0·002	0·066	38·765	0·004	30·85	18·353	0·034	15·624	0·002	38·454	0·036
GAV181	18·684	0·001	8·5	15·651	0·001	0·062	38·824	0·003	32·08	18·414	0·032	15·637	0·002	38·500	0·038
GAV193	18·694	0·000	11·5	15·641	0·000	0·084	38·837	0·001	50·34	18·329	0·044	15·623	0·002	38·330	0·059
NS27	18·436	0·004	8·2	15·635	0·003	0·060	38·597	0·007	35·06	18·176	0·031	15·622	0·003	38·243	0·042
NS28	18·539	0·002	10·0	15·642	0·002	0·074	38·776	0·005	44·91	18·221	0·038	15·625	0·003	38·323	0·053
NEW3	18·589	0·008	9·1	15·644	0·006	0·067	38·707	0·016	34·80	18·301	0·035	15·629	0·007	38·356	0·044
NEW136C	18·550	0·020	8·3	15·634	0·017	0·061	38·623	0·042	34·60	18·288	0·037	15·621	0·017	38·275	0·059
NEW16	18·567	0·001	8·8	15·638	0·001	0·064	38·692	0·001	34·21	18·294	0·033	15·624	0·002	38·354	0·040
NEW17	18·567	0·001	8·8	15·646	0·001	0·064	38·660	0·001	34·20	18·289	0·033	15·632	0·002	38·315	0·040
NEW18	18·576	0·000	8·0	15·663	0·000	0·059	38·746	0·001	35·15	18·329	0·030	15·650	0·002	38·402	0·041
NEW69	18·618	0·000	9·6	15·658	0·001	0·070	38·777	0·002	33·94	18·315	0·036	15·642	0·002	38·435	0·040
NEW133	18·678	0·002	16·5	15·656	0·002	0·121	38·718	0·004	18·91	18·155	0·062	15·629	0·004	38·528	0·022
NEW52	18·923	0·001	11·1	15·653	0·001	0·082	38·820	0·003	34·77	18·569	0·042	15·635	0·002	38·470	0·041
NEW68	18·887	0·001	10·3	15·659	0·001	0·076	38·816	0·002	35·63	18·561	0·039	15·643	0·002	38·456	0·042
NEW73	19·015	0·001	11·7	15·663	0·001	0·086	38·939	0·003	37·55	18·642	0·044	15·644	0·002	38·561	0·044
NEW74	18·961	0·001	11·6	15·661	0·001	0·085	38·904	0·003	42·53	18·591	0·044	15·642	0·003	38·475	0·050
NEW134	18·887	0·001	11·6	15·659	0·001	0·085	38·816	0·002	42·43	18·519	0·044	15·640	0·002	38·388	0·050
CUL6	18·547	0·001	9·0	15·645	0·001	0·066	38·644	0·002	26·48	18·261	0·034	15·631	0·002	38·377	0·031
CUL13	18·606	0·001	9·3	15·652	0·001	0·069	38·757	0·003	23·57	18·310	0·035	15·637	0·002	38·519	0·028
CUL25	18·581	0·002	11·4	15·675	0·001	0·084	38·768	0·004	31·30	18·219	0·043	15·657	0·003	38·452	0·037
CUL28	18·853	0·002	10·6	15·663	0·001	0·078	38·804	0·003	33·54	18·518	0·040	15·646	0·002	38·466	0·039
CUL8	18·961	0·001	9·1	15·661	0·001	0·067	38·904	0·003	41·69	18·671	0·035	15·646	0·002	38·483	0·049
CUL9	18·949	0·001	8·1	15·640	0·001	0·060	38·834	0·002	34·95	18·691	0·031	15·627	0·002	38·482	0·041
CUL67	18·681	0·003	9·5	15·682	0·003	0·070	38·902	0·007	35·93	18·380	0·036	15·667	0·003	38·540	0·043

$\varepsilon Nd_{ini.}$ calculated at 201 Ma using the present-day values for CHUR: $(^{143}Nd/^{144}Nd)_{chur} = 0{\cdot}512638$, $^{147}Sm/^{144}Nd = 0{\cdot}1967$ (Jacobsen & Wasserburg, 1980).

Table 2: Re–Os isotope data for the ENA CAMP basalts

Unit	Sample	Group	MgO	[Os] (ppt)	[Re] (ppt)	^{188}Os (mol g^{-1})	$(^{187}Os/^{188}Os)_{meas.}$	±2σ	$^{187}Re/^{188}Os$	$(^{187}Os/^{188}Os)_{ini.}$	±2σ	Error (%)
Fundy												
NMB Lower flow	NS6	Orange Mt	6·64	23	495	1·50E–14	0·51197	0·00270	111	0·1387	0·0065	4·7
NMB Upper flow	NS21	Orange Mt	8·90	69	326	4·74E–14	0·22522	0·00101	23·2	0·1474	0·0015	1·0
GAV Middle flow	GAV81	Orange Mt	6·49	22	457	1·50E–14	0·49063	0·00423	103	0·1451	0·0068	4·7
GAV Lower flow	GAV181	Orange Mt	6·18	16	462	1·08E–14	0·58827	0·01076	144	0·1058	0·0141	13·4
Shelburne dyke	NS27	Orange Mt	8·46	440	458	3·06E–13	0·14695	0·00067	5·0	0·1300	0·0007	0·6
Shelburne dyke	NS28	Orange Mt	6·80	85	641	5·87E–14	0·25660	0·00120	36·9	0·1329	0·0021	1·6
Newark												
Palisades sill	NEW3	Orange Mt	6·86	82	393	5·66E–14	0·21440	0·00128	23·3	0·1362	0·0020	1·5
Palisades sill	NEW136C	Orange Mt	16·82	1670	236	1·16E–12	0·13139	0·00057	0·7	0·1291	0·0006	0·4
Palisades sill	NEW17	Orange Mt	12·91	744	386	5·18E–13	0·13698	0·00063	2·5	0·1286	0·0007	0·5
Orange Mt	NEW69	Orange Mt	7·91	50	566	3·41E–14	0·32170	0·00156	55·8	0·1346	0·0037	2·8
Orange Mt	NEW133	Orange Mt	8·20	56	599	3·82E–14	0·31357	0·00157	52·7	0·1368	0·0032	2·4
Preakness	NEW68	Preakness	7·33	7·7	568	4·47E–15	1·62717	0·02042	427	0·1935	0·0319	16·5
Hook Mt	NEW73	Hook Mt	5·60	5·9	1008	2·61E–15	4·52975	0·11504	1300	0·1701	0·1335	78·5
Hook Mt	NEW74	Hook Mt	5·66	18	1098	1·06E–14	1·31229	0·00915	348	0·1459	0·0218	15·0
Culpeper												
Mt Zion Church	CUL6	Orange Mt	7·65	56	522	3·82E–14	0·28173	0·00148	45·9	0·1276	0·0029	2·3
Hickory Grove	CUL13	Preakness	7·78	14	496	9·28E–15	0·79020	0·00613	180	0·1874	0·0123	6·6
Sander	CUL25	Preakness	5·62	3·5	620	1·49E–15	4·94438	0·21833	1397	0·2600	0·2332	89·7
Rapidan sill	CUL8	Orange Mt	11·75	369	245	2·57E–13	0·14344	0·00094	3·2	0·1327	0·0010	0·7

Os isotopic ratios were normalized to $^{192}Os/^{188}Os = 3·08271$. Uncertainties for the measured $^{187}Os/^{188}Os$ ratios include in-run 2SE, long-term 2σ reproducibility of the liquid standard (~0·2%) and uncertainties on blanks (isotopic composition and quantity). All data are blank corrected, using blank values given in the Supplementary Data. Uncertainties on initial ratios include in-run errors and uncertainties on blank corrections and on $^{187}Re/^{188}Os$ ratios and ages used for radiogenic corrections (all 2σ). Initial ratios were calculated using a decay constant $\lambda = 1·666 \times 10E{-}11$ (Smoliar *et al.*, 1996).

($Dy/Yb_N = 1·20–1·36$; $La/Sm_N = 1·76–2·21$; hereafter the lower NMB sub-group).

Sr–Nd–Pb isotopes

All data plot within the field of previously analysed CAMP low-Ti basalts in the Sr–Nd and Pb–Pb isotope diagrams (Figs 7–10).

In the $^{208}Pb/^{204}Pb$ and $^{207}Pb/^{204}Pb$ vs $^{206}Pb/^{204}Pb$ diagrams (Fig. 7), the data plot well above the Northern Hemisphere Reference Line (NHRL) with relatively high $^{207}Pb/^{204}Pb$ and $^{208}Pb/^{204}Pb$ at low to moderate $^{206}Pb/^{204}Pb$. The ENA samples can be distinguished on the basis of whether their $^{206}Pb/^{204}Pb$ values are higher or lower than 18·5. With the exception of the Rapidan sill, all the samples of the Orange Mt group have Pb isotopic compositions typical of low-Ti CAMP basalts ($^{206}Pb/^{204}Pb = 18·155–18·440$; $^{207}Pb/^{204}Pb = 15·616–15·667$; $^{208}Pb/^{204}Pb = 38·160–38·540$) and form a rough trend parallel to the NHRL. This range of Pb isotope compositions corresponds approximately to the average Pb isotopic composition of low-Ti basalts from other CFBs (see Carlson, 1991). In contrast, with the exception of CUL25 (Sander basalt) and CUL13 (Hickory basalt), all samples of the upper units (Hook Mt and Preakness groups), have $^{206}Pb/^{204}Pb > 18·5$ and seem to be shifted towards the NHRL (Fig. 7). Unlike the first group, these samples have both Δ7/4 less than 15 and Δ8/4 less than 50 (Fig. 8), where Δ values represent the relative vertical deviation in $^{207}Pb/^{204}Pb$ or $^{208}Pb/^{204}Pb$ from the NHRL.

In a Sr–Nd isotope diagram (Fig. 9), the ENA samples can be subdivided into three clusters, according to their Nd isotope composition. Samples of the Hook Mt group have the highest Nd initial ratios ($^{143}Nd/^{144}Nd = 0·512388–0·512499$), but similar Sr initial ratios to those

observed in the other samples ($^{87}Sr/^{88}Sr \sim 0{\cdot}7054$–$0{\cdot}7073$). The second isotopic cluster, which has lower Nd initial ratios ($^{143}Nd/^{144}Nd = 0{\cdot}512260$–$0{\cdot}512347$), includes all the units of the Preakness group and the units of the Orange Mt group in the USA. It also contains samples of the lower unit of the NMB and the intermediate unit of the GAV drill hole in the Fundy basin. In contrast, the Shelburne sub-group, including the upper and intermediate units of the NMB flows and the Shelburne dyke, compose the third isotopic cluster, which has the lowest $^{143}Nd/^{144}Nd$ ($0{\cdot}512169$–$0{\cdot}512211$) and relatively high $^{87}Sr/^{86}Sr$ ($0{\cdot}7067$–$0{\cdot}7082$). Within each group, the trend to high $^{87}Sr/^{86}Sr$ (>$0{\cdot}708$) at nearly constant $^{143}Nd/^{144}Nd$ (HB29, NS7 and NEW133) suggests that the $^{87}Sr/^{86}Sr$ composition of a few samples might have been affected by post-emplacement alteration.

In a $^{143}Nd/^{144}Nd$ vs $^{206}Pb/^{204}Pb$ diagram (Fig. 10), the same groups can be distinguished as in the Sr–Nd isotope diagram. Overall, the four groups define a positive correlation between Nd and Pb isotopic ratios, from the Shelburne sub-group with the lowest Pb and Nd isotopic ratios, which plots at the extremity of the field of the Meguma terrane basement rocks, towards the Hook Mt group with the highest Pb and Nd isotopic ratios. The

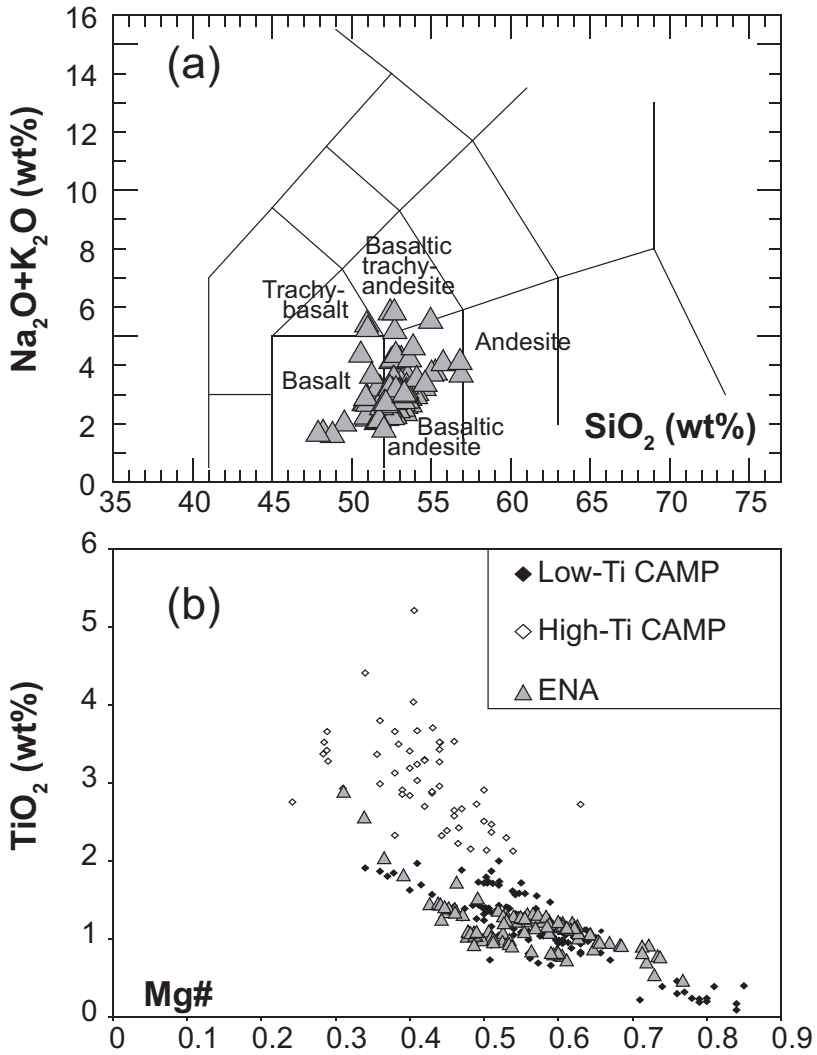

Fig. 3. (a) Total alkalis–silica (TAS) diagram. The abundances of major elements have been recalculated on a volatile-free basis (Le Maitre *et al.*, 2002). (b) TiO_2 vs Mg# diagram for the ENA CAMP basalts. CAMP data are from the GEOROC website. Data for low-Ti and high-Ti CAMP tholeiites are from Dupuy *et al.* (1988), Nomade *et al.* (2002), De Min *et al.* (2003), Jourdan *et al.* (2003), Deckart *et al.* (2005), Verati *et al.* (2005) and Merle *et al.* (2011). The data have been recalculated to 100% on a volatile-free basis; cumulative rocks have been excluded. $Mg\# = Mg^{2+}/(Mg^{2+} + Fe^{2+})$. (c, d) MgO vs Co and MgO vs Ni diagrams. Range expected for magmas in equilibrium with their mantle source: Ni = 200–500 ppm, Co = 50–70 ppm (Allègre *et al.*, 1977).

(continued)

cluster with intermediate $^{143}Nd/^{144}Nd$ values (Preakness group and part of the Orange Mt group) shows decreasing $^{206}Pb/^{204}Pb$ at constant or very slightly increasing $^{143}Nd/^{144}Nd$ trending through the field of the Meguma terrane rocks. However, samples from the Preakness group do not plot in the latter field; except for the two samples from the Sander–Hickory Grove units (CUL13 and CUL25) with $^{206}Pb/^{204}Pb$ lower than 18·5. The Hook Mt group also shows a very approximate trend with decreasing Pb and increasing Nd isotopic ratios.

Os isotopes and Re and Os concentrations

Os concentrations range from 4 to 1670 ppt, whereas Re concentrations vary from 236 to 1098 ppt. An approximate positive correlation is observed between Os and MgO, whereas an approximate negative relationship exists between Re concentration and MgO (Fig. 11), consistent with the compatible and incompatible behaviours of Os and Re, respectively, during fractional crystallization–accumulation processes. Measured $^{187}Os/^{188}Os$ ratios range from 0·1314 to 4·9444 and the initial ratios from 0·1058 to 0·2600. Five samples (GAV181, NEW68, NEW73, NEW74 and CUL25) have very low Os concentrations (3·5–17·6 ppt) and $^{187}Re/^{188}Os$ higher than 140, which leads to uncertainties higher than 10% on the calculated initial ratios owing to the error propagation related to the blank and age corrections. As a consequence, these data are not considered precise enough and are not considered further (Fig. 12). A sixth sample (CUL13, Hickory Grove) also has a low Os concentration (14·4 ppt) coupled with a more reliable elevated initial $^{187}Os/^{188}Os$ ratio ($0·1874 \pm 0·0123$). Such characteristics are observed in basalts that have experienced differentiation accompanied by contamination with material from the continental crust

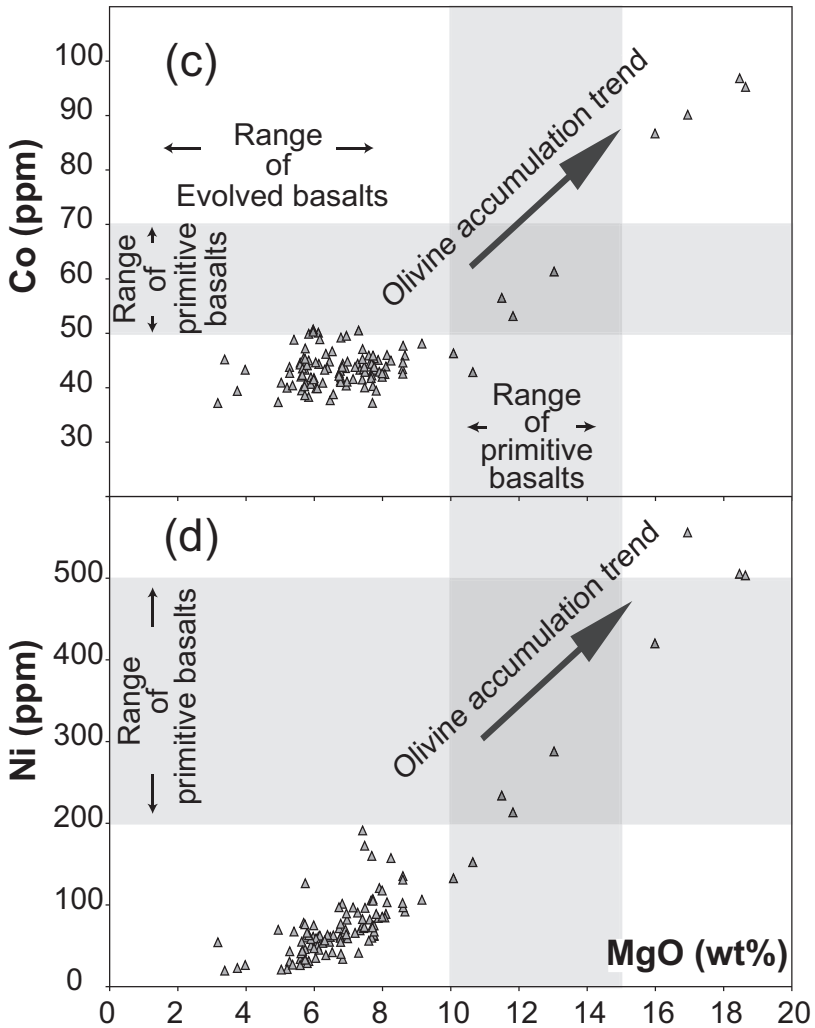

Fig. 3. Continued.

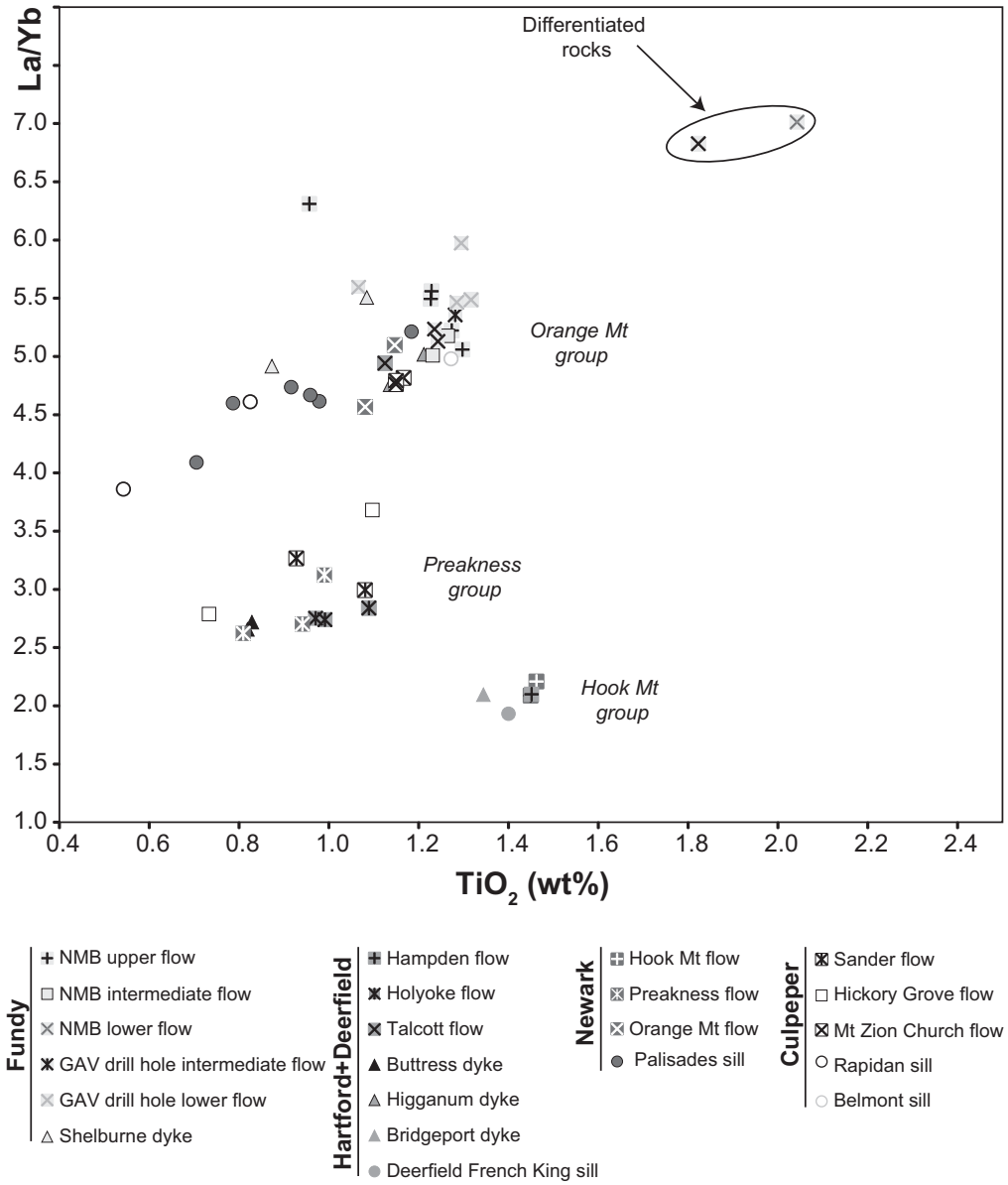

Fig. 4. Variation of TiO_2 vs La/Yb showing the chemical groups of the ENA CAMP basalts.

(Fig. 13). Indeed, this sample plots in the field expected for basalts contaminated by the upper continental crust (Fig. 13).

The remaining 12 samples have initial $^{187}Os/^{188}Os$ lower than 0·150, which are characteristic of mantle-derived magmas, coupled with Os concentrations ranging from 22·5 to 1670 ppt; these samples all belong to the Orange Mountain group. The isotopic compositions of three samples (CUL6, NEW136C and NEW17) overlap with the Primitive Upper Mantle (PUM) value at 201 Ma (0·1281 ± 0·0008, based on the present-day value of PUM of 0·1296; Meisel *et al.*, 2001; Fig. 13). Samples with Os concentrations higher than 300 ppt have initial $^{187}Os/^{188}Os$ in the restricted range of 0·1286–0·1327 (Fig. 13) and all are intrusive (sills or dykes: NS27, CUL8, NEW17 and NEW136C) with MgO contents higher than 8 wt % reflecting olivine and pyroxene accumulation.

There are no obvious correlations between the initial isotopic ratios of Os and those of Pb and Nd (Fig. 14). However, in the $^{187}Os/^{188}Os$ vs $^{143}Nd/^{144}Nd$ plot (Fig. 14), the ENA samples plot close to the field of the low-Ti CAMP basalts from Maranhão basin (Merle *et al.*, 2011) and do not show any trend toward the modern OIB.

DISCUSSION

The possible mantle sources of the CAMP

The CAMP basalts are clearly mantle-derived magmas as shown by their unradiogenic Os isotopic compositions, which are characteristic of mantle melts. Nevertheless, they have negative Nb and positive Pb anomalies in normalized trace element patterns and Sr–Nd–Pb isotopic ratios approaching those typically found in crustal rocks. Regardless of the geodynamic process that generated their parental magmas, several hypotheses could explain this enigma, including the following: (i) direct derivation from a mantle plume with the trace element and isotopic characteristics described above (Wilson, 1997);

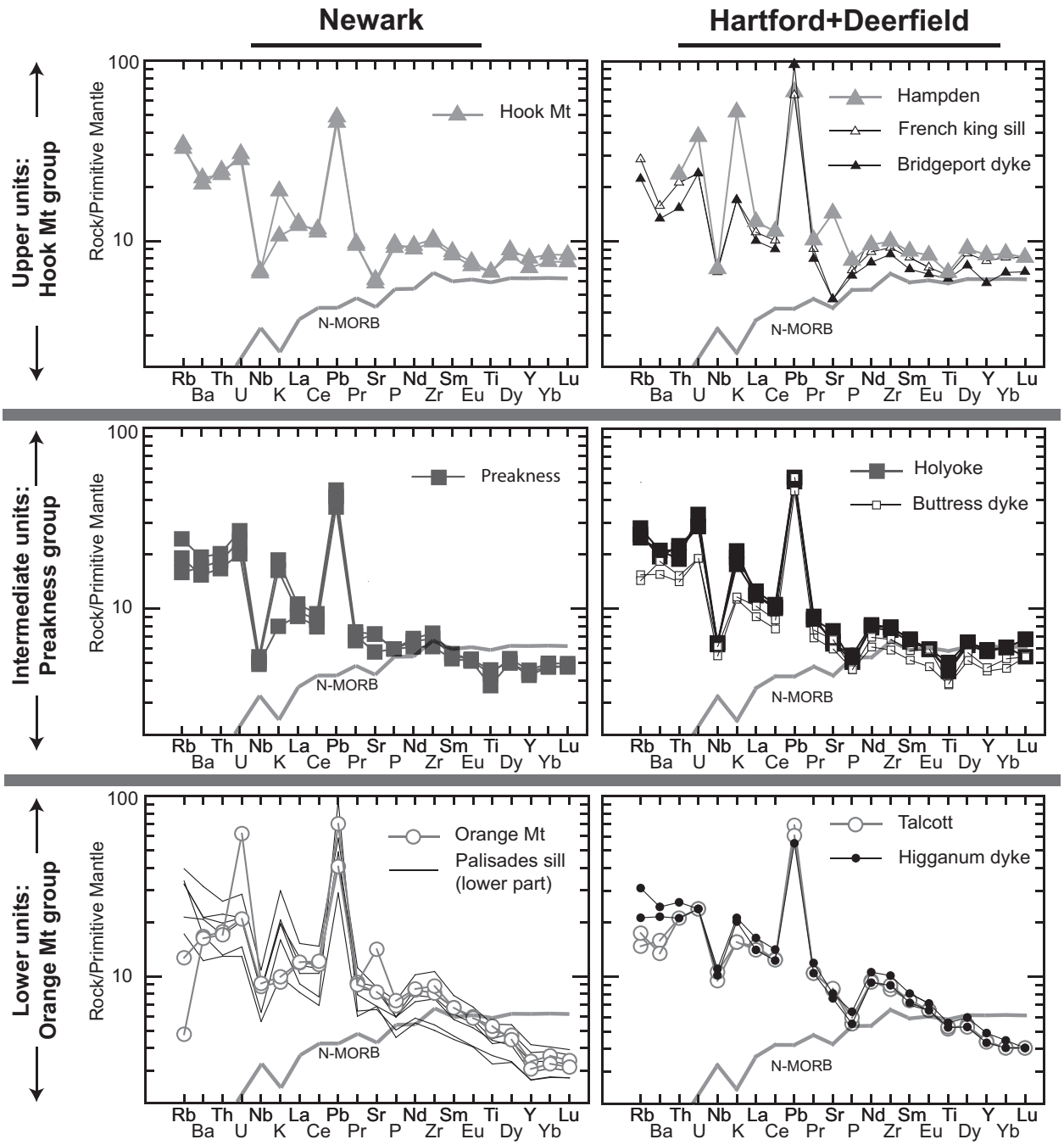

Fig. 5. Multi-element patterns of the Newark, Hartford–Deerfield, Culpeper and Fundy basin samples. Primitive mantle normalization values are from Sun & McDonough (1989).

(continued)

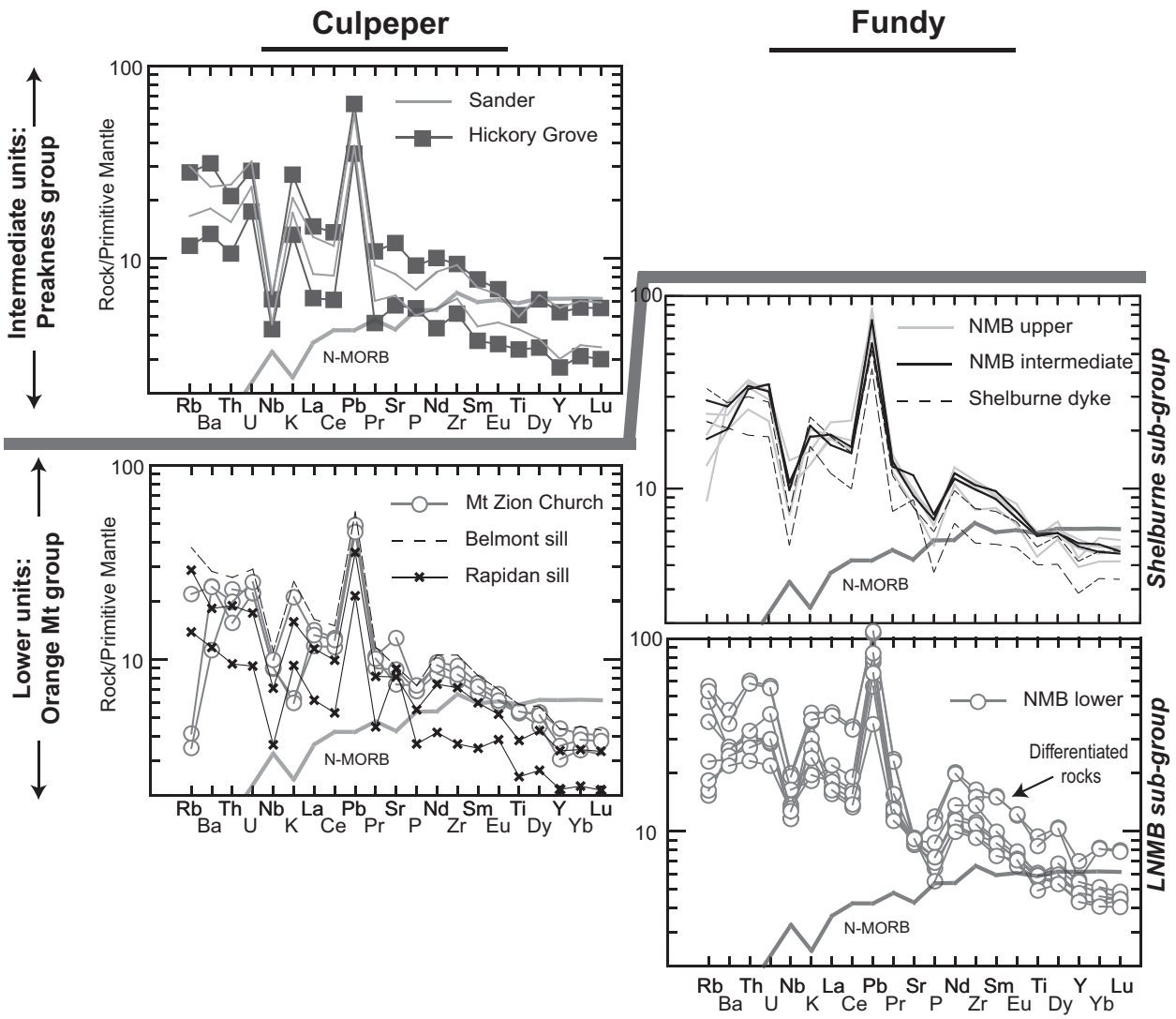

Fig. 5. Continued.

(ii) contamination of magmas derived from a mantle plume by continental crust (Arndt *et al.*, 1993); (iii) mixing between OIB or asthenospheric melts and ultra-alkaline mafic melts, such as lamproite, kimberlite, and kamafugite-type liquids assumed to be derived from metasomatized SCLM (Arndt & Christensen, 1992; Gibson *et al.*, 2006; Heinonen *et al.*, 2010), possibly followed by crustal contamination; (iv) derivation from oceanic plateau basalt (OPB)-type melts (e.g. Kerr & Mahoney, 2007); (v) ternary mixing between OIB, MORB and SCLM-related melts, possibly followed by crustal contamination; (vi) direct melting of a shallow source enriched in incompatible elements such as metasomatized SCLM or the mantle wedge above subduction zones (Puffer, 2001; De Min *et al.*, 2003; Deckart *et al.* 2005; Dorais & Tubrett, 2008). We will examine each of these models in turn to see which one is most compatible with the geological and geochemical constraints placed by the CAMP volcanism, and in particular, the ENA sub-province.

Plume-related origin without crustal contamination (hypothesis i)

It has commonly been proposed that CFB are derived from mantle plumes as the latter can provide large amounts of heat capable of producing large volumes of melt. Plumes may include a significant proportion of recycled crust and/or sediment (e.g. Zindler & Hart, 1986) and it is possible that these may contribute to the enriched Sr–Nd–Pb isotopic characteristics observed in the CAMP basalts. However, as previously noted by Merle *et al.* (2011) in their study of the Brazilian CAMP, plume-related (OIB) lavas with the required isotopic characteristics are lacking in

the Atlantic region. Generally, there are no OIB displaying $^{187}Os/^{188}Os$ values in the range of the ENA CAMP basalts with $^{143}Nd/^{144}Nd$ as low as found in the CAMP basalts (Fig. 14). The Savai'i lavas from Samoa, representing an extreme end-member EM-II mantle component, are the only OIB free of any shallow contamination by the continental crust but with the required negative Nb anomalies (Jackson *et al.*, 2007). Whereas these OIB lavas have $^{187}Os/^{188}Os$ ratios of 0·1270–0·1353 (Workman *et al.*, 2004) similar to the CAMP basalts, they show significantly

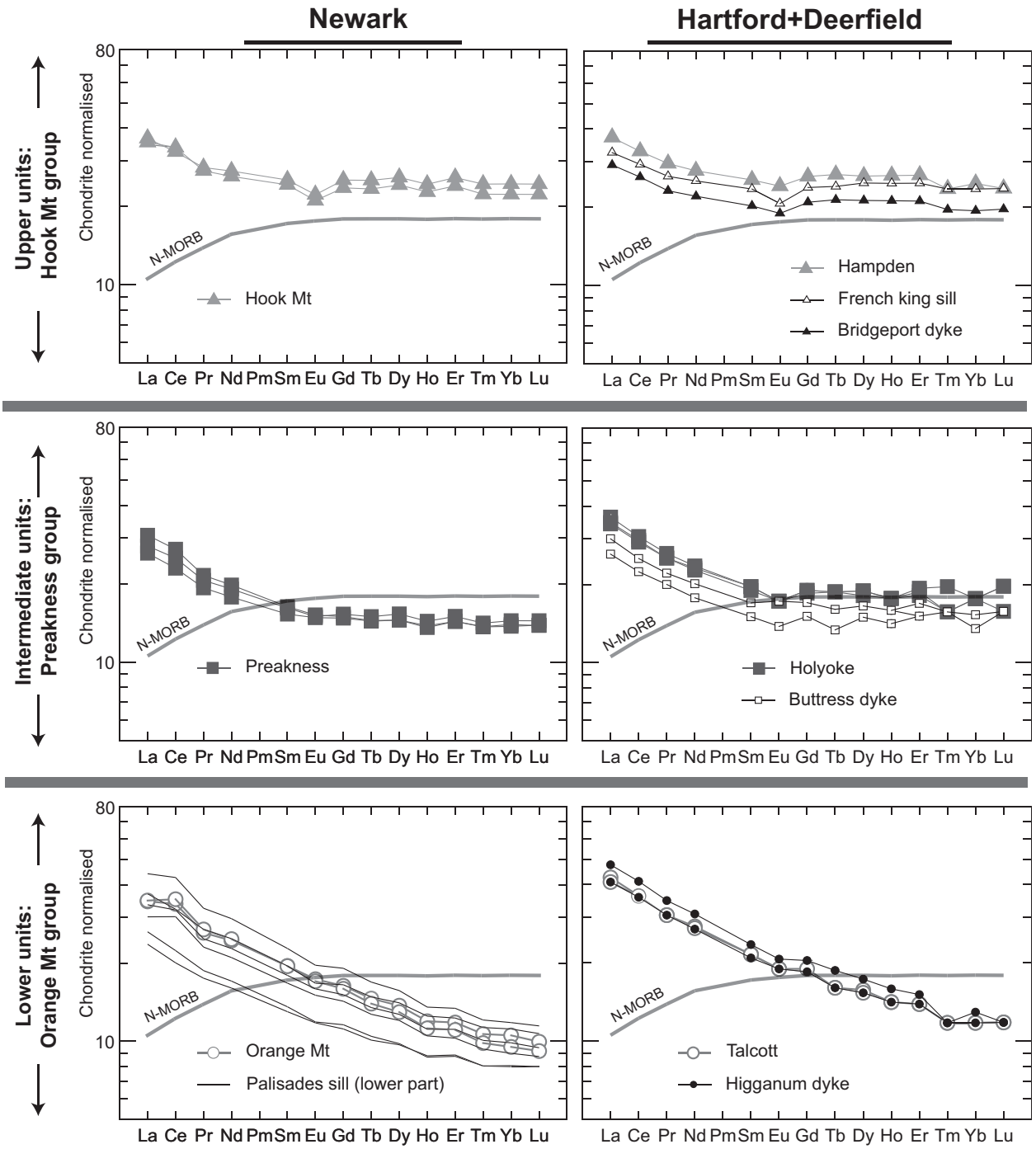

Fig. 6. Rare earth elements patterns of the Newark, Hartford–Deerfield, Culpeper and Fundy basin samples. Chondrite normalization values and average value for N-MORB are from Sun & McDonough (1989).

(continued)

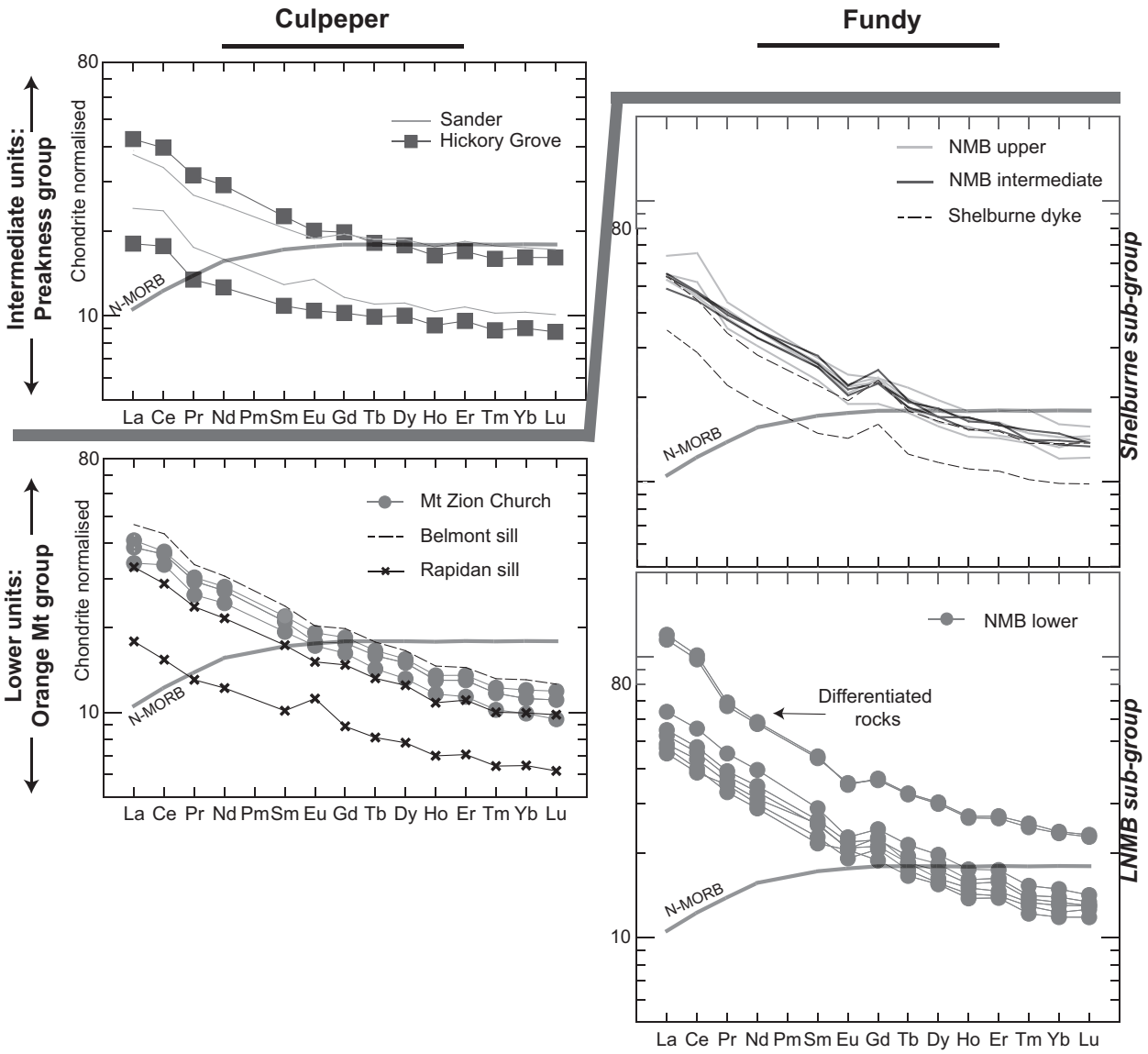

Fig. 6. Continued.

higher $^{143}Nd/^{144}Nd$, $^{206}Pb/^{204}Pb$ and $^{208}Pb/^{204}Pb$ than the CAMP basalts. Moreover, these extreme EM-II OIB are rare and it is difficult to imagine that a plume of this composition could have affected the entire Central Atlantic region at 200 Ma with no trace of it remaining today.

Plume-related origin with involvement of crustal contamination (hypothesis ii)

The CAMP basalts could be derived from a mantle plume with a composition close to those of central Atlantic OIB (i.e. Cape Verde, Fernando de Noronha, Ascension, Canaries), with their enriched continental crust-like character acquired through contamination by the continental crust. Considering that Atlantic OIB have higher $^{206}Pb/^{204}Pb$ and $^{143}Nd/^{144}Nd$ and lower $^{207}Pb/^{204}Pb$ than the CAMP basalts (e.g. Zindler & Hart, 1986; Halliday *et al.*, 1992), a large amount of crustal contamination would be required to produce the observed isotopic compositions. In this case, a simple assimilation–fractional crystallization (AFC) process would be expected to produce trends of decreasing differentiation indices (such as MgO content) with decreasing $^{143}Nd/^{144}Nd$ among samples of each group of ENA CAMP basalts or even a part of the dataset. However, there is no such correlation for the dataset but instead a decrease of $^{143}Nd/^{144}Nd$ at constant MgO content is observed between and within the groups (Fig. 15). This observation argues against extensive crustal contamination by AFC processes. Another

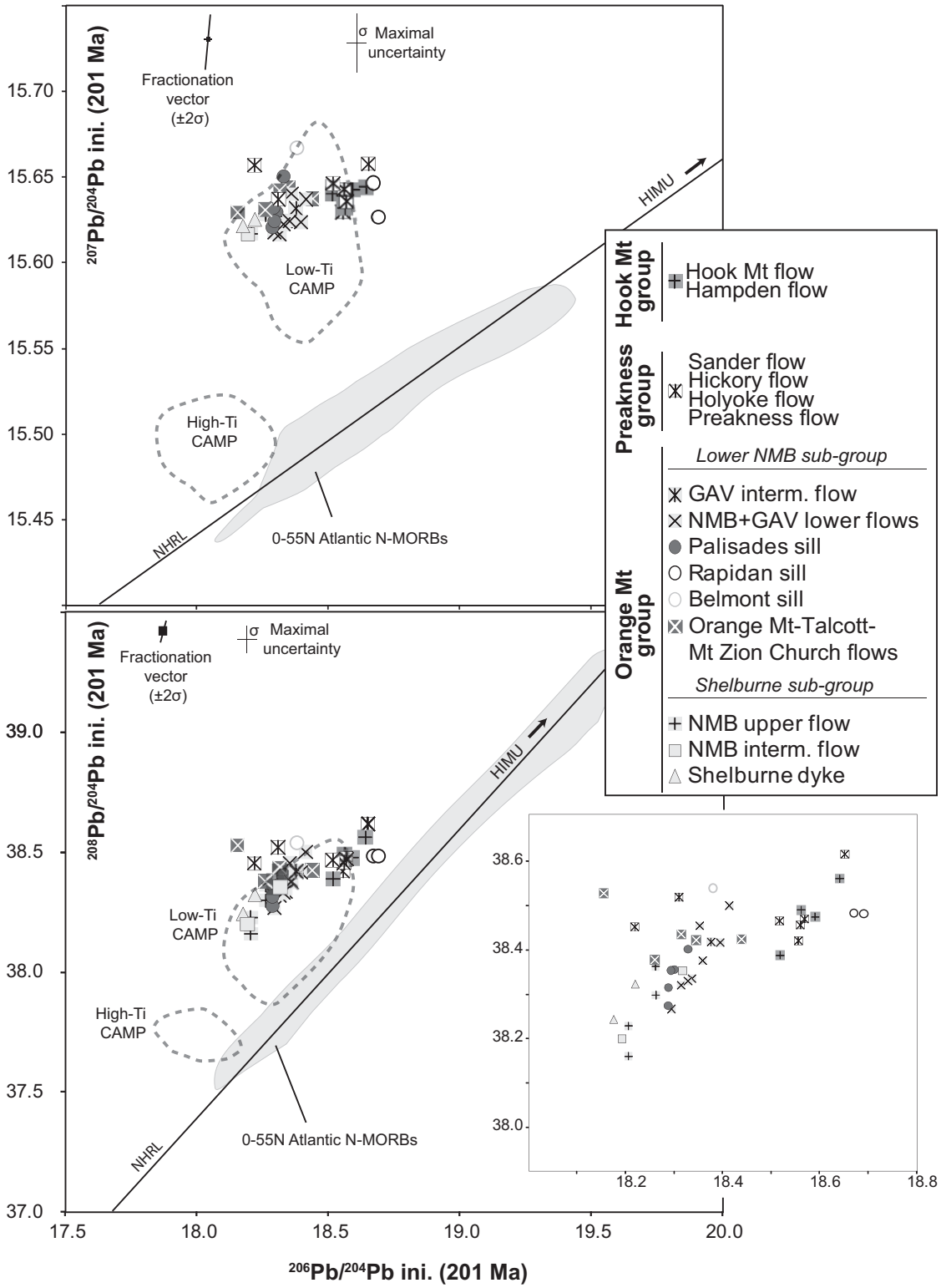

Fig. 7. Variation of $^{207}Pb/^{204}Pb$ and $^{208}Pb/^{204}Pb$ vs $^{206}Pb/^{204}Pb$ for samples of ENA CAMP basalts, all back-calculated to 201 Ma. Fields for CAMP low- and high-Ti tholeiites are based on data from Dupuy *et al.* (1988), Cebria *et al.* (2003), Jourdan *et al.* (2003), Deckart *et al.* (2005) and Merle *et al.* (2011). Trajectories of mass fractionation and maximal analytical error (calculated based on error propagation with analytical errors of U and Pb and measured isotopic ratios) are shown.

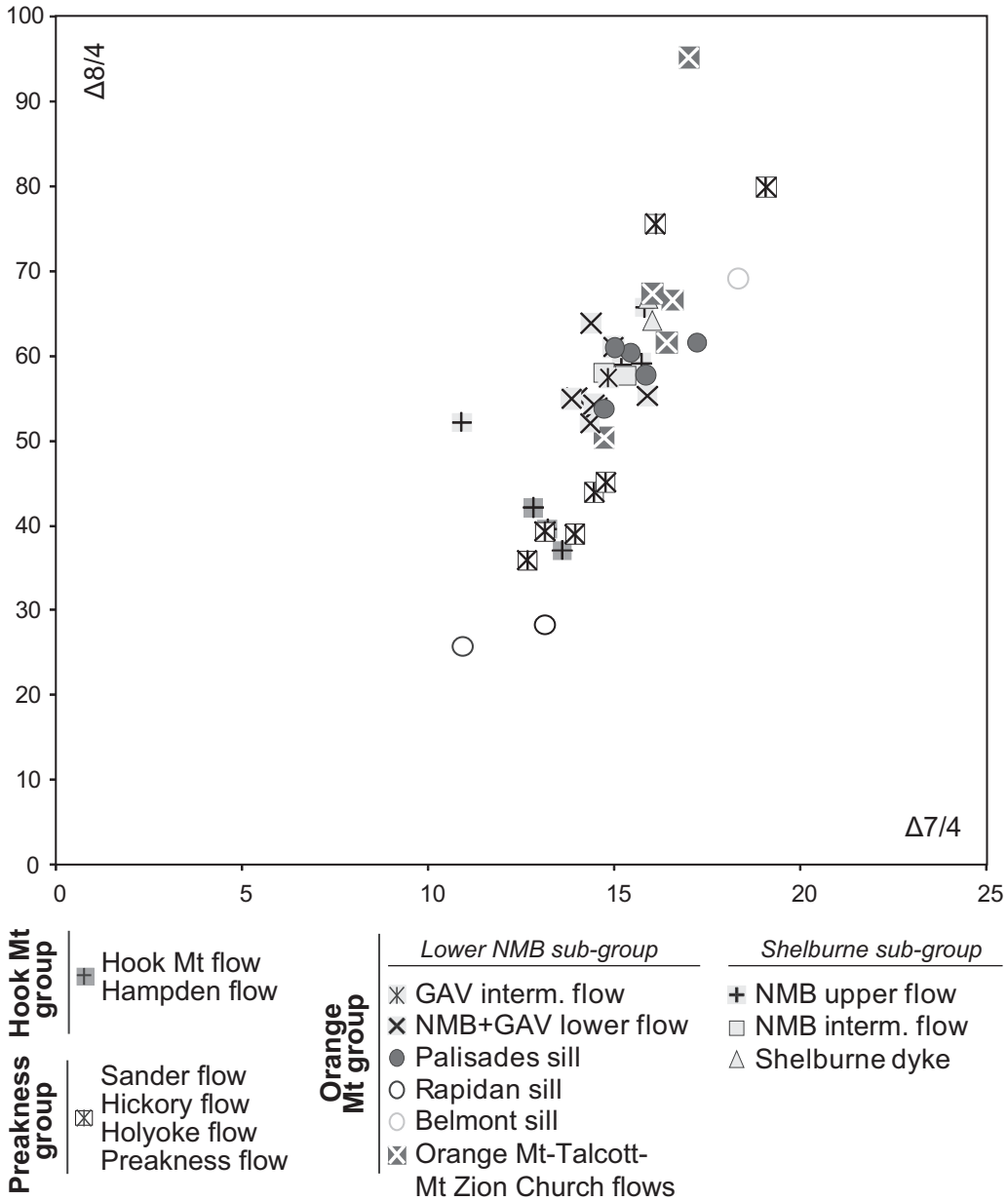

Fig. 8. Δ7/4 vs Δ8/4 for the ENA CAMP basalts.

argument against AFC is that this process would result in high incompatible element contents (Aitcheson & Forrest, 1994), which are never observed for the CAMP basalts. Perhaps the most compelling argument is that extensive crustal contamination by AFC is not compatible with the mantle-like Os isotopic ratios of the ENA CAMP samples. Magmas significantly contaminated by the crust should have initial $^{187}Os/^{188}Os$ ratios higher than 0·15 at Os concentrations lower than 50 ppt (e.g. Widom, 1997). Indeed, Os is a compatible trace element, so basalts are generated with relatively low Os concentrations that decrease rapidly during fractional crystallization. As continental crust has much more radiogenic Os isotopic compositions than the mantle ($^{187}Os/^{188}Os$ ~1–1·5 for the crust; ~0·1100–0·1500 for the mantle), Os isotopic ratios would be rapidly modified during AFC processes as basaltic Os concentration decreases. There are no trends in the Os–Pb or Os–Nd diagrams from any OIB components toward crustal compositions through the CAMP basalts that may be interpreted as reflecting crustal contamination (Fig. 14).

Nevertheless, more complex models of differentiation coupled with contamination might be considered. For

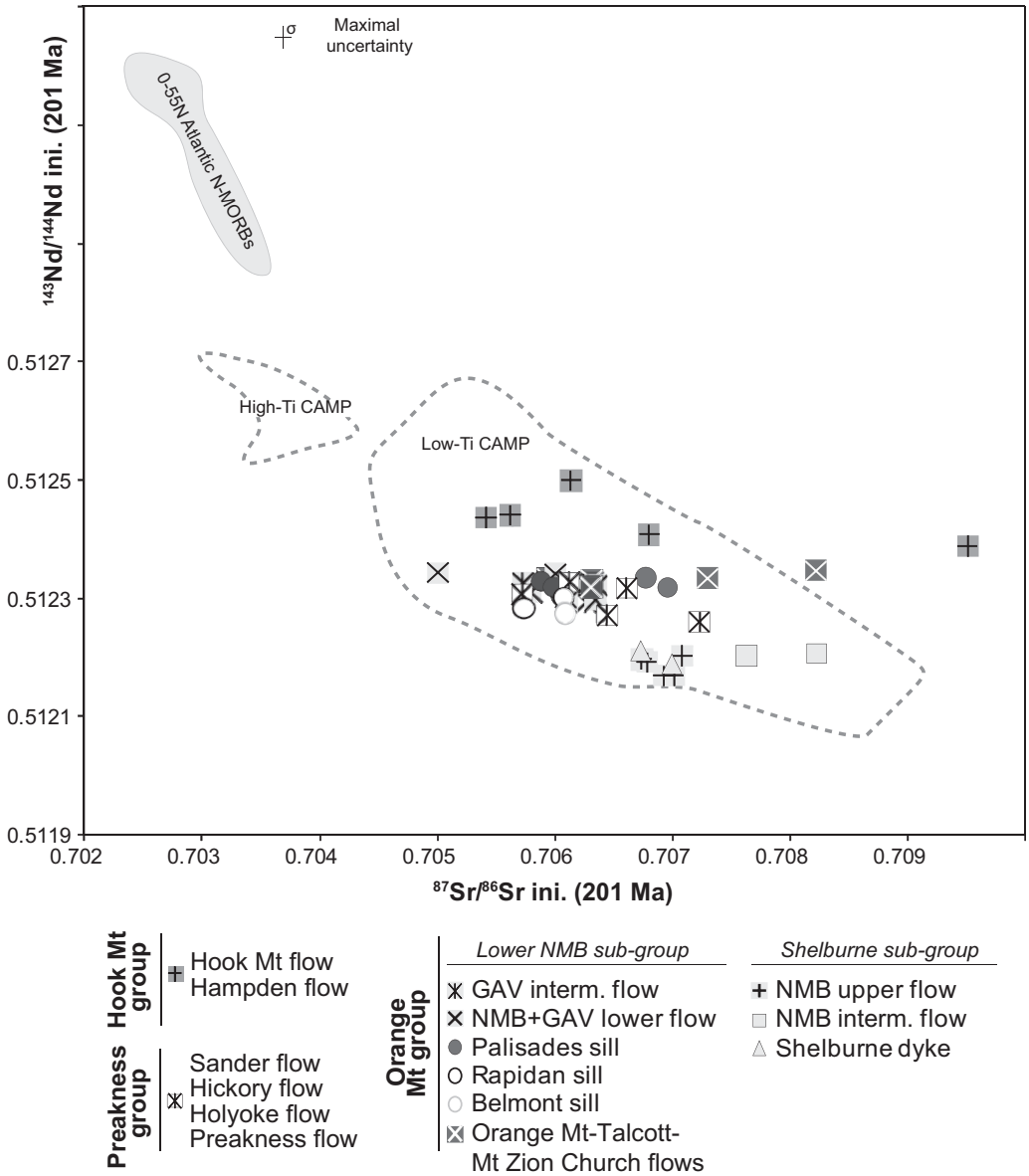

Fig. 9. Variation of $^{143}Nd/^{144}Nd$ vs $^{87}Sr/^{86}Sr$ in ENA CAMP basalts back-calculated to 201 Ma. Fields for CAMP low- and high-Ti tholeiites are based on data from Dupuy *et al.* (1988), Cebria *et al.* (2003), Jourdan *et al.* (2003), Deckart *et al.* (2005), Verati *et al.* (2005) and Merle *et al.* (2011).

instance, models of crystallizing magma chambers periodically refilled with primitive magma such as picritic liquids cannot be fully excluded [for discussion, see Molzahn *et al.* (1996)]. However, such models were designed for CFBs in which picritic magma types are common. This model could not be applied to the CAMP as no related picrites or primitive basalts have been identified so far. Moreover, picritic melts are not consistent with the relatively low mantle potential temperatures calculated for the CAMP (<1500°C; Herzberg & Gazel, 2009).

Alternatively, large amounts of assimilation of continental crust by hot and primitive mafic magmas flowing turbulently through conduits with very limited crystallization [assimilation through turbulent ascent (ATA); Huppert & Sparks, 1985] suggest that the more primitive samples should show greater evidence of crustal contamination (e.g. Kerr *et al.*, 1995*a*). It should be noted that ATA is mathematically equivalent to simple bimodal mixing between primitive melts and the continental crust (Kerr *et al.*, 1995*a*). In this case, different isotopic compositions should be expected between the more primitive (more contaminated) and the more evolved samples (less contaminated). However, this is never observed for the ENA CAMP basalts (Fig. 15).

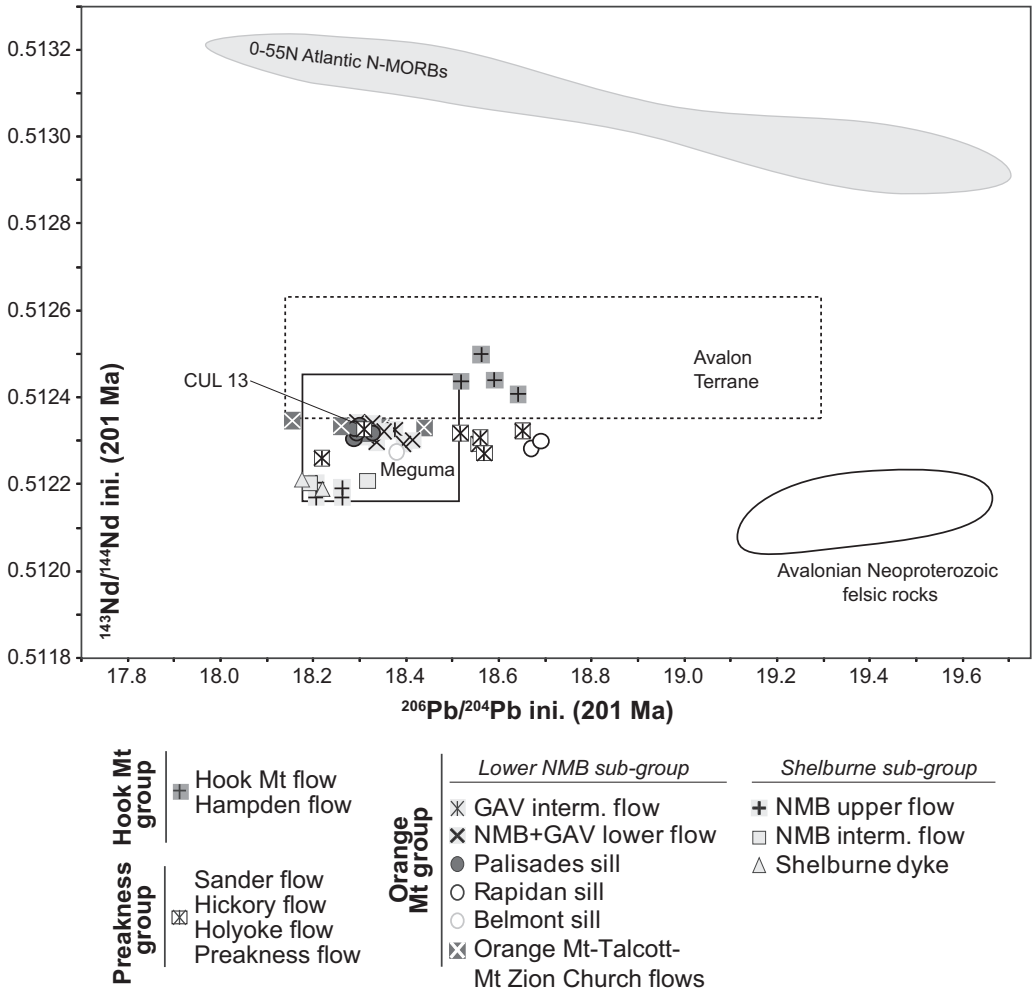

Fig. 10. Variation of initial isotopic ratios (back-calculated at 201 Ma) of $^{143}Nd/^{144}Nd$ vs $^{206}Pb/^{204}Pb$ for samples from ENA CAMP basalts. The fields for the local continental crust have been compiled from published data combining Pb and Nd and back-calculated to 201 Ma. Initial Pb isotopic ratios measured on feldspars have been included. Data for the Avalon terrane and Avalonian Neoproterozoic felsic rocks (Bass River block) are from Pe-Piper & Piper (1998); data for the Meguma terrane are from Currie *et al.* (1998) and Pe-Piper & Jansa (1999).

For all of the reasons stated above, the chemical characteristics of the CAMP basalts and in particular the enriched signature seem unlikely to be related to substantial crustal contamination of OIB- or MORB-type parental magmas.

Mixing between OIB or asthenospheric melts and ultra-alkaline mafic melts (hypothesis iii)

An alternative mechanism for generating enriched Sr–Nd–Pb isotopic compositions in tholeiitic basalts would be to mix asthenospheric or OIB-type melts with ultra-alkaline melts derived from metasomatized SCLM (Arndt & Christensen, 1992; Gibson *et al.*, 2006; Heinonen *et al.*, 2010), followed by contamination by the continental crust. This hypothesis is essentially based on the occurrence of SCLM-derived ultra-alkaline mafic rocks (lamproites, kimberlites or carbonatites) that are associated with tholeiitic magmatism in some flood basalt provinces such as the Parana–Etendeka province (Gibson *et al.*, 2006). However, no such compositions are known to be related (spatially or temporally) with the CAMP event. Nevertheless, this process has been modelled to see whether it might provide a feasible explanation for the isotopic compositions of the ENA CAMP basalts. A two-step process is assumed: (1) simple mixing between OIB- or MORB-type melts and SCLM-related melts; (2) subsequent contamination involving components of the local continental crust. For the contamination process, both AFC (DePaolo, 1981) and ATA (Huppert & Sparks, 1985) have been modeled.

Because ultra-alkaline SCLM-derived rocks are not associated with the CAMP, we used the composition of such rocks associated with the Mesozoic Paraná LIP. Our choice is driven by the geodynamic similarity of the

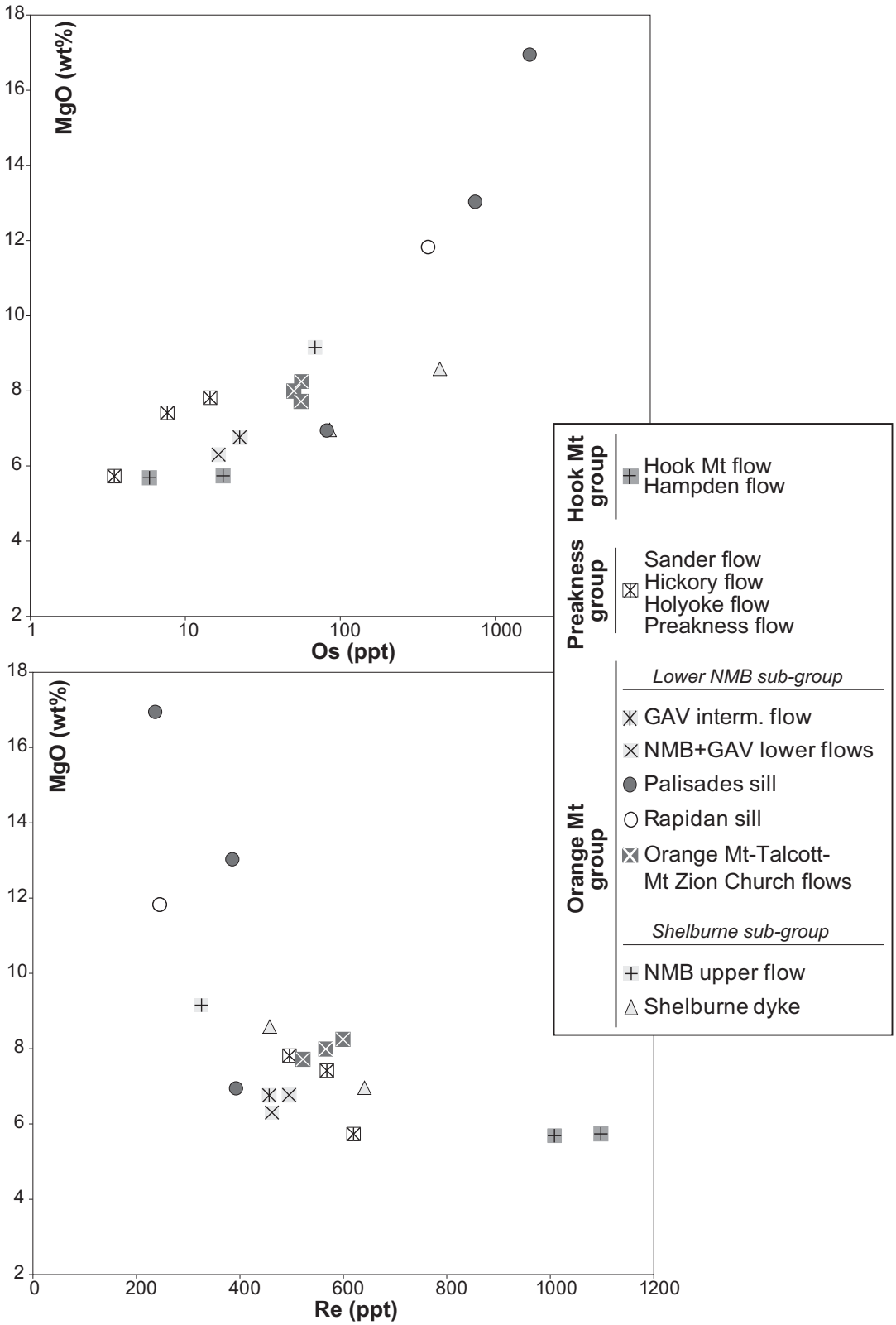

Fig. 11. Variation of Re and Os (ppt) vs MgO (wt %).

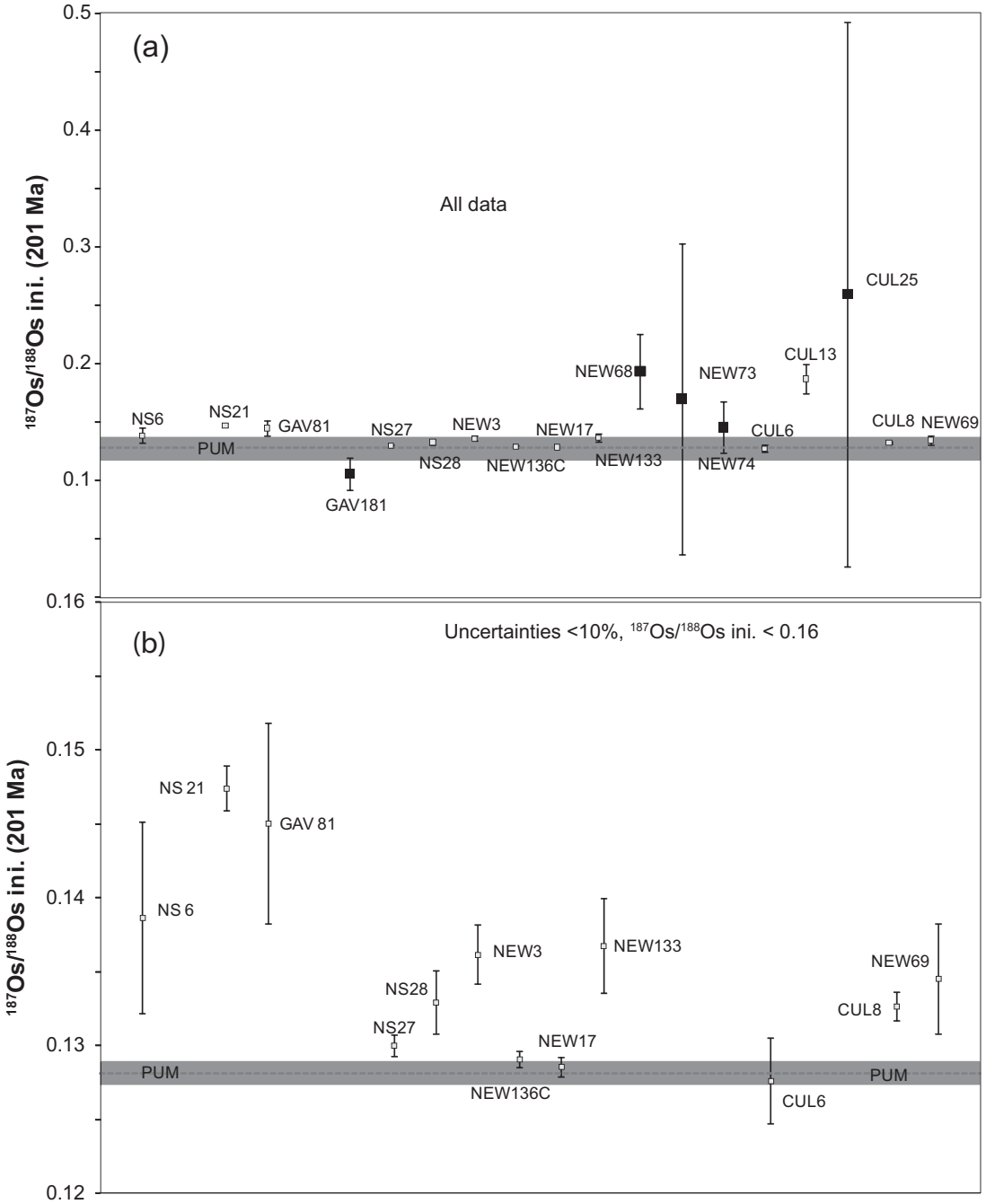

Fig. 12. Initial $^{187}Os/^{188}Os$ (back-calculated to 201 Ma) with uncertainties. Error bars are given at the 2σ level. (a) All data shown. Filled black rectangles, data with uncertainties higher than 10%; open rectangles, data with uncertainties lower than 10%. (b) Samples with $^{187}Os/^{188}Os < 0{\cdot}16$ and uncertainties lower than 10%. Value of the Primitive Upper Mantle (PUM) back-calculated to 201 Ma (present-day PUM values: $^{187}Os/^{188}Os = 0{\cdot}1296 \pm 0{\cdot}0008$; $^{187}Re/^{188}Os = 0{\cdot}4353$; Meisel *et al.*, 2001).

CAMP and Paraná, both LIPs being associated with the opening of the Atlantic Ocean. Because there is no modern equivalent of the hypothetical CAMP mantle plume, the composition of the OIB end-member is poorly constrained. Considering the large range of OIB compositions worldwide and the fact that the results are strongly dependent on this parameter, the best proxy needs to be constrained by the geology of the CAMP. As a consequence, we assumed an average OIB composition close to that of Atlantic OIB (i.e. Cape Verde, Fernando de Noronha, Ascension, Canaries). For the assimilation model, we considered several components of the local

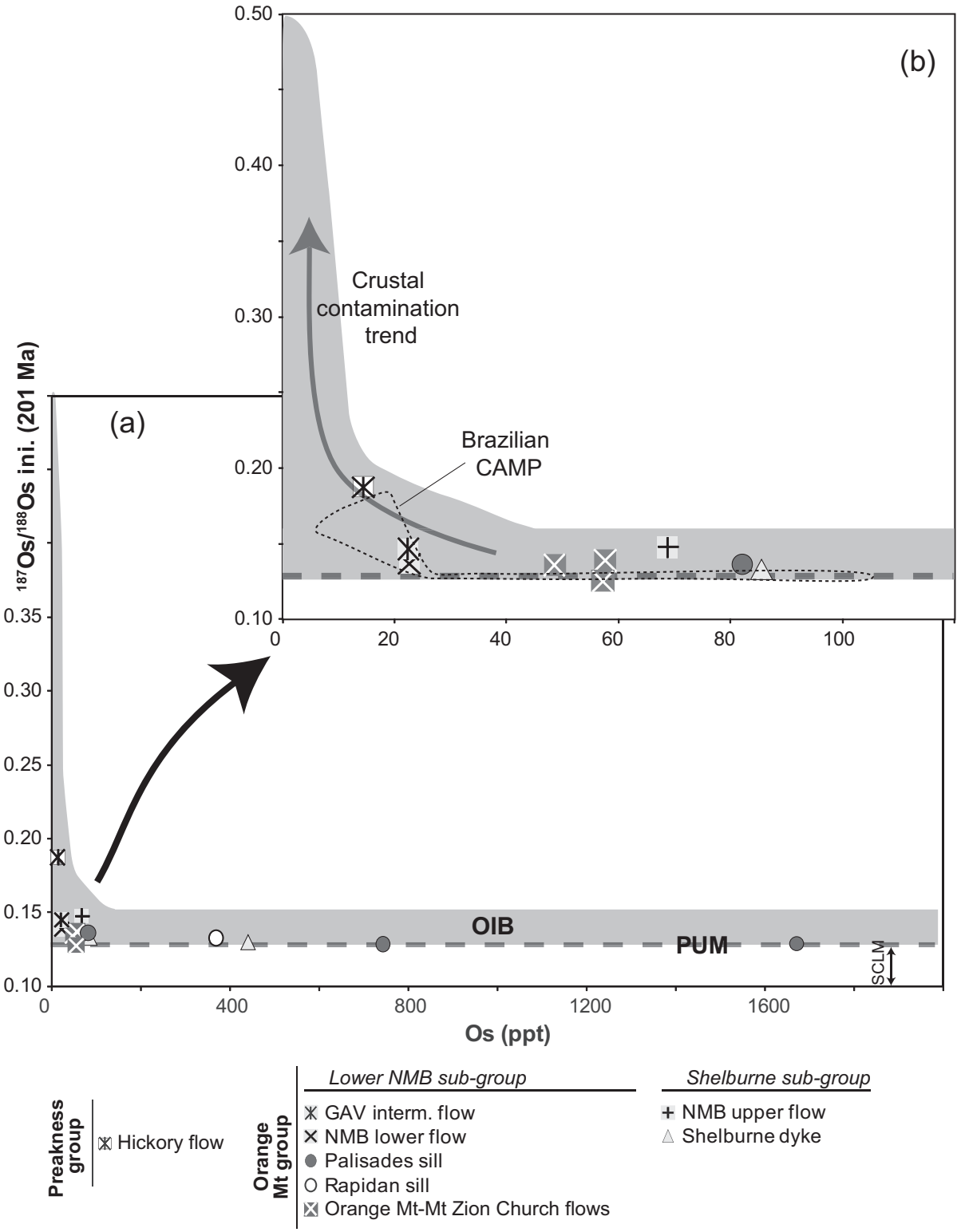

Fig. 13. Variation of initial $^{187}Os/^{188}Os$ (back-calculated to 201 Ma) vs Os concentration. (a) All ENA data represented. (b) Samples with Os contents lower than 120 ppt. The general crustal contamination trend is based on upper continental crust with low [Os] and high $^{187}Os/^{188}Os$. The grey field corresponds to worldwide occurrences of OIB. The value of the Primitive Upper Mantle (PUM) has been back-calculated to 201 Ma (present-day PUM values: $^{187}Os/^{188}Os = 0{\cdot}1296 \pm 0{\cdot}0008$; $^{187}Re/^{188}Os = 0{\cdot}4353$; Meisel *et al.*, 2001). Field for Brazilian CAMP is from Merle *et al.* (2011).

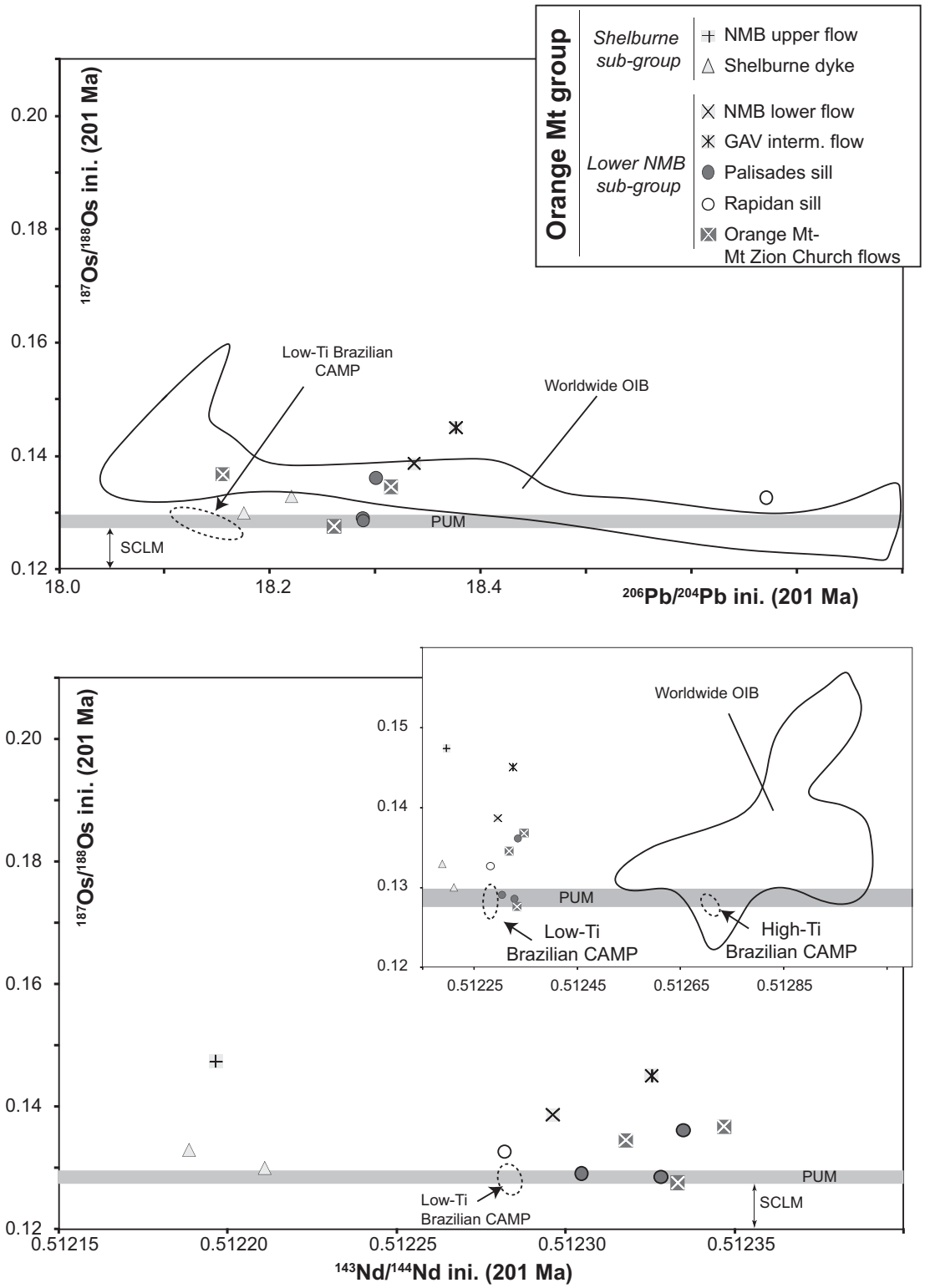

Fig. 14. Variation of initial $^{187}Os/^{188}Os$ vs $^{143}Nd/^{144}Nd$ and $^{206}Pb/^{204}Pb$ for ENA CAMP basalts (data back-calculated to 201 Ma). Primitive upper mantle (PUM) value is from Meisel *et al.* (2001), back-calculated to 201 Ma. Field for modern worldwide OIB is based on data from the Georoc database. The OIB data have been filtered for lithosphere contamination: samples with [Os] < 30 ppt and $^{187}Os/^{188}Os > 0{\cdot}16$ have been discarded. It should be noted that sample CUL13 (Hickory Grove), which shows characteristics of contamination by the continental crust, is not plotted. The fields for Brazilian CAMP basalts are from Merle *et al.* (2011).

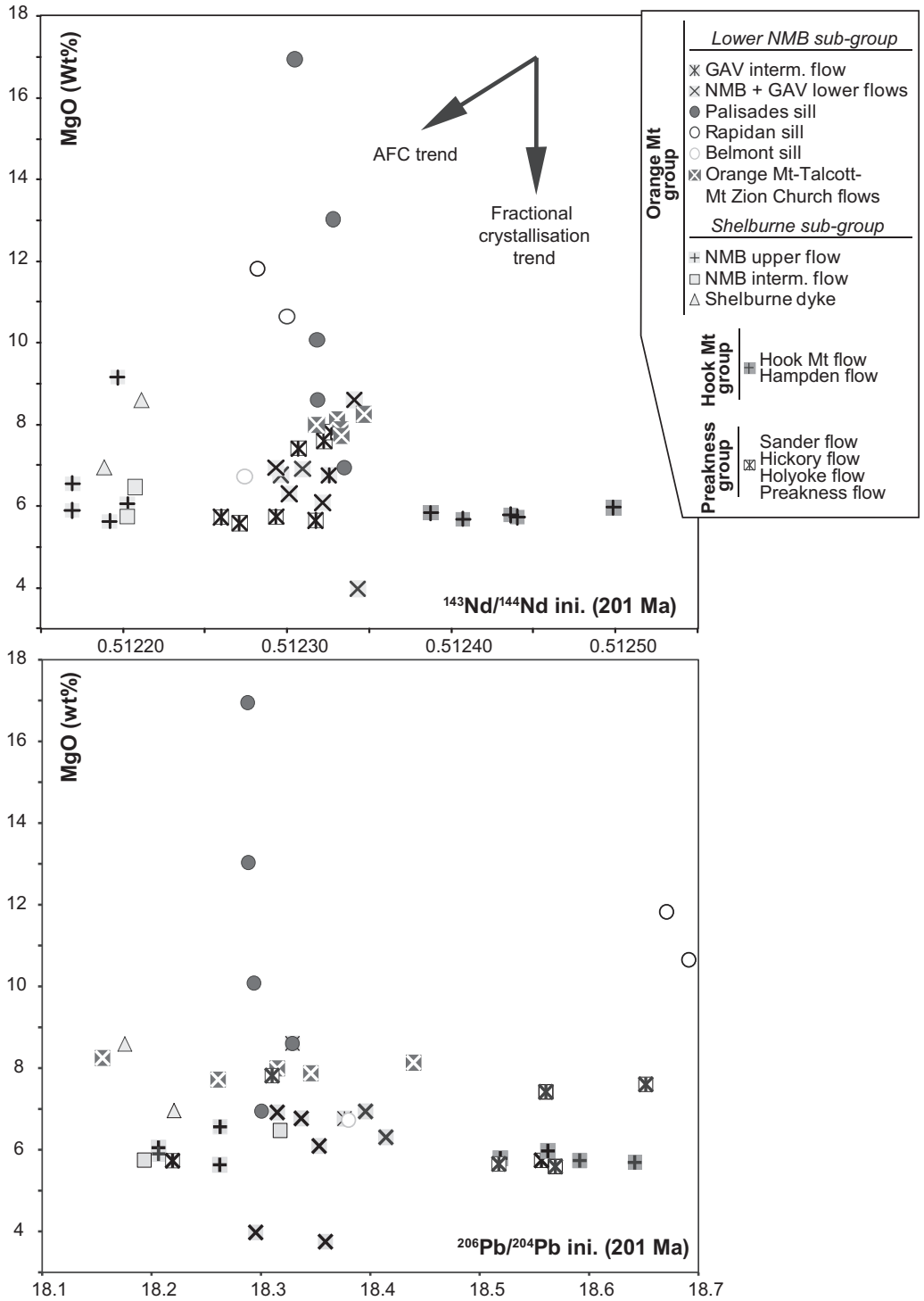

Fig. 15. Variation of initial $^{143}Nd/^{144}Nd$ and $^{206}Pb/^{204}Pb$ vs MgO for the ENA CAMP basalts. The AFC trend indicates the general evolution of the chemistry of the basalts when contaminated by average upper continental crust with a low MgO content and low $^{143}Nd/^{144}Nd$.

crust. The chemical characteristics of the ENA CAMP basalts were best reproduced using the composition of Avalonian Neoproterozoic felsic crust (Pe-Piper & Piper, 1998).

According to the numerical modelling, mixing involving either OIB or MORB-like parental melts followed by crustal contamination partially reproduces the compositions of the three chemical ENA CAMP groups (Figs 16–19;

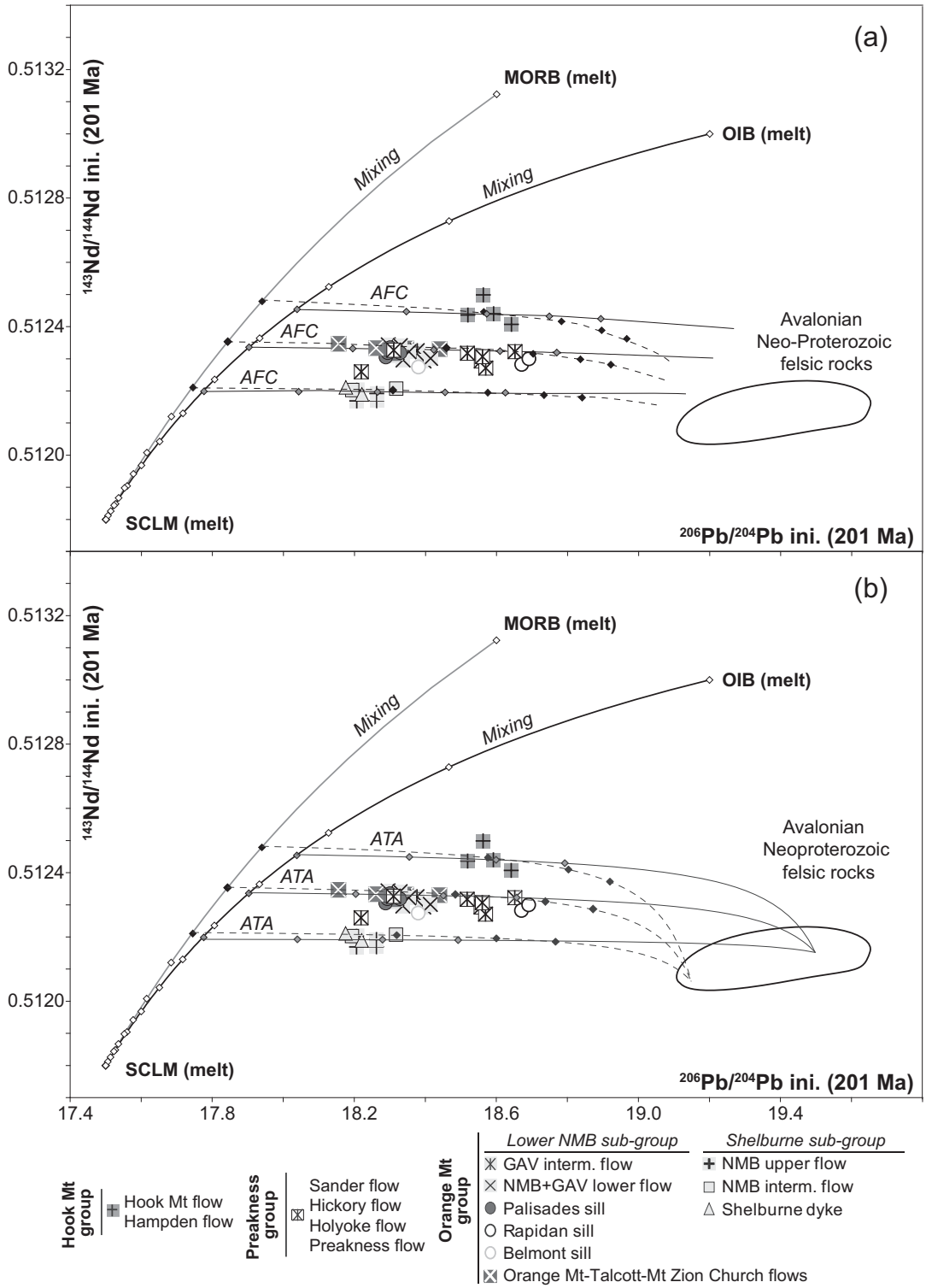

Fig. 16. Models combining mixing of OIB or MORB compositions with SCLM-derived melts followed by crustal contamination. (a) $^{143}Nd/^{144}Nd$ vs $^{206}Pb/^{204}Pb$ assuming an AFC contamination process. (b) $^{143}Nd/^{144}Nd$ vs $^{206}Pb/^{204}Pb$ assuming an ATA contamination process. The lozenges on the mixing and AFC or ATA lines represent 10% increments. Composition of Avalonian Neoproterozoic felsic rocks is from Pe-Piper & Piper (1998). All model parameters are given in Supplementary Data Tables A4 and A5.

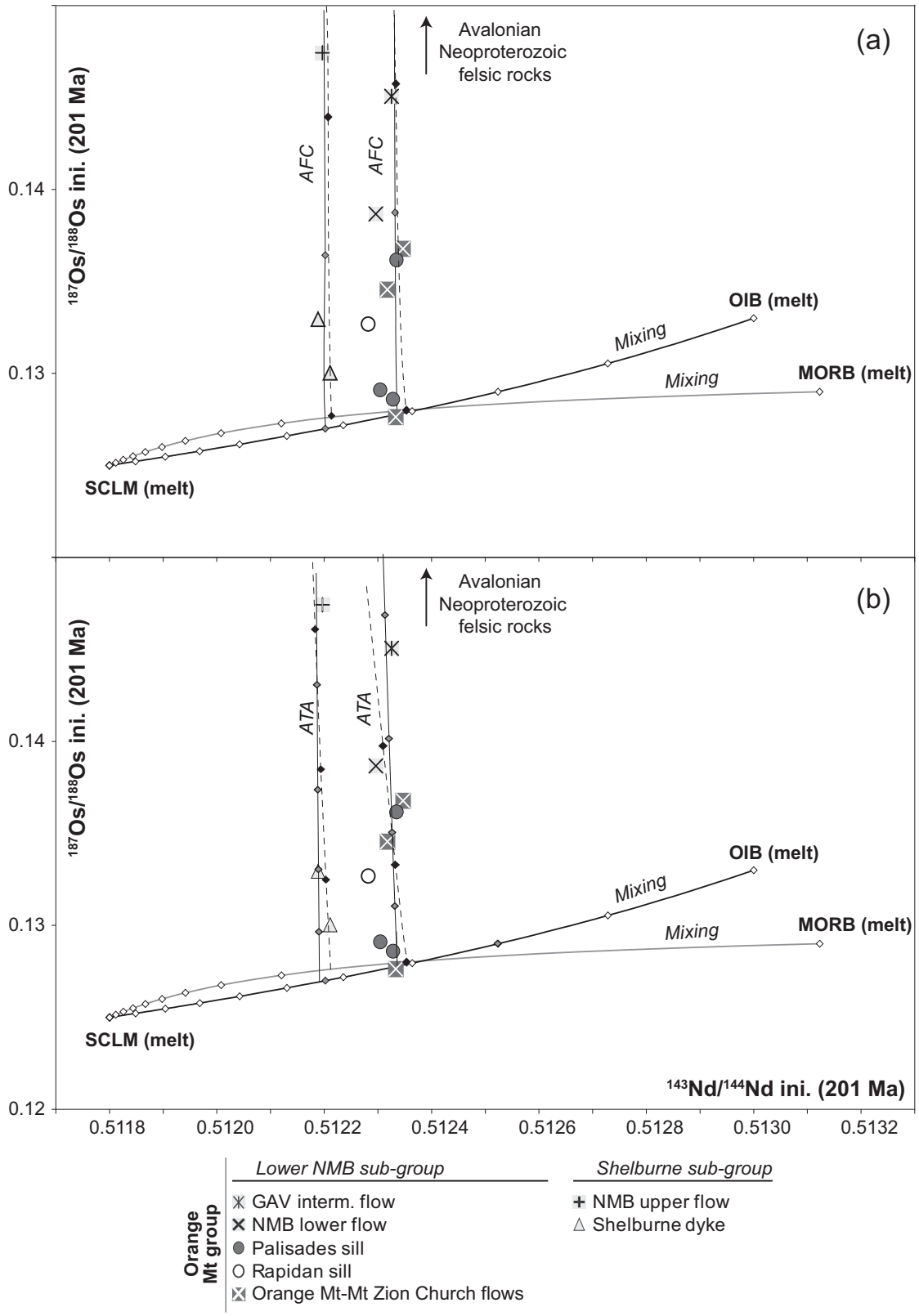

Fig. 17. Models combining mixing of OIB or MORB compositions with SCLM-derived melts followed by crustal contamination. (a) $^{143}Nd/^{144}Nd$ vs $^{187}Os/^{188}Os$ assuming an AFC contamination process. (b) $^{143}Nd/^{144}Nd$ vs $^{187}Os/^{188}Os$ assuming an ATA contamination process. The lozenges on the mixing and AFC or ATA lines represent 10% increments. Composition of the Avalonian Neoproterozoic felsic rocks is from Pe-Piper & Piper (1998). All model parameters are given in Supplementary Data Tables A4 and A5.

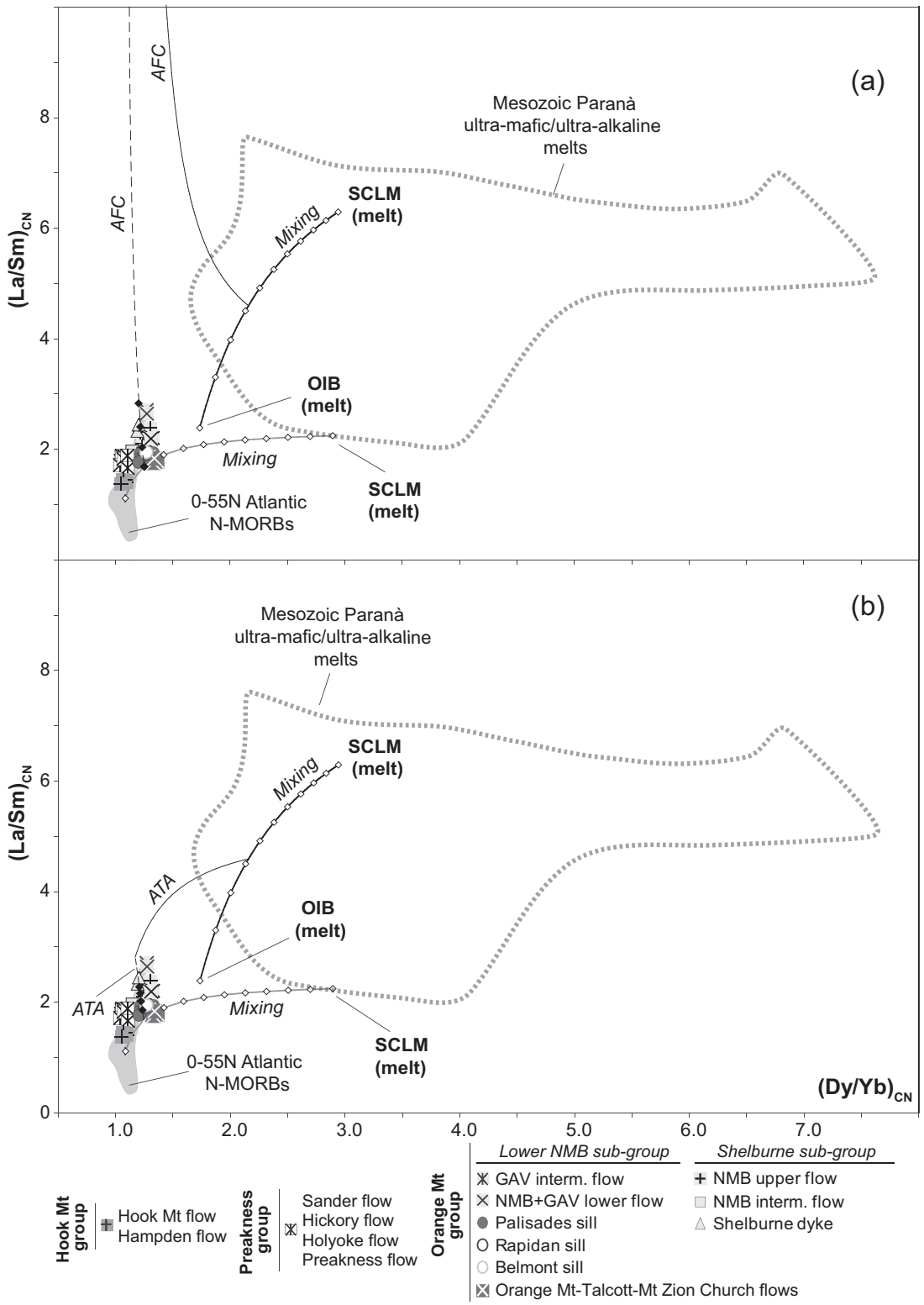

Fig. 18. Models combining mixing of OIB or MORB compositions with SCLM-derived melts followed by crustal contamination. (a) La/Sm_{CN} vs Dy/Yb_{CN} assuming an AFC contamination process. (b) La/Sm_{CN} vs Dy/Yb_{CN} assuming an ATA contamination process. The lozenges on the mixing and AFC or ATA lines represent 10% increments. All model parameters are given in Supplementary Data Tables A4 and A5. Composition of Mesozoic ultramafic or ultra-alkaline rocks of the Parana LIP are from the Georoc database. CN, chrondrite normalization values from Sun & McDonough (1989).

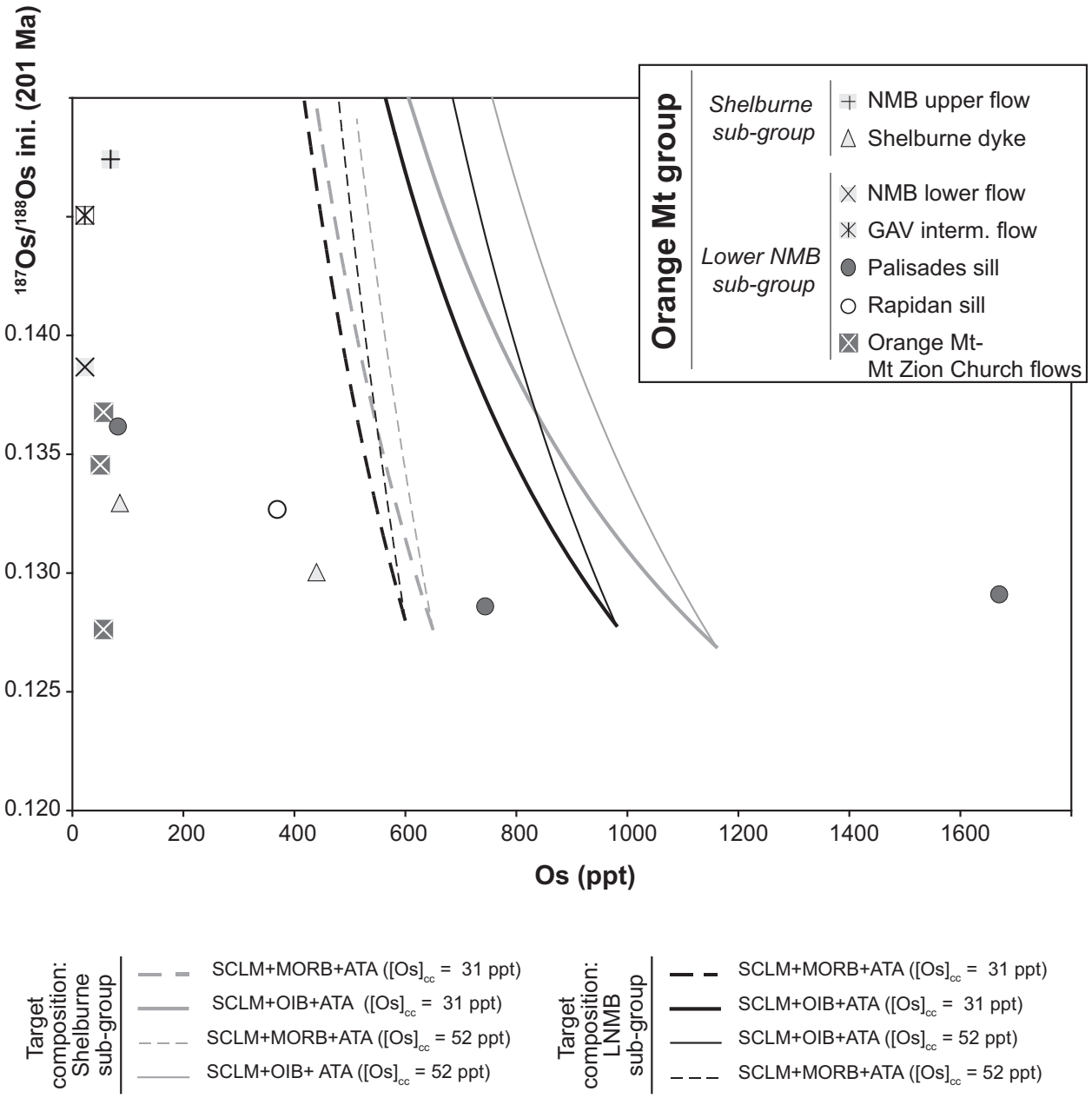

Fig. 19. Variation of Os concentration in ppt vs initial $^{187}Os/^{188}Os$ (at 201 Ma) showing models of mixing between OIB or MORB melts and SCLM-derived melts followed by ATA involving different compositions of continental crust. (See further explanation in the text.)

parameters and results are given in Supplementary Data Tables A4 and A5). In the case of mixing of OIB with SCLM-related melts, the isotopic composition of the ENA CAMP basalts can be modelled by mixing with 24% (Hook Mt group) and 44% (Shelburne sub-group) of SCLM-related melts followed by very large amounts of assimilation of continental crust, regardless of the process of assimilation (AFC: 13–35%; ATA: 12–32%; Figs 16–18). However, this model presents some problems. First, the Nd–Pb–Os isotopic compositions of the ENA CAMP basalts can be matched only for very high Os and very low Nd contents (2000 ppt and 100 ppm, respectively) in the primary SCLM-related melt (Fig. 16). Second, and, more significantly, the main problem of this modelling concerns the incompatible elements and in particular the REE ratios of the resulting melts. Whereas the large majority of OIB and Paranà SCLM-related melts have $La/Sm_N > 2$ (Sun & McDonough, 1989; Gibson *et al.*, 1999), most of the ENA CAMP basalts have $La/Sm < 2$ (Fig. 18). An AFC or ATA process following the mixing would

result in more enriched REE contents that would never match the compositions of the ENA CAMP basalts regardless of the composition of the continental crust (Fig. 18). Moreover, the trends observed in the Nd–Pb and Os–Nd isotopic diagrams require up to 35% of contamination by the local continental crust (Figs 16–18). Such high degrees of assimilation should have been observed in the MgO vs $^{143}Nd/^{144}Nd$ and MgO vs $^{206}Pb/^{204}Pb$ diagrams as trends for an AFC process or as significant differences between more primitive and more evolved samples for an ATA process (Fig. 15). In addition, assimilation of more than 20% of continental crust is thermodynamically unrealistic (Spera & Bohrson, 2001). Consequently, the hypothesis of a magma originating from mixing between OIB and SCLM-related melts and further contaminated by the continental crust is unlikely.

When MORB and SCLM-related melts mix, the Nd–Pb–Os isotopic compositions of the ENA CAMP basalts could be matched by between 15% (Shelburne sub-group) and 7% (Hook Mt group) of SCLM-related melts and by assimilation of 5–20% of the local continental crust through an AFC process and by 5–18% through an ATA process (Figs 16–18). As for mixing between OIB- and SCLM-related melts, the compositions of the ENA CAMP basalts can be obtained only for very low Nd contents (100 ppm) in the SCLM-related melt. As for the OIB–SCLM model, the main flaw concerns the REE ratios, as the ENA CAMP basalt compositions can be matched only by involving depleted compositions of N-MORB and extreme compositions (lowest La/Sm and Dy/Yb observed for the ultra-alkaline melts) of the SCLM-related melts.

In the case of an AFC process, the trends observed in the Nd–Pb and Nd–Os isotopic variations of the ENA CAMP basalts can be matched only if a very low Pb content (5 ppm) is assumed for the local continental crust. The main problem with this scenario concerns the discrepancy between the amount of assimilation required to match the isotopic (*c.* 20%) and the REE (*c.* 30%) compositions of the ENA tholeiites (Fig. 17). This issue is not resolved when ATA is considered instead of AFC and the same composition of continental crust is assumed. Indeed, the Nd–Pb isotopic compositions require smaller amounts of assimilation (less than 20%) than suggested by the Os isotopic compositions (up to 30%) or the REE contents (up to 50%).

This discrepancy could be eliminated by considering a continental crust component with a slightly atypical composition ([La] = 39 ppm, [Sm] = 3·1 ppm, [Dy] = 3·6 ppm, [Yb] = 2 ppm), which would match the CAMP compositions for approximately 20% crustal contamination (both AFC and ATA considered). In the case of the AFC process, the composition of the lower NMB sub-group is modelled by assuming a crust with a very low Os concentration ([Os] = 2·6 ppt). Such low Os contents are rare in the continental crust, and similar concentrations have been found only in lower crustal plagioclase-rich cumulates (Saal *et al.*, 1998). However, the latter rocks have higher initial Os and Nd isotopic ratios and lower initial Pb isotopic ratios than the composition of the crust required to model the ENA CAMP basalts (Saal *et al.*, 1998, and references included). Moreover, this kind of plagioclase cumulate has not been documented in the NE USA. In the case of an ATA process, crust with an Os concentration up to 52 ppt is required. Nevertheless, this process cannot produce the Os concentrations of the ENA CAMP basalts (Fig. 19).

In conclusion, mixing between OIB and SCLM-related melts seems rather unrealistic and can be ruled out. The MORB–SCLM-related model seems more plausible but also has some limitations.

Derivation from OPB-type melts (hypothesis iv)

Because most OIB compositions are extreme end-members that result from small degrees of partial melting of the mantle, they might not be representative of the composition produced by the large-scale melting proposed for generation of LIPs. Moreover, for continental LIP magmas, even the least evolved, crustal contamination cannot be entirely ruled out. High-MgO OPB compositions might, therefore, be a better proxy for the primary melts derived from a deep mantle source (Kerr *et al.*, 1995*b*). In addition, many continental flood basalts show evidence for depleted (MORB-like) components in their sources that are not related to a shallow contamination by the asthenosphere (entrainment of the asthenosphere by a rising plume) but are genuinely deep mantle components (Kerr *et al.*, 1995*b*). As a consequence, the uncontaminated magmas share characteristics of both MORB and OIB (Kerr *et al.*, 1995*b*).

We therefore tested the possibility that the ENA CAMP basalts were derived from magmas analogous to OPB melts that experienced crustal contamination, possibly preceded by mixing with SCLM-derived melts. For the primitive parental magma composition, we used the average compositions of primitive melts (i.e. tholeiitic, picritic and komatiitic compositions with MgO > 8%) from both the Caribbean and the Ontong–Java plateaux (e.g. Kerr & Mahoney, 2007). Considering that no Os data are available for the latter, we used the average $^{187}Os/^{188}Os$ initial ratio and Os concentration of the Caribbean plateau basalts. Because OPBs are clearly distinct from the CAMP basalts, continental crustal contamination is required to achieve the enriched signature observed in the latter. However, simple crustal contamination of OPB-type primitive melts by either ATA or AFC mechanisms fails to reproduce the chemical characteristics of the ENA CAMP basalts (Fig. 20). A slightly better fit is achieved if the OPB melts are first mixed with SCLM-derived melts and then contaminated by the continental crust; nevertheless, in this case also, only part of ENA CAMP compositions can be reproduced, in particular the REE compositions of the

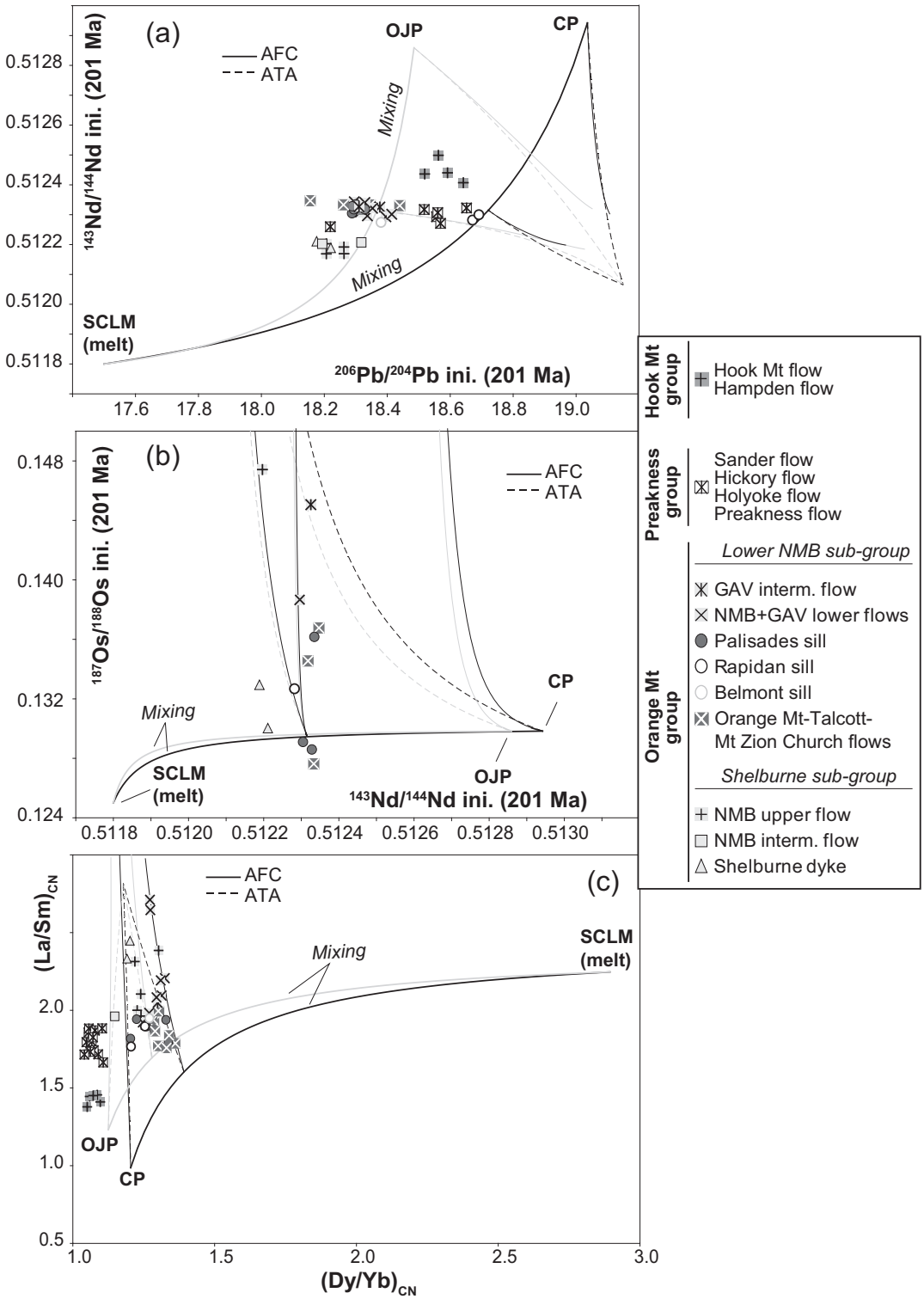

Fig. 20. Variation of (a) ^{143}Nd/^{144}Nd vs ^{206}Pb/^{204}Pb, (b) ^{143}Nd/^{144}Nd vs ^{187}Os/^{188}Os and (c) La/Sm$_{CN}$ vs Dy/Yb$_{CN}$ showing combined models of mixing + AFC and ATA between Ontong–Java Plateau (OJP) or Caribbean Plateau (CP) melts and SCLM-derived melts. Average composition of OJP and CP primitive basaltic melts is from the Georoc database. All model parameters are given in Supplementary Data Table A6.

Hook Mt and Preakness groups and the Pb–Nd isotopic compositions of the Orange Mt group (Fig. 20). It should be noted that the composition of the SCLM end-member is similar to that used in the previous modeling, and hence presents the same problems. Nevertheless, it is the only composition able to partly reproduce the composition of the CAMP basalts.

Because the OPB compositions used in this modeling are averages it could be argued that they are not representative of the oceanic plateau and different compositions could perhaps match the ENA CAMP basalts. Nevertheless, extreme compositions are more rare and less representative of large-scale mantle melting. Moreover, tholeiitic OPB compositions are close to those of MORB, leading to the same problems as encountered for mixing between MORB and SCLM melts. Conversely, more enriched OPB compositions tend to display the same problems as observed for mixing between OIB and SCLM melts.

As a consequence, although this model can plausibly reproduce the compositions of the ENA CAMP basalts it still presents some limitations.

Ternary mixing between OIB or asthenospheric melts and ultra-alkaline mafic melts (hypothesis v)

The chemical characteristics of the ENA CAMP basalts could result from ternary mixing between OIB, MORB and SCLM compositions, possibly followed by crustal assimilation (AFC or ATA). In this model the compositions for OIB, MORB and SCLM melts are the same as for the binary mixing models of hypothesis iii (parameters are given in Supplementary Data Tables A4 and A5) and the composition of the continental crust is similar to that used in the models of MORB–SCLM mixing (see parameters in Supplementary Data Tables A4 and A5). The isotopic composition of the lower NMB sub-group and Preakness group can be modeled by mixing 69% MORB, 15% OIB and 16% SCLM melt followed by approximately 4% crustal contamination (both by ATA or AFC; Fig. 21). The Hook Mt group isotopic composition can be reproduced by mixing 73% MORB, 16% OIB and 11% SCLM, followed by 8% crustal contamination (ATA or AFC). The isotopic composition of the Shelburne sub-group can be reproduced with 63% MORB, 14% OIB and 23% SCLM melt, followed by approximately 7% crustal contamination (ATA or AFC). In this model, the proportion of the MORB end-member is dominant, with very limited crustal contamination. However, this model fails to reproduce the REE and Os contents of the lower NMB sub-group (Fig. 22).

Melting of a metasomatized SCLM-type source (hypothesis vi)

In this scenario, the continental crust-like isotopic characteristics of the ENA CAMP basalts (e.g. high Sr and low Nd initial isotopic ratios; negative Nb and positive Pb anomalies) reflect the composition of the SCLM source, without the need for significant crustal assimilation. Indeed, except for one sample with high initial $^{187}Os/^{188}Os$ (CUL13: $^{187}Os/^{188}Os = 0{\cdot}1874$), all the ENA CAMP samples have initial $^{187}Os/^{188}Os < 0{\cdot}1500$, which is compatible with them being virtually uncontaminated mantle-derived magmas. As noted above, even small amounts of crustal contamination by AFC or ATA processes very rapidly drive the Os isotopic composition outside the mantle field. Considering the intensive sampling of the ENA province, in particular the lava units in the Triassic–Jurassic basins, the dataset is expected to encompass chemical and isotopic variations related to possible crustal contamination. The lack of correlations between MgO and the Nd, Os, or Pb isotopic ratios between or within the groups (Fig. 15) precludes significant assimilation of crustal rocks through an AFC process. Moreover, most of the samples with the highest MgO (8–11 wt %) and compatible trace element contents (Co = 43–53 ppm, Ni = 102–213 ppm, Cr = 358–850 ppm), display Sr, Pb and Nd isotopic compositions comparable with those of the more evolved rocks. These observations argue against extensive contamination by the continental crust by either AFC or ATA processes and favour a mantle source with a low $^{187}Os/^{188}Os$. Hence, the continental crust-like characteristics of the ENA CAMP rocks may directly reflect the characteristics of their mantle source(s). Recent studies have suggested that such contrasting chemical characteristics may be derived from a metasomatized SCLM-type source (e.g. Brauns *et al.*, 2000). Regardless of the nature of the source, the uncontaminated magmas need an initial $^{187}Os/^{188}Os$ that is lower than or similar to ~0·1276 (Fig. 7), which is the lowest value for the ENA samples. In this case, the Os isotopic composition of the source is within the range of $^{187}Os/^{188}Os$ of off-cratonic SCLM (0·1180–0·1290; Carlson, 2005).

We next consider the process that may have enriched a shallow section of the asthenospheric mantle beneath eastern North America. The mantle at present underlying this region experienced several subduction events during the Palaeozoic related to the accretion of peri-Laurentia and peri-Gondwana terranes such as Avalonia and Meguma (e.g. Van Staal *et al.*, 2009; Nance *et al*, 2010). As a consequence, this mantle may not have been refractory during the CAMP event. This suggestion is supported by evidence of several episodes of tholeiitic mafic magmatism in the Avalonia–Meguma terranes since the Late Neoproterozoic. These mafic magmas are suspected to have originated in the SCLM (Pe-Piper & Piper, 1999; Puffer, 2001, 2003; Murphy *et al.*, 2008, 2011) and show a progressive time-related decrease in their initial εNd that could reflect a progressive enrichment of their source (Murphy *et al.*, 2011). The similarities between these rocks and the ENA

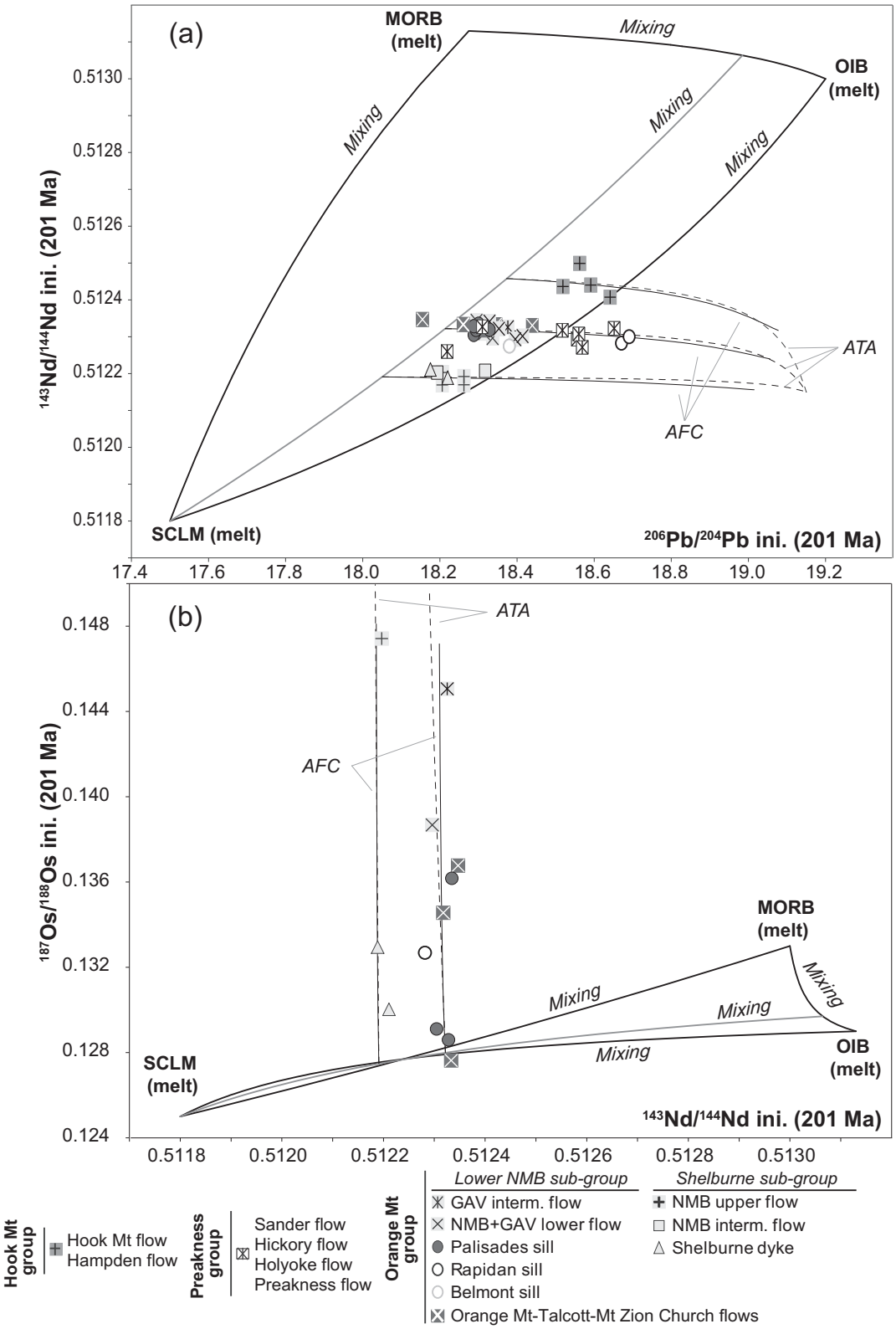

Fig. 21. Variation of (a) $^{143}Nd/^{144}Nd$ vs $^{206}Pb/^{204}Pb$ and (b) $^{143}Nd/^{144}Nd$ vs $^{187}Os/^{188}Os$ showing combined models of ternary mixing between OIB, MORB and SCLM-derived compositions followed by AFC or ATA.

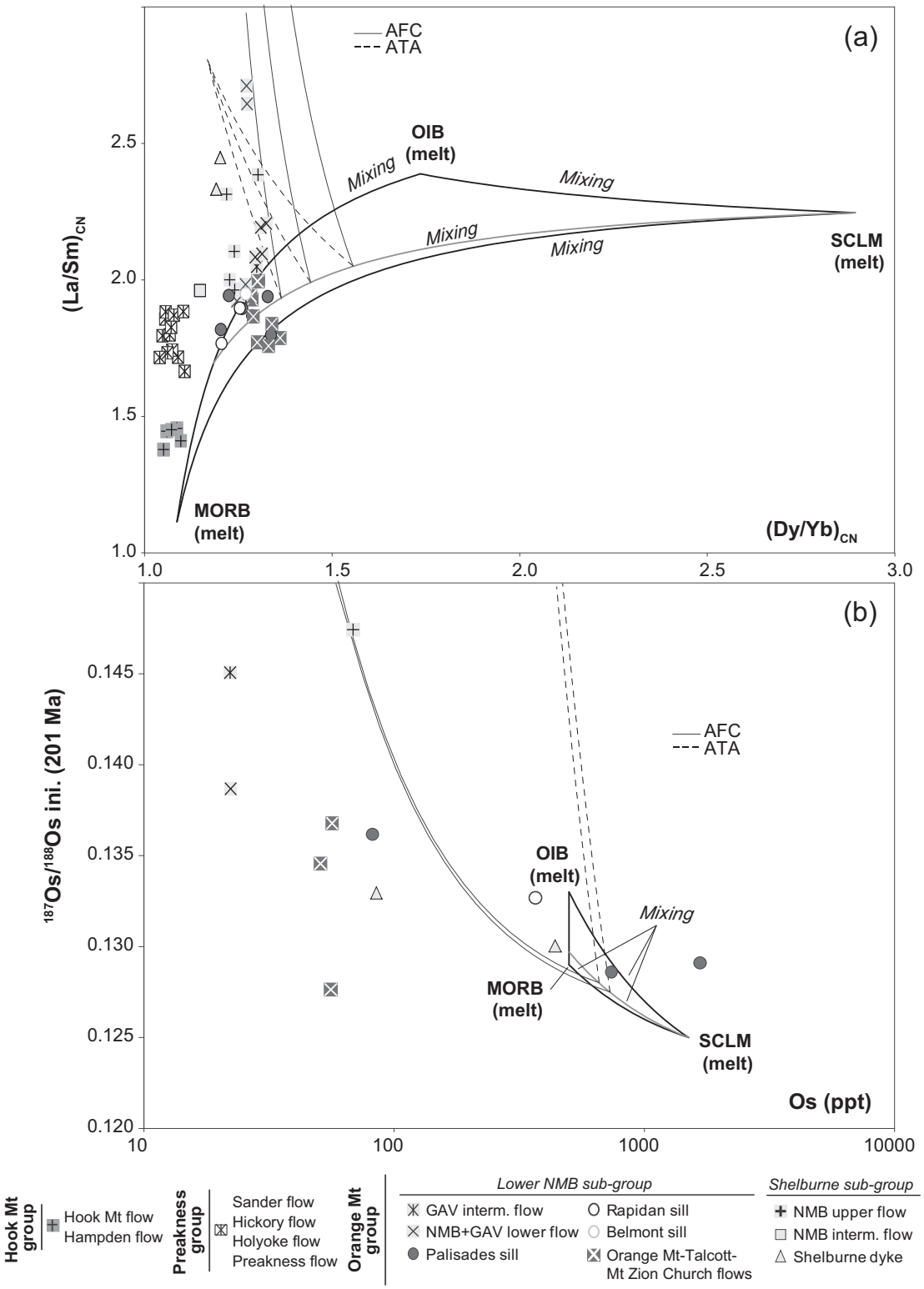

Fig. 22. Variation of (a) La/Sm_{CN} vs Dy/Yb_{CN} and (b) Os concentration vs initial $^{187}Os/^{188}Os$ showing combined models of ternary mixing between OIB, MORB and SCLM-derived compositions followed by AFC or ATA. Models use the same compositions for OIB, MORB, SCLM and continental crust as in the binary mixing models (Figs 16 and 17). All parameters are reported in Supplementary Data Tables A4 and A5.

CAMP basalts in terms of Nd–Pb isotopic compositions might suggest that the ENA basalts were derived from the same SCLM-like source, which acquired its crustal-like enrichment during episodes of Palaeozoic subduction (Puffer, 2003) when the accretion of the Avalonia–Meguma terranes to the Laurentia margin occurred.

Involvement of subduction-related sediments and fluids is suggested by the isotopic and trace element characteristics of the ENA CAMP basalts. Among the various groups, a broadly negative correlation exists between incompatible element ratios (IE), such as La/Sm and Th/Yb, and initial $^{143}Nd/^{144}Nd$ (Fig. 23). The highest incompatible element ratios and lowest initial $^{143}Nd/^{144}Nd$ are found in the Shelburne sub-group, whereas the lowest incompatible element ratios and highest $^{143}Nd/^{144}Nd$ belong to the Hook Mt group; the other Orange Mt samples and Preakness group samples plot between these groups. Increasing Th/Yb coupled with decreasing initial $^{143}Nd/^{144}Nd$ has also been documented in present-day arc-related lavas and suggests variable enrichment of the mantle source by subduction of sediments. In contrast, a decrease of initial $^{143}Nd/^{144}Nd$ at constant Th/Yb argues for enrichment through slab-derived fluids (Woodhead *et al.*, 2001). Correlations between Th/Yb and $^{143}Nd/^{144}Nd$ have been used successfully to distinguish between fluid and sediment input in the source (SCLM-like source) of the Karoo CFB (Jourdan *et al.*, 2007). Because a similar correlation is observed between initial Nd isotopic composition and La/Sm, the LREE enrichment within the ENA CAMP basalts may also be related to the progressive increase of a sedimentary contribution from the Hook Mountain group to the Shelburne sub-group. In this scenerio, the sources of the lower NMB sub-group and those of the Preakness group would have experienced similar extents of sediment input, and the variation of Th/Yb and La/Sm at constant initial $^{143}Nd/^{144}Nd$ (Fig. 23) would reflect a decreasing degree of melting from the Preakness to the Orange group. The Shelburne sub-group has a lower initial $^{143}Nd/^{144}Nd$ but similar Th/Yb to the lower NMB sub-group (Fig. 23) that suggests source enrichment by an increasing fluid contribution from the latter towards the former.

An alternative source model for the CAMP magmas

As demonstrated above, crustal contamination by AFC or ATA processes of typical mantle-derived magmas (MORB, OIB, OPB) is very unlikely to produce the geochemical characteristics of the ENA CAMP basalts. Mixing of such magmas (particularly MORB or OPB) with lithosphere-derived melts, possibly followed by limited amounts of crustal contamination, is somewhat more successful, but nevertheless does not produce fully satisfactory results, assuming probable end-member compositions. We therefore examine the alternative possibility that the ENA CAMP basalts were derived from a mantle source enriched in incompatible elements, more specifically, an SCLM-like source that has been metasomatized by subduction-related processes. This suggestion is supported by the fact that the ENA region underwent successive episodes of subduction during the Paleozoic Era. The presumably highly refractory nature of the lithospheric mantle has been used to argue that this reservoir could not produce massive volumes of basaltic volcanism (Arndt *et al.*, 1993). However, significant metasomatic enrichment events, such as earlier subduction, may facilitate melting of the SCLM (e.g. Gallagher & Hawkesworth, 1992). Several geochemical studies of CFBs, including the CAMP (Pegram, 1990; Puffer, 2001, 2003; De Min *et al.*, 2003; Deckart *et al.*, 2005; Merle *et al.*, 2011; Murphy *et al.*, 2011) have suggested a dominant contribution from a mantle source with geochemical characteristics similar to metasomatized SCLM. An alternative source might be the so-called 'Perisphere', which has been defined as the less refractory, enriched and hydrated uppermost part of the asthenosphere that is isolated from the convecting mantle under the continents and which may share the chemical characteristics of the SCLM (Anderson, 1994).

To determine whether such a mantle source would be able to produce the ENA CAMP basalts we modelled the geochemical effects of long-lasting subduction on the sub-arc mantle, assuming a starting composition similar to that of the depleted asthenosphere.

Modelling the effects of subduction-related metasomatism on a section of sub-arc mantle

Geodynamic reconstructions suggest that the Avalonia–Meguma terranes were rifted away from the Gondwana margin and accreted to the Laurentia margin during a complex succession of subduction episodes. However, there is no general consensus for the timing of these events. Nevertheless, the most recent studies suggest that the Avalonia–Meguma terranes were separated from Gondwana and accreted to Laurentia during one or several events from *c.* 540 until *c.* 370 Ma (e.g. Puffer, 2003; Van Staal *et al.*, 2009; Nance *et al.*, 2010). This suggests that the asthenospheric (DMM-like) sub-arc mantle underneath the terranes underwent progressive enrichment owing to continuous injection of sediments, melts and fluids between 540 Ma and 370 Ma. At *c.* 370 Ma, the continental collision between Gondwana and Laurentia occurred with cessation of subduction and isolation of the former sub-arc mantle from more injection of material (e.g. Murphy *et al.*, 2006; Van Staal *et al.*, 2009). Considering these geodynamic reconstructions, we infer that the source of the ENA CAMP basalts was originally MORB-source depleted mantle (DMM) into which subduction-derived melts or fluids were continuously injected between 540 and 370 Ma. This metasomatized mantle-wedge was then isolated from further sedimentary input

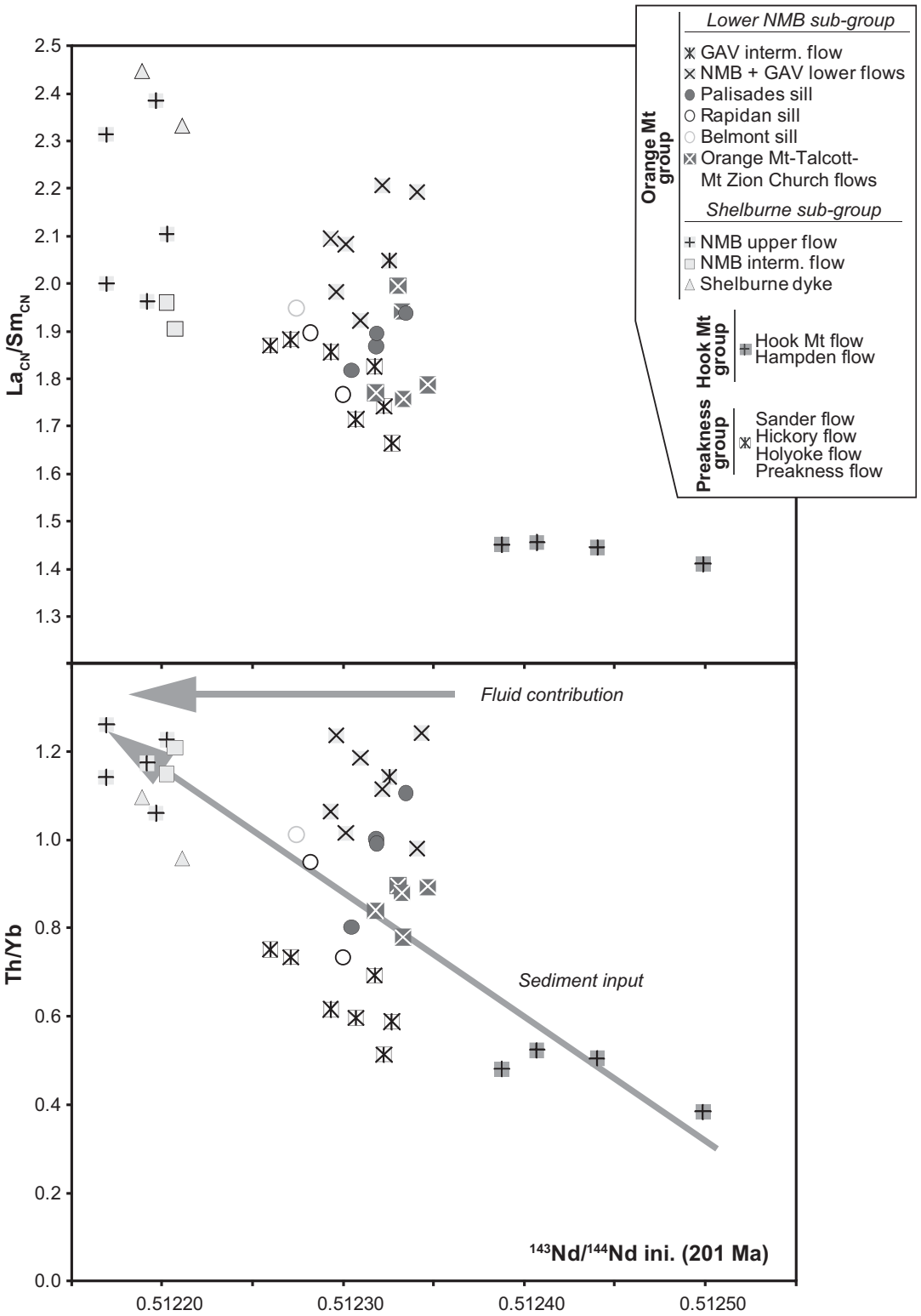

Fig. 23. Variation of La/Sm$_N$ and Th/Yb vs ^{143}Nd/^{144}Nd initial (at 201 Ma). The trends (grey arrows) represent sediment input and slab-derived fluid contribution as discussed by Woodhead *et al.* (2001). The Nd isotopic data have been back-calculated to 201 Ma.

from 370 Ma until 201 Ma when the CAMP event occurred; during this period the evolution of the Sr–Nd–Pb–Os isotopic ratios would be due to only radioactive decay.

Based on these considerations, we designed a mathematical mantle evolution model to evaluate the time-dependent change of the Nd–Pb–Os isotopic composition of this mantle region. The model assumes a period of 170 Myr (540–370 Ma) during which sediments were progressively incorporated into the depleted mantle wedge through a mixing process (open-system behaviour). In terms of the evolution of the isotopic composition during this period, the effects of sediment addition must be integrated with the effects of radioactive decay. The period of open-system behaviour was followed by a period of *c.* 170 Myr (370–201 Ma) of closed-system behaviour during which the isotopic composition of the sediment-contaminated mantle was modified only by radioactive decay. The open-system period model is approximated by a mass-balanced flux box model. The mathematical development of the model is presented in the Supplementary Material.

For the open-system period, we start with a sub-arc mantle with a composition close to the average value of the present-day DMM (see parameters in Supplementary Data Table A5). The Nd–Pb–Os isotopic composition of this mantle is back-calculated to the period between 540 and 370 Ma in increments of 10 Ma. The composition of the subducted sediment is considered to be equivalent to the present-day local continental crust (see parameters in Supplementary Data Table A5) and its Nd–Pb–Os isotopic composition is also back-calculated to the period between 540 and 370 Ma, again in increments of 10 Ma. All the Pb isotopic compositions of the sediments involved in the modelling are in the range of the values of the upper continental crust and close to those for mature arc sediments (Zartman & Doe, 1981), which are expected for a subduction system lasting 170 Myr.

The equations translating the evolution of the isotopic composition resemble the classic binary mixing equation, but the mixing parameter F is a function of time, sediment input rate, and the ratio of the number of moles per unit volume of the non-radiogenic isotope of a given element in the depleted mantle and the sediments at 540 Ma (see details in Supplementary Material). The calculated percentages of sediment represent the mass of sediment accumulated over a period of 170 Myr in a given volume of depleted mantle. We stress that the mantle segments into which sediments have been incorporated are also those that are most likely to melt (e.g. Merle *et al.*, 2011).

According to the model, the Nd–Pb–Os isotopic composition of the Hook Mountain group can be reproduced by incorporating into the depleted mantle ~3% sediment with a composition identical to that of the present-day Avalonian Neoproterozoic felsic crust (Figs 24 and 25). The isotopic composition of the Preakness group and the Rapidan sill can be modelled by incorporating 5% of two slightly different sediment components derived from the Avalonian Neoproterozoic felsic crust close to that involved in the source of the Hook Mt group (see Supplementary Data Table A5). The lower NMB sub-group can be modelled by incorporating 5% sediment, which would have a present-day composition equivalent to the Meguma terrane felsic rocks. The isotopic composition of the Shelburne sub-group can be modelled by incorporating 10% sediment with a present-day composition slightly different from that involved in the lower NMB sub-group, yet still within the range of the Meguma terrane rocks. The contaminant incorporated in the Shelburne sub-group source has a lower $^{143}Nd/^{144}Nd$ ratio and Nd content than that which influenced the lower NMB sub-group, perhaps reflecting the involvement of fluids or more hydrated sediments in the source of the Shelburne sub-group.

It is worth noting that the percentages of sediment calculated for the source of the ENA CAMP basalts are not too different from those assumed for recycled sediments in EMII-type OIB (e.g. 3–8% in Samoa–Society; Eiler *et al.*, 1997) or continental arc lavas (2–6%; Plank, 2005). In the case of the source of the ENA CAMP basalts, the percentage of sediment input is related to a specific section of depleted mantle. These percentages are not inconsistent with the production of basaltic magmas.

As stated above, all of the reliable (uncertainty <10%) initial $^{187}Os/^{188}Os$ ratios but one (CUL13) are less than 0·1500 and were obtained only for the Orange Mt group (see Fig. 24). Nevertheless, the percentage range of sediment input in the sources of the different groups would be unable to produce very large variations of the initial $^{187}Os/^{188}Os$ ratio (Fig. 24). As has been often shown (e.g. Chesley *et al.*, 2004), the low Os concentrations of most sediments are unable to substantially modify the $^{187}Os/^{188}Os$ ratios of mantle peridotites, which typically have high Os concentrations. The differences in initial Os isotopic composition observed between samples of the Orange Mt group could reflect heterogeneity of the mantle source rocks prior to sediment incorporation and variations of the Os concentration and/or isotopic composition of the incorporated sediments. In particular, sediments rich in ancient mafic material or black shales could add non-negligible amounts of radiogenic Os. Because most of the ENA CAMP basalts have low Os concentrations, very small amounts (2–3%) of shallow contamination by the upper continental crust could also lead to minor variation of the $^{187}Os/^{188}Os$ ratio (Merle *et al.*, 2011) without significantly affecting the other isotope systems. Minor shallow contamination could, in particular, explain the high initial $^{187}Os/^{188}Os$ ratio of sample CUL13, given the very low Os concentration of this sample.

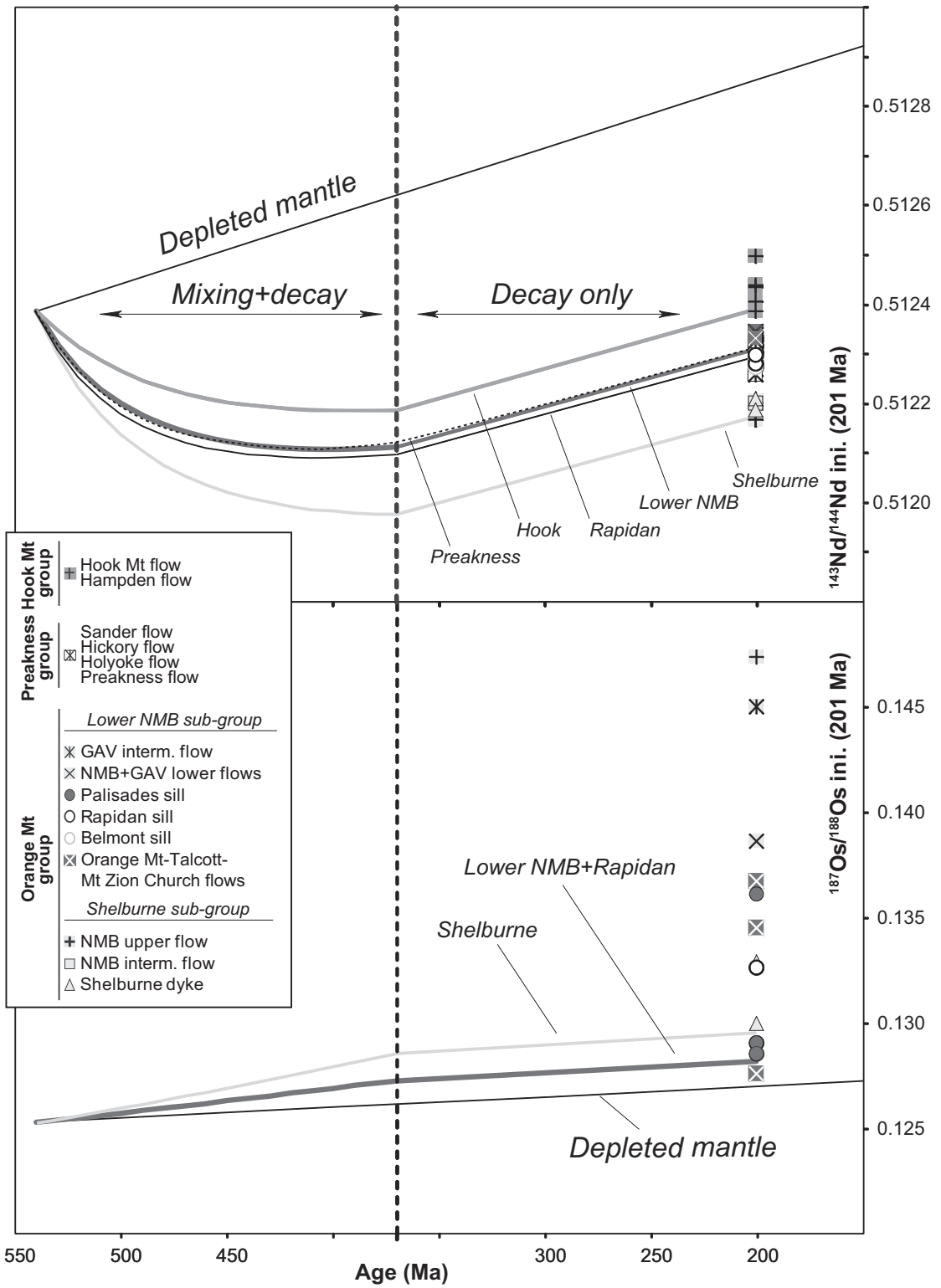

Fig. 24. Time evolution of $^{143}Nd/^{144}Nd$ and $^{187}Os/^{188}Os$ for an asthenospheric sub-arc mantle wedge undergoing continuous input of subducted sediment over 170 Myr (open-system behaviour) and evolving by isotopic decay (closed-system behaviour) during the following 170 Myr until the CAMP magmatic event. Model details are given in the text and in the Supplementary Material.

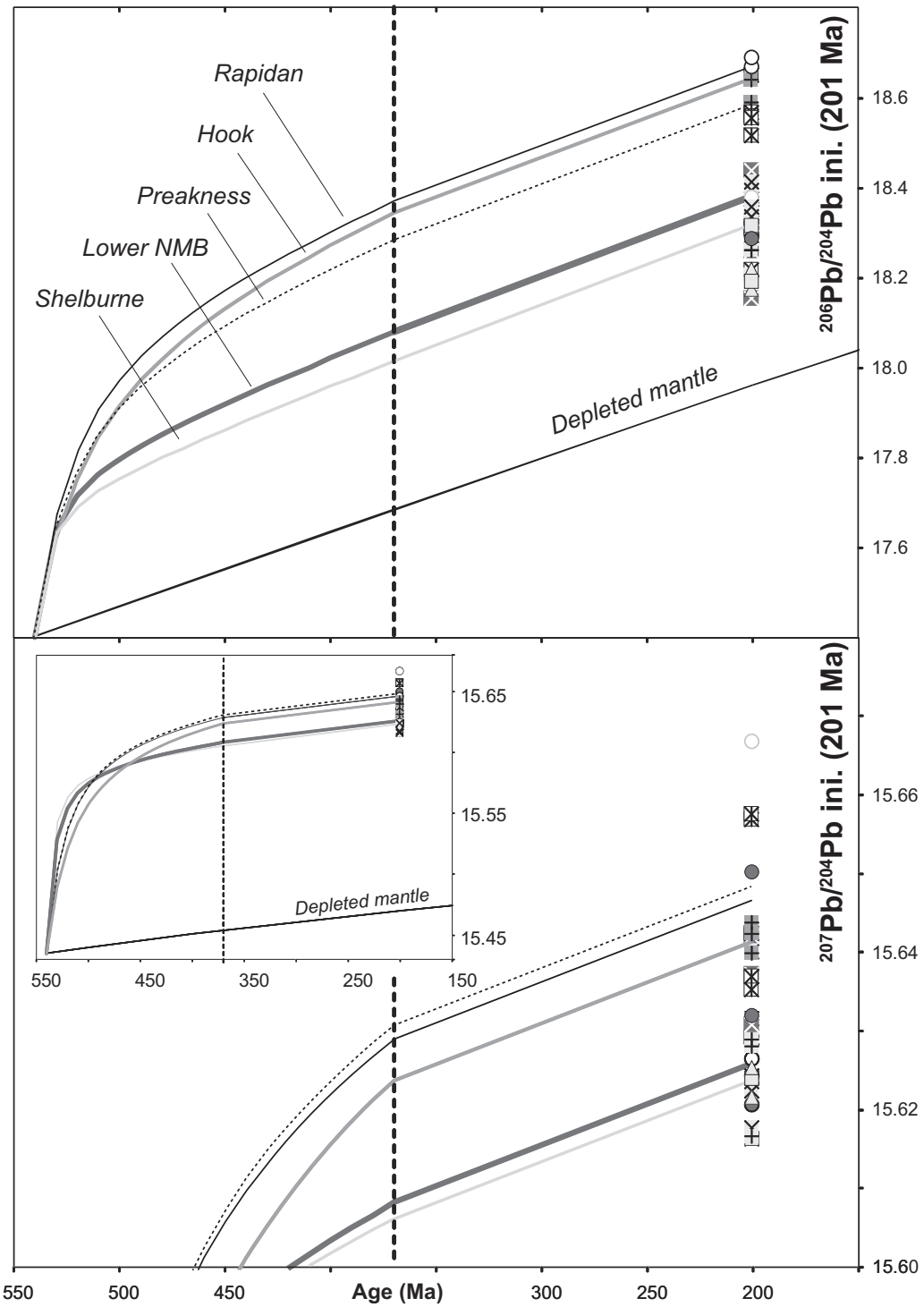

Fig. 25. Time evolution of $^{206}Pb/^{204}Pb$ and $^{207}Pb/^{204}Pb$ for an asthenospheric sub-arc mantle wedge undergoing continuous input of subducted sediment over 170 Myr (open-system behaviour) and evolving by isotopic decay (closed-system behaviour) during the following 170 Myr until the CAMP magmatic event. The symbols representing the ENA CAMP basalts are identical to those of Fig. 24. Model details are given in the text and in the Supplementary Material.

Consequences for the CAMP

According to our model, the isotope composition of the CAMP basalts might originate from progressive incorporation of subducted sediments derived from the local continental crust into a depleted sub-arc mantle wedge above a subduction zone. The age and duration of the enrichment process during subduction (open-system phase), as well as the duration of the subsequent isolation (radioactive decay phase), might vary throughout the CAMP province. For instance, by changing these parameters in the model in a manner consistent with the geological constraints from the Maranhão basin in Brazil (subduction between 660 and 575 Ma then isolation phase until 201 Ma), the isotopic characteristics of the Brazilian CAMP basalts can be modelled assuming the same starting mantle composition as the ENA CAMP basalts. As the isotopic composition of the local Brazilian crust is not well constrained [for details about the geological setting of the Maranhão basin see Merle *et al.* (2011)], we assumed the present-day composition of mature-arc sediments ($^{143}Nd/^{144}Nd = 0{\cdot}51185$, $^{206}Pb/^{204}Pb = 18{\cdot}520$, $^{207}Pb/^{204}Pb = 15{\cdot}640$, $^{208}Pb/^{204}Pb = 38{\cdot}75$, $^{187}Os/^{188}Os = 2$, Nd = 38 ppm, Pb = 12 ppm, Os = 50 ppt; Ben Othman *et al.*, 1989; Esser & Turekian, 1993; Fig. 26).

It should be noted that the isotopic characteristics of the CAMP basalts in the Maranhão basin are similar to those of the majority of the CAMP basalts including those from ENA. As a consequence, this model can be applied to all of the CAMP sub-provinces studied to date and is probably able to yield the isotopic compositions of the CAMP basalts in any given area using the same parameters as for the Maranhão CAMP basalts. Nevertheless, such modelling may be more accurate and geologically meaningful by applying the correct geodynamic constraints (duration of the subduction, length of isolation after continental collision for a specific area) and composition of the local crust as a proxy for the subducted sediments.

Both the modalities of sediment incorporation into the sub-arc mantle and the fate of the modified mantle wedge after collision stops subduction are currently highly speculative. However, this mantle segment could have been incorporated into the lithosphere and might form an enriched portion of the SCLM. Alternatively, it could have remained on top of the depleted asthenosphere as an enriched layer (i.e. Perisphere). In either case this mantle would probably have been hydrated and would include very fusible portions that could melt in response to an increase in the ambient temperature (e.g. Coltice *et al.*, 2007, 2009).

The case of CUL13

Samples CUL13 and CUL25 plot away from the other Preakness group samples yet close to those of the Orange

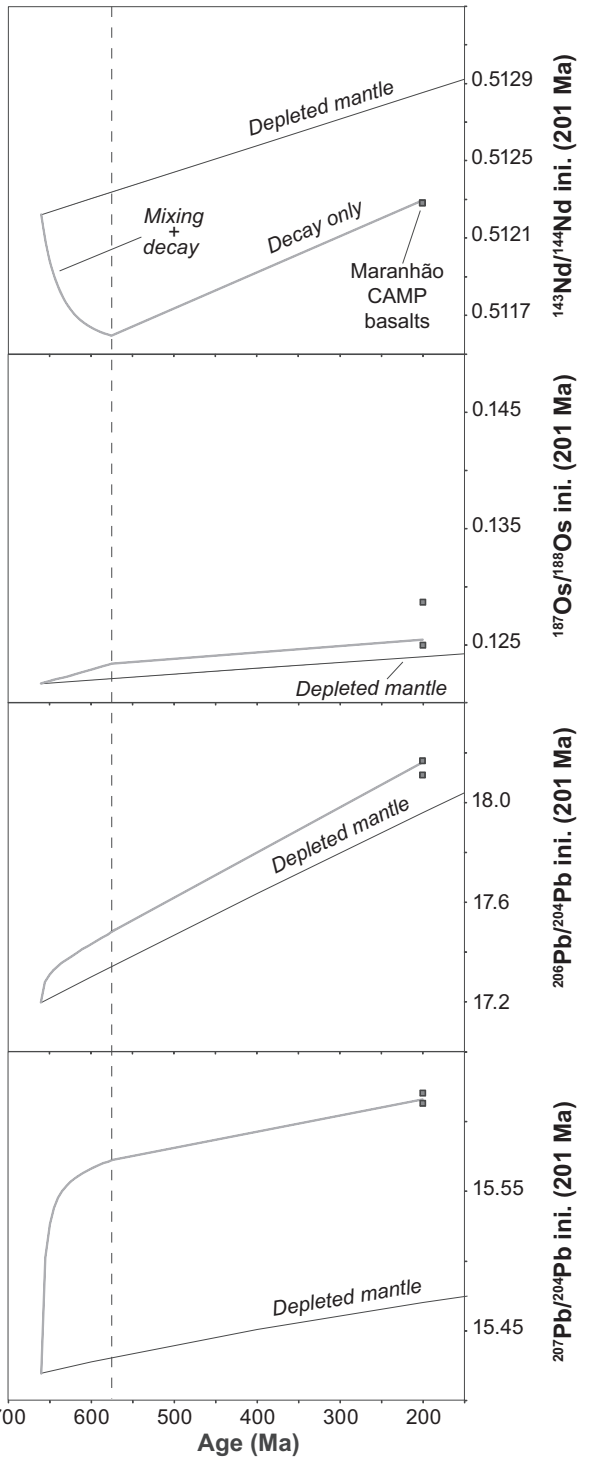

Fig. 26. Modelling of the source of the CAMP basalts in the Maranhão basin, showing the time evolution of $^{143}Nd/^{144}Nd$, $^{187}Os/^{188}Os$, $^{206}Pb/^{204}Pb$ and $^{207}Pb/^{204}Pb$ for an asthenospheric sub-arc mantle wedge undergoing continuous input of subducted sediment from 660 Ma until 575 Ma (open-system behaviour) and evolving by isotopic decay (closed-system behaviour) until the CAMP magmatic event. Data for CAMP Maranhão basalts are from Merle *et al.* (2011).

Mt in the Pb–Pb and initial $^{206}Pb/^{204}Pb$ vs initial $^{143}Nd/^{144}Nd$ diagrams (Figs 7 and 10). In contrast to sample CUL25, CUL13 has a reliable high initial Os ratio ($^{187}Os/^{188}Os = 0{\cdot}1874 \pm 0{\cdot}0123$) and low Os content ([Os] = 14·4 ppt), which may be accounted for by shallow-level contamination by the upper continental crust. We assume that the other samples of the Preakness group represent uncontaminated or very slightly contaminated magmas, based on the previous discussion. None of these samples are primitive and considering that the contamination occurred in the upper crust, we consider the least evolved of the Preakness group basalts (the Buttress dyke sample HB102) as the parental magma composition. We also assumed an isotopic composition of $^{187}Os/^{188}Os = 0{\cdot}1282$ for the uncontaminated magma, which is that calculated at 201 Ma by our sediment-enriched mantle model for the Preakness group. Based on these parameters, we modelled the $^{143}Nd/^{144}Nd$ and $^{206}Pb/^{204}Pb$ initial ratios of sample CUL13 through an AFC process (Fig. 14). The modelling failed to reach the isotopic composition of CUL13 using a contaminant composition similar to that of the felsic rocks of the Meguma terrane. However, the composition of CUL13 can be reached through an AFC process by involving *c.* 10% of a contaminant with an isotopic and IE composition close to that of Devonian plutonic rocks in New Hampshire and Western Maine (Tomascak *et al.*, 2005). This modelling may also explain the slight variation in the isotopic compositions observed within the Preakness group samples, as outlined above, by less than 4% of shallow contamination by the local crust. The isotopic composition of sample CUL25 can be explained by more than 10% contaminant (Fig. 27).

Further remarks about the CAMP

Many features of the CAMP suggest that it might be different from other LIPs and that the common models for LIP generation may not be applicable. Indeed, the tectonic context of the CAMP is difficult to reconcile with the classic mantle plume hypothesis (e.g. Campbell, 2007). CAMP lacks geological evidence (e.g. hotspot track with decreasing age toward an active volcano, radiating dyke pattern, lithospheric uplift preceding basalt eruption, high-temperature melts such as picrites and ultramafic and ultra-alkaline liquids) for the involvement of a mantle plume (McHone, 2000; Coltice *et al.*, 2009). Moreover, the mantle potential temperatures calculated for CAMP are substantially lower than those calculated for the Deccan or Siberian Traps (Herzberg & Gazel, 2009).

In terms of chemistry, the CAMP basalts are also distinct from other LIP basalts. Whereas several LIPs such as Parana–Etendeka, North Atlantic or Deccan have experienced crustal contamination by ATA (Devey & Cox, 1987; Kerr *et al.*, 1995*a*; Peate & Hawkesworth, 1996), this process probably did not significantly affect the CAMP basalts. The large majority of the CAMP basalts show rather homogeneous REE contents at the scale of the whole province. Indeed, they have flat HREE patterns, which have been modelled as resulting from the melting of a spinel-bearing source (e.g. Bellieni *et al.*, 1990; Jourdan *et al.*, 2003; Verati *et al.*, 2005) and are thus indicative of a shallow melting zone. However, plume models predict that as the plume head impinges on the base of the lithosphere the initial average depth of melting is relatively deep but decreases as the degree of melting increases (White & McKenzie, 1995). This should produce compositional trends that are inconsistent with the homogeneity of the CAMP basalts (Salters *et al.*, 2003).

The high abundance of evolved basalts and the lack of picritic rocks might be related to the composition of the mantle source. Indeed, during subduction recycled crustal material might form garnet-pyroxenitic veins or layers in the shallow mantle. Melts of these garnet-pyroxenites may react with the ambient depleted mantle to produce fertile spinel lherzolite that has a lower MgO content than average lherzolite and retains the signature of recycled crustal material (Marchesi *et al.*, 2013).

Although metasomatic or refertilization processes may promote melting of the SCLM or the perisphere by lowering the solidus, a source of heat is still needed to initiate magma generation. Physical models suggest that large-scale mantle warming under supercontinents such as Pangaea, resulting from accumulation of internal heat beneath the insulating lithosphere, an lead to an increase in temperature of up to 100°C that might be sufficient to melt metasomatized SCLM (Coltice *et al.*, 2007, 2009). However, the timescales of melting of the SCLM by heat conduction from the underlying convecting mantle may be far too long to be consistent with the rapid timescales of eruption of CFB-type magmas (Gibson *et al.*, 2006). As a consequence, the involvement of one or more deep-rooted mantle plumes as heat suppliers cannot be ruled out, and may contribute to the melting of an SCLM source.

CONCLUSIONS

New data for the ENA CAMP sills, dykes, and lava flows define three groups (Orange Mt, Preakness and Hook Mt groups) based on the stratigraphy and chemistry of the units. Geochemical and Sr–Nd–Pb–Os isotopic data for selected samples allow the following conclusions to be reached.

(1) The continental crust-like characteristics of the CAMP basalts probably do not result from extensive contamination by the upper continental crust of plume-derived or other asthenospheric melts. Furthermore, derivation from a plume source with an unusual isotopic composition is also unlikely.
(2) Numerical modelling shows that mixing between two enriched melts, such as OIB-type and SCLM-related

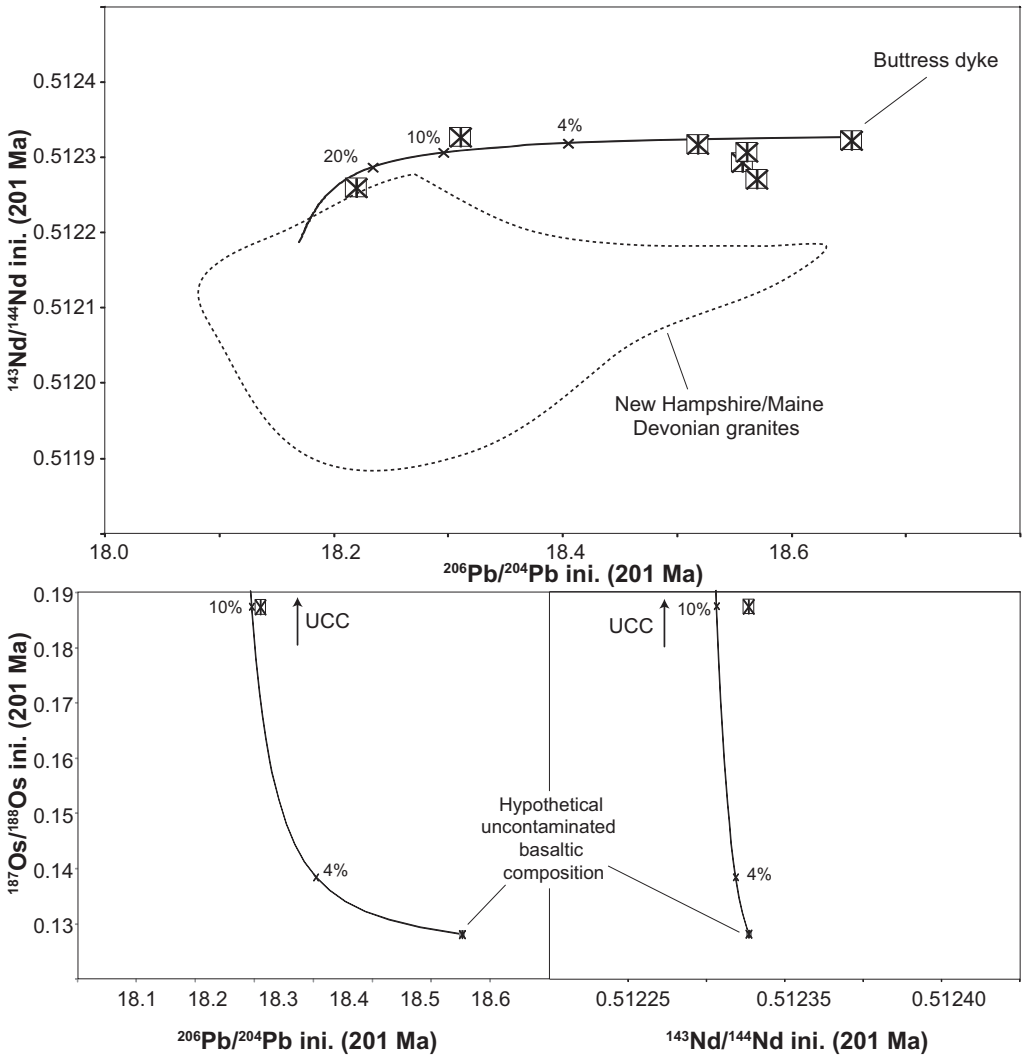

Fig. 27. AFC modelling of the composition of the Preakness samples. Uncontaminated basaltic magma composition: [Nd] = 9 ppm, [Pb] = 2 ppm, [Os] = 300 ppt, $^{143}Nd/^{144}Nd = 0{\cdot}512327$, $^{187}Os/^{188}Os = 0{\cdot}1282$, $^{206}Pb/^{204}Pb = 18{\cdot}65$; continental crust contaminant: [Nd] = 5 ppm, [Pb] = 49 ppm, [Os] = 31 ppt, $^{143}Nd/^{144}Nd = 0{\cdot}51195$, $^{187}Os/^{188}Os = 1{\cdot}7$, $^{206}Pb/^{204}Pb = 18{\cdot}16$ (Esser & Turekian, 1993; Tomascak *et al.*, 2005). AFC parameters: $K_D(Nd) = 0{\cdot}25$, $K_D(Pb) = 0{\cdot}5$, $K_D(Os) = 8{\cdot}5$, $r = 0{\cdot}4$. (See text for details.)

melts (ultra-alkaline–ultramafic liquids), possibly followed by limited contamination by the upper continental crust, is unlikely to produce the composition of the ENA CAMP basalts.

(3) The mixing of MORB-like or OPB-like magmas with melts derived from the SCLM is more plausible; however, the REE contents of the ENA CAMP basalts require extreme compositions of such SCLM-derived melts and up to 30% assimilation of upper continental crust, which is rather unrealistic.

(4) Our numerical model shows that incorporation of subducted sediments into an asthenospheric mantle wedge during episodes of Paleozoic subduction can reconcile the paradoxical coexistence of continental crust-like isotopic and trace element signatures (i.e. high $^{87}Sr/^{86}Sr$, high $^{207}Pb/^{204}Pb$ for moderate $^{206}Pb/^{204}Pb$, low $^{143}Nd/^{144}Nd$, higher LILE contents than MORB, specific Nb and Pb anomalies) with low, SCLM-like, $^{187}Os/^{188}Os$ ratios. The small range of initial $^{187}Os/^{188}Os$ (0·128–0·15) observed in the ENA CAMP basalts could reflect initial heterogeneity in the asthenospheric mantle, variations in the nature and/or the amount of subducted sediment incorporated, and a limited amount of shallow contamination by the local crust.

ACKNOWLEDGEMENTS

Angelo De Min, Robert Weems, Larry Tanner, Simonetta Cirilli and Paolo Podestà, as well as Paul Olsen,

participated in the field trip to the ENA CAMP and they are all thanked for their contributions. Sampling of the drill hole that penetrated the North Mountain Basalt was made possible by the Nova Scotia Department of Natural Resources and the Department of Geology, Acadia University, Wolfville, Nova Scotia. Finally, we thank C. Zimmerman, C. Keller, C. Douchet and P. Capiez for their capable laboratory assistance. Drs A. Kerr, B. Murphy and two anonymous reviewers are thanked for their comments on the earlier versions of this paper. J. Gamble is thanked for editorial handling of this paper.

FUNDING

Financial assistance for the project came from grants CARIPARO 2008 and PRIN-2008 (to A.M.) and from the GDR Marges CNRS-INSU program (to H.B.).

SUPPLEMENTARY DATA

Supplementary data for this paper are available at *Journal of Petrology* online.

REFERENCES

Aitcheson, S. J. & Forrest, A. H. (1994). Quantification of crustal contamination in open magmatic systems. *Journal of Petrology* **35**, 461–488.

Alibert, C. (1985). A Sr–Nd isotope and REE study of late Triassic dolerites from the Pyrenées (France) and the Messejana dyke (Spain and Portugal). *Earth and Planetary Science Letters* **73**, 81–90.

Allègre, C. J., Treuil, M., Minster, J. F., Minster, B. & Albarède, F. (1977). Systematic use of trace elements in igneous processes: part I. Fractional crystallisation processes in volcanic suites. *Contributions to Mineralogy and Petrology* **60**, 57–75.

Anderson, D. L. (1994). The sublithospheric mantle as the source of subcontinental flood basalts; the case against the continental lithosphere and plume head reservoir. *Earth and Planetary Science Letters* **123**, 269–280.

Arndt, N. & Christensen, U. (1992). The role of lithospheric mantle in continental flood volcanism; thermal and geochemical constraints. *Journal of Geophysical Research* **97**, 10967–10981.

Arndt, N. T. & Goldstein, S. L. (1987). Use and abuse of crust formation ages. *Geology* **15**, 893–895.

Arndt, N. T., Czamanske, G. K., Wooden, J. L. & Fedorenko, V. A. (1993). Mantle and crustal contributions to continental flood volcanism. *Tectonophysics* **223**, 39–52.

Ayuso, R. A. & Bevier, M. L. (1991). Regional differences in Pb isotopic compositions of feldspars in plutonic rocks of the northern Appalachian Mountains, USA, Canada: A geochemical method of terrane correlation. *Tectonics* **10**, 191–212.

Barr, S. M. & Hegner, E. (1992). Nd isotopic compositions of felsic igneous rocks in Cape Breton Island, Nova Scotia. *Canadian Journal of Earth Sciences* **29**, 650–657.

Bellieni, G., Picirillo, E. M., Cavazzini, G., Petrini, R., Comin-Chiaramonti, P., Nardy, A. J. R., Civetta, L., Melfi, A. J. & Zantedeschi, P. (1990). Low- and high TiO_2, Mesozoic tholeiitic magmatism of the Maranhão basin (NE Brazil): K–Ar age, geochemistry, petrology, isotope characteristics and relationships with Mesozoic low- and high-TiO_2 flood basalts of the Paraná Basin (SE Brazil). *Neues Jahrbuch für Mineralogie, Abhandlungen* **162**, 1–33.

Ben Othman, D., White, W. M. & Patchett, J. (1989). The geochemistry of marine sediments, island arc magma genesis, and crust–mantle recycling. *Earth and Planetary Science Letters* **94**, doi: 10.1016/0012-821X(89)90079-4.

Bertrand, H. (1991). The Mesozoic Tholeiitic Province of Northwest Africa: a volcano-tectonic record of the early opening of Central Atlantic. In: Kampunzu, A. B. & Lubala, R. T. (eds) *Magmatism in Extensional Structural Settings. The Phanerozoic African Plate.* Springer, pp. 147–188.

Bertrand, H., Dostal, J. & Dupuy, C. (1982). Geochemistry of early Mesozoic tholeiites from Morocco. *Earth and Planetary Science Letters* **58**, 225–239.

Brauns, C. M., Hergt, J. M., Woodhead, J. D. & Maas, R. (2000). Os isotopes and the origin of the Tasmanian dolerites. *Journal of Petrology* **41**, 905–918.

Campbell, I. H. (2007). Testing the plume thoery. *Chemical Geology* **241**, 153–176.

Carlson, R. W. (1991). Physical and chemical evidence on the cause and source characteristics of flood basalt volcanism. *Australian Journal of Earth Sciences* **38**, 525–544.

Carlson, R. W. (2005). Application of the Pt–Re–Os isotopic systems to mantle geochemistry and geochronology. *Lithos* **82**, 249–272.

Cebria, J. M., Lopez-Ruiz, J., Doblas, M., Martins, L. T. & Munha, J. (2003). Geochemistry of the Early Jurassic Messejana–Plasencia dyke (Portugal–Spain); implications on the origin of the Central Atlantic Magmatic Province. *Journal of Petrology* **44**, 547–568.

Chesley, J., Righter, K. & Ruiz, J. (2004). Large-scale mantle metasomatism: a Re–Os perspective. *Earth and Planetary Science Letters* **219**, 49–60.

Cirilli, S., Marzoli, A., Tanner, L., Bertrand, H., Buratti, N., Jourdan, F., Bellieni, G., Kontak, D. & Renne, P. R. (2009). Latest Triassic onset of the Central Atlantic magmatic province (CAMP) volcanism in the Fundy basin (Nova Scotia): new stratigraphic constraints. *Earth and Planetary Science Letters* **286**, 514–525.

Coltice, N., Phillips, B. R., Bertrand, H., Ricard, Y. & Rey, P. (2007). Global warming of the mantle at the origin of flood basalts over supercontinents. *Geology* **35**, 391–394.

Coltice, N., Bertrand, H., Rey, P., Jourdan, F., Philipps, B. R. & Ricard, Y. (2009). Global warming of the mantle beneath continents back to the Archean. *Gondwana Research* **15**, 254–266.

Courtillot, V., Jaupart, C., Manighetti, I., Tapponnier, P. & Besse, J. (1999). On causal links between flood basalts and continental breakup. *Earth and Planetary Science Letters* **166**, 177–195.

Currie, K. L., Whalen, J. B., Davis, W. J., Longstaffe, F. J. & Cousens, B. L. (1998). Geochemical evolution of peraluminous plutons in southern Nova Scotia, Canada—a pegmatite-poor suite. *Lithos* **44**, 117–140.

Deckart, K., Féraud, G. & Bertrand, H. (1997). Age of Jurassic continental tholeiites of French Guyana, Surinam and Guinea: implications for the initial opening of the Central Atlantic Ocean. *Earth and Planetary Science Letters* **150**, 205–220.

Deckart, K., Bertrand, H. & Liegeois, J.-P. (2005). Geochemistry and Sr, Nd, Pb isotopic composition of the Central Atlantic Magmatic Province (CAMP) in Guyana and Guinea. *Lithos* **82**, 289–314.

De Min, A., Piccirillo, E. M., Marzoli, A., Bellieni, G., Renne, P. R., Ernesto, M. & Marques, L. (2003). The Central Atlantic Magmatic Province (CAMP) in Brazil: Petrology, Geochemistry, $^{40}Ar/^{39}Ar$ ages, paleomagnetism and geodynamic implications. In: Hames, W. E., McHone, J. G., Renne, P. R. & Ruppel, C. (eds) *The Central Atlantic Magmatic Province: Insights from Fragments of*

Pangea. Geophysical Monograph, American Geophysical Union **136**, 209–226.

DePaolo, D. J. (1981). Trace element and isotopic effects of combined wall rock assimilation and fractional crystallization. *Earth and Planetary Science Letters* **53**, 189–202.

Devey, C. W. & Cox, K. G. (1987). Relationships between crustal contamination and crystallisation in continental flood basalt magmas with special reference to the Deccan Traps of the Western Ghats, India. *Earth and Planetary Science Letters* **84**, 59–68.

Dorais, M. J. & Tubrett, M. (2008). Identification of a subduction zone component in the Higganum dyke, Central Atlantic Magmatic province: a LA-ICP-MS study of clinopyroxenes with implication for flood basalt petrogenesis. *Geochemistry, Geophysics, Geosystems* **9**, doi:10.1029/2008GC002079.

Dostal, J. & Dupuy, C. (1984). Geochemistry of the North Mountain Basalts (Nova Scotia, Canada). *Chemical Geology* **45**, 245–261.

Dostal, J. & Durning, M. (1998). Geochemical constraints on the origin and evolution of early Mesozoic dykes in Atlantic Canada. *European Journal of Mineralogy* **10**, 79–93.

Dostal, J. & Greenough, J. D. (1992). Geochemistry and petrogenesis of the early Mesozoic North Mountain basalts of Nova Scotia, Canada. In: Puffer, J. H. & Ragland, P. C. (eds) *Eastern North American Mesozoic Magmatism. Geological Society of America, Special Papers* **268**, 149–159.

Drake, A. A., Jr, Sinha, A. K., Laird, J. & Guy, R. E. (1989). The Taconic orogen. In: Hatcher, R. D., Jr, Thomas, W. A. & Viele, G. W. (eds) *The Appalachian–Ouachita Orogen in the United States. Geological Society of America, The Geology of North America* **F-2**, 101–177.

Dupuy, C., Marsh, J., Dostal, J., Michard, A. & Testa, S. (1988). Asthenospheric and lithospheric sources for Mesozoic dolerites from Liberia (Africa): trace element and isotopic evidence. *Earth and Planetary Science Letters* **87**, 100–110.

Eiler, J. M., Farley, K. A., Valley, J. W., Hauri, E., Craig, H., Hart, S. R. & Stolper, E. (1997). Oxygen isotope variations in ocean island basalt phenocrysts. *Geochimica et Cosmochimica Acta* **61**, 2281–2293.

Ernst, R. E. & Buchan, K. L. (2002). Maximum size and distribution in time and space of mantle plumes: evidence from large igneous provinces. *Journal of Geodynamics* **31**, 309–342.

Esser, B. K. & Turekian, K. K. (1993). The osmium isotopic composition of the continental crust. *Geochimica et Cosmochimica Acta* **57**, 3093–3104.

Fowell, S. J. & Olsen, P. E. (1993). Time calibration of Triassic–Jurassic microfloral turnover, eastern North America. *Tectonophysics* **222**, 361–369.

Gallagher, K. & Hawkesworth, C. (1992). Dehydration melting and generation of continental flood basalts. *Nature* **358**, 57–59.

Gibson, S. A., Thompson, R. N., Leonardos, O. H., Dickin, A. P. & Mitchell, J. G. (1999). The limited extent of plume–lithosphere interactions during continental flood-basalt genesis: geochemical evidence from Cretaceous magmatism in southern Brazil. *Contributions to Mineralogy and Petrology* **137**, 147–169.

Gibson, S. A., Thompson, R. N. & Day, J. A. (2006). Timescales and mechanisms of plume–lithosphere interactions: $^{40}Ar/^{39}Ar$ geochronology and geochemistry of alkaline igneous rocks from the Paraná–Etendeka large igneous province. *Earth and Planetary Science Letters* **251**, 1–17.

Gorring, M. L. & Naslund, H. R. (1995). Geochemical reversals within the lower 100 m of the Palisades sill, New Jersey. *Contributions to Mineralogy and Petrology* **119**, 263–276.

Greenough, J. D., Jones, L. M. & Mossman, D. J. (1989). Petrochemical and stratigraphic aspects of North Mountain Basalt from the north shore of the Bay of Fundy, Nova Scotia, Canada. *Canadian Journal of Earth Sciences* **26**, 2710–2717.

Halliday, A. N., Davies, G. R., Lee, D. C., Tommasini, S., Paslick, C. R., Fitton, J. G. & James, D. E. (1992). Lead isotopic evidence for young trace element enrichment in the oceanic upper mantle. *Nature* **359**, 623–627, [correction (1993) *Nature* **362**, 184].

Hames, W. E., Renne, P. R. & Ruppel, C. (2000). New evidence for geologically instantaneous emplacement of earliest Jurassic Central Atlantic magmatic province basalts on the North American margin. *Geology* **28**, 859–862.

Hart, S. R., Hauri, E. H., Oschmann, L. A. & Whitehead, J. A. (1992). Mantle plumes and entrainment: isotopic evidence. *Science* **256**, 517–520.

Hatcher, R. D., Jr, Thomas, W. A., Geiser, P. A., Snoke, A. W., Mosher, S. & Wiltschko, D. V. (1989). Alleghanian orogen. In: Hatcher, R. D., Jr, Thomas, W. A. & Viele, G. W. (eds) *The Appalachian–Ouachita Orogen in the United States. Geological Society of America, The Geology of North America* **F-2**, 233–318.

Heatherington, A. L. & Mueller, P. A. (1999). Lithospheric sources of North Florida, USA tholeiites and implications for the origin of the Suwannee terrain. *Lithos* **46**, 215–233.

Heatherington, A. L. & Mueller, P. A. (2003). Mesozoic igneous activity in the Suwannee Terrane, Southeastern USA: petrogenesis and Gondwanan affinities. *Gondwana Research* **2**, 296–311.

Heinonen, J. S., Carlson, R. W. & Luttinen, A. V. (2010). Isotopic (Sr, Nd, Pb, and Os) composition of highly magnesian dykes of Vestfjella, western Dronning Maud Land, Antarctica: A key to the origins of the Jurassic Karoo large igneous province? *Chemical Geology* **277**, 227–244.

Herzberg, C. & Gazel, E. (2009). Petrological evidence for secular cooling in mantle plumes. *Nature* **458**, 619–623.

Hibbard, J. P., Stoddard, E. F., Secor, D. T. & Dennis, A. J. (2002). The Carolina Zone: Overview of Neoproterozoic to early Paleozoic peri-Gondwanan terranes along the eastern flank of the southern Appalachians. *Earth-Science Reviews* **57**, 299–339.

Hibbard, J. P., van Staal, C. R. & Rankin, D. W. (2007). Links among Carolinia, Avalonia, and Ganderia in the Appalachian peri-Gondwanan realm. In: Sears, J. W., Harms, C. A. & Evenchick, C. A. (eds) *Whence the Mountains? Inquiries into the Evolution of Orogenic Systems. Geological Society of America, Special Papers* **433**, 291–311.

Hill, R. I. (1991). Starting plumes and continental break-up. *Earth and Planetary Science Letters* **104**, 398–416.

Huppert, H. E. & Sparks, R.S. J. (1985). Cooling and contamination of mafic and ultramafic magmas during ascent through continental crust. *Earth and Planetary Science Letters* **74**, 371–386.

Hush, J. (1990). Palisades sill: origin of the olivine zone by separate magmatic injection rather than gravity settling. *Geology* **18**, 699–702.

Jackson, M. G., Hart, S. R., Koppers, A. A. P., Staudigel, H., Konter, J., Blusztajn, J., Kurz, M. & & Russell, J. A. (2007). The return of subducted continental crust in Samoan lavas. *Nature* **448**, 684–687.

Jacobsen, S. B. & Wasserburg, G. J. (1980). Sm–Nd isotopic evolution of chondrites. *Earth and Planetary Science Letters* **50**, 139–155.

Jourdan, F., Marzoli, A., Bertrand, H., Cosca, M. & Fontignie, D. (2003). The northernmost CAMP: $^{40}Ar/^{39}Ar$ age, petrology and Sr–Nd–Pb isotope geochemistry of the Kerforne dyke, Brittany, France. In: Hames, W. E., McHone, J. G., Renne, P. R. & Ruppel, C. (eds) *The Central Atlantic Magmatic Province: Insights from Fragments of Pangea. Geophysical Monograph, American Geophysical Union* **136**, 209–226.

Jourdan, F., Bertrand, H., Schärer, U., Blichert-Toft, J., Féraud, G. & Kampunzu, A. B. (2007). Major and trace element and Sr, Nd, Hf and Pb isotope compositions of the Karoo Large Igneous

Province, Botswana–Zimbabwe: lithosphere vs mantle plume contribution. *Journal of Petrology* **48**, 1043–1077.

Jourdan, F., Marzoli, A., Bertrand, H., Cirilli, S., Tanner, L., Kontak, D. J., McHone, G., Renne, P. R. & Bellieni, G. (2009). $^{40}Ar/^{39}Ar$ ages of CAMP in North America: implications for the Triassic–Jurassic boundary and the ^{40}K decay constant bias. *Lithos* **110**, 167–180.

Kent, D. V. & Olsen, P. E. (2000). Magnetic polarity stratigraphy and paleolatitude of the Triassic–Jurassic Blomidon Formation in the Fundy Basin (Canada): implications for early Mesozoic tropical climate gradients. *Earth and Planetary Science Letters* **179**, 311–324.

Kerr, A. C. & Mahoney, J. J. (2007). Oceanic plateaus: problematic plumes, potential paradigms. *Chemical Geology* **241**, 332–353.

Kerr, A. C., Kempton, P. D. & Thompson, R. N. (1995*a*). Crustal assimilation during turbulent magma ascent (ATA): new isotopic evidence from the Mull Tertiary lava succession, N. W. Scotland. *Contributions to Mineralogy and Petrology* **119**, 142–154.

Kerr, A. C., Saunders, A. D., Tarney, J., Berry, N. H. & Hards, V. L. (1995*b*). Depleted mantle-plume geochemical signatures: no paradox for plume theories. *Geology* **23**, 843–846.

Knight, K. B., Nomade, S., Renne, P. R., Marzoli, A., Bertrand, H. & Youbi, N. (2004). The Central Atlantic Magmatic Province at the Triassic–Jurassic boundary: paleomagnetic and $^{40}Ar/^{39}Ar$ evidence from Morocco for brief, episodic volcanism. *Earth and Planetary Science Letters* **228**, 143–160.

Kontak, D. J. (2008). On the edge of CAMP: Geology and volcanology of the Jurassic North Mountain Basalt, Nova Scotia. *Lithos* **101**, 74–101.

Le Maitre, R. W. (2002). *Igneous Rocks: A Classification and Glossary of Terms: Recommendations of the International Union of Geological Sciences Subcommission on the Systematics of Igneous Rocks*. Cambridge University Press, 240 p.

Marchesi, C., Garrido, C. J., Bosch, D., Bodinier, J.-L., Gervilla, F. & Hidas, K. (2013). Mantle refertilization by melts of crustal-derived garnet pyroxenite: Evidence from the Ronda peridotite massif, southern Spain. *Earth and Planetary Science Letters* **362**, 66–75.

Marzoli, A., Renne, P. R., Picirillo, E. M., Ernesto, M. & De Min, A. (1999). Extensive 200-million-year-old continental flood basalts of the Central Atlantic Magmatic Province. *Science* **284**, 616–618.

Marzoli, A., Bertrand, H., Knight, K., Cirilli, S., Buratti, N., Verati, C., Nomade, S., Renne, P. R., Youbi, N., Martini, R., Allenbach, K., Neuwerth, R., Rapaille, C., Zaninetti, L. & Bellieni, G. (2004). Synchrony of the Central Atlantic magmatic province and the Triassic–Jurassic boundary climatic and biotic crisis. *Geology* **32**, 376–973.

Marzoli, A., Jourdan, F., Puffer, J. H., Cuppone, T., Tanner, L. H., Weems, R. E., Bertrand, H., Cirilli, S., Bellieni, G. & De Min, A. (2011). Timing and duration of the Central Atlantic magmatic province in the Newark and Culpeper basins, eastern USA. *Lithos* **122**, 175–188.

May, P. R. (1971). Pattern of Triassic diabase dykes around the North Atlantic in the context of predrift position of the continents. *Geological Society of America Bulletin* **82**, 1285–1292.

McHone, J. G. (2000). Non-plume magmatism and rifting during the opening of the Central Atlantic Ocean. *Tectonophysics* **316**, 287–296.

McHone, J. G. (2003). Volatile emissions of Central Atlantic Magmatic Province basalts: mass assumptions and environmental consequences. In: Hames, W. E., McHone, J. G., Renne, P. R. & Ruppel, C. (eds) *The Central Atlantic Magmatic Province: Insights from Fragments of Pangea. Geophysical Monograph, American Geophysical Union* **136**, 241–254.

McHone, J. G., Anderson, D. L., Beutel, E. K. & Fialko, Y. A. (2005). Giant dikes, rifts, flood basalts, and plate tectonics: A contention of mantle models. In: Foulger, G. R., Natlund, J. H., Presnall, D. C. & Anderson, D. L. (eds) In: *Plates, Plumes, and Paradigms, Geological Society of America, Special Paper* **388**, 401–420.

Meisel, T., Walker, R. J., Irving, A. J. & Lorand, J.-P. (2001). Osmium isotopic compositions of mantle xenoliths: A global perspective. *Geochimica et Cosmochimica Acta* **65**, 1311–1323.

Merle, R., Marzoli, A., Bertrand, H., Reisberg, L., Verati, C., Zimmermann, C., Chiaradia, M., Bellieni, G. & Ernesto, M. (2011). $^{40}Ar/^{39}Ar$ ages and Sr–Nd–Pb–Os geochemistry of CAMP tholeiites from the western Maranhão basin (NE Brazil). *Lithos* **122**, 137–151.

Moench, R. H. & Aleinikoff, J. N. (2002). Stratigraphy, geochronology, and accretionary terrane settings of two Bronson Hill arc sequences, northern New England. *Physics and Chemistry of the Earth* **27**, 47–95.

Molzahn, M., Reisberg, L. & Wörner, G. (1996). Os, Sr, Nd, Pb and O isotope data from the Ferrar flood basalts, Antarctica: Evidence for an enriched subcontinental lithospheric source. *Earth and Planetary Science Letters* **144**, 529–546.

Morgan, W. J. (1983). Hotspot tracks and the early rifting of the Atlantic. *Tectonophysics* **94**, 123–139.

Murphy, J. B. & Dostal, J. (2007). Continental mafic magmatism of different ages in the same terrane: constraints on the evolution of an enriched mantle source. *Geology* **35**, 335–338.

Murphy, J. B. & Keppie, J. D. (1998). Late Devonian palinspastic reconstruction of the Avalon–Meguma terrane boundary: Implications for terrane accretion and basin development in the Appalachian orogen. *Tectonophysics* **284**, 221–231.

Murphy, J. B. & Nance, R. D. (2002). Sm–Nd isotopic systematics as tectonic tracers: an example from West Avalonia in the Canadian Appalachians. *Earth-Science Reviews* **59**, 77–100.

Murphy, J. B., Pisarevsky, S. A., Nance, R. D. & Keppie, J. D. (2004). Neoproterozoic–early Paleozoic configuration of peri-Gondwanan terranes: Implications for Laurentia–Gondwanan connections. *International Journal of Earth Sciences* **93**, 659–682.

Murphy, J. B., Gutierrez-Alonso, G., Damian Nance, R. D., Fernandez-Suarez, J., Keppie, J. D., Quesada, C., Strachan, R. A. & Dostal, J. (2006). Origin of the Rheic Ocean: Rifting along a Neoproterozoic suture? *Geology* **34**, 325–328.

Murphy, J. B., Dostal, J. & Keppie, J. D. (2008). Neoproterozoic–Early Devonian magmatism in the Antigonish Highlands, Avalon terrane, Nova Scotia: tracking the evolution of the mantle and crustal sources during the evolution of the Rheic Ocean. *Tectonophysics* **461**, 181–201.

Murphy, J. B., Dostal, J., Gutiérrez-Alonso, G. & Keppie, J. D. (2011). Early Jurassic magmatism on the northern margin of CAMP: Derivation from a Proterozoic sub-continental lithospheric mantle. *Lithos* **123**, 158–164.

Nance, R. D. & Murphy, J. B. (1996). Basement isotopic signatures and Neoproterozoic paleogeography of Avalonian–Cadomian and related terranes in the circum North Atlantic. In: Nance, R. D. & Thompson, M. D. (eds) *Avalonian and Related Peri-Gondwanan Terranes of the Circum North Atlantic. Geological Society of America, Special Papers* **304**, 333–346.

Nance, R. D., Gutiérrez-Alonso, G., Keppie, J. D., Linnemann, U., Murphy, J. B., Quesada, C., Strachan, R. A. & Woodcock, N. H. (2010). Evolution of the Rheic Ocean. *Gondwana Research* **17**, 194–222.

Nomade, S., Pouclet, A. & Chen, Y. (2002). The French Guyana doleritic dykes: geochemical evidence of three populations and new data for the Jurassic Central Atlantic Magmatic Province. *Journal of Geodynamics* **34**, 595–614.

Nomade, S., Knight, K. B., Beutel, E., Renne, P. R., Verati, C., Féraud, G., Marzoli, A., Youbi, N. & Bertrand, H. (2007).

Chronology of the Central Atlantic Magmatic Province: Implications for the Central Atlantic rifting processes and the Triassic–Jurassic biotic crisis. *Palaeogeography Palaeoclimatology Palaeoecology* **244**, 326–344.

Olsen, P. E., Kent, D. V., Et-Touhami, M. & Puffer, J. H. (2003). Cyclo-, magneto-, and biostratigraphic constraints on the duration of the CAMP event and its relationship to the Triassic–Jurassic boundary. In: Hames, W. E., McHone, J. G., Renne, P. R. & Ruppel, C. (eds) *The Central Atlantic Magmatic Province: Insights from Fragments of Pangea. Geophysical Monograph, American Geophysical Union* **136**, 7–32.

Osberg, P. H., Tull, J. F., Robinson, P., Hon, R. & Butler, J. R. (1989). The Acadian orogen. In: Hatcher, R. D., Jr, Thomas, W. A. & Viele, G. W. (eds) *The Appalachian–Ouachita Orogen in the United States. Geological Society of America, The Geology of North America* **F-2**, 179–232.

Peate, D. W. & Hawkesworth, C. J. (1996). Lithospheric to asthenospheric transition in Low-Ti flood basalts from the southern Paraná, Brazil. *Chemical Geology* **127**, 1–24.

Pegram, W. J. (1990). Development of continental lithospheric mantle as reflected in the chemistry of the Mesozoic Appalachian tholeiites, USA. *Earth and Planetary Science Letters* **97**, 316–331.

Pe-Piper, G. & Jansa, L. F. (1999). Pre-Mesozoic basement rocks offshore Nova Scotia, Canada: New constraints on the origin and Paleozoic accretionary history of the Meguma terrane. *Geological Society of America Bulletin* **111**, 1773–1791.

Pe-Piper, G. & Piper, D. J. W. (1998). Geochemical evolution of Devonian–Carboniferous igneous rocks of the Magdalen basin, eastern Canada: Pb and Nd isotope evidence for mantle and lower crustal sources. *Canadian Journal of Earth Sciences* **35**, 201–221.

Philpotts, A. R. (1998). Nature of flood-basalt-magma reservoir based on the compositional variation in a single flood-basalt flow and its feeder dyke in the Mesozoic Hartford basin, Connecticut. *Contributions to Mineralogy and Petrology* **133**, 69–82.

Philpotts, A. R. & Martello, A. (1986). Diabase feeder dykes for the Mesozoic basalts in southern New England. *American Journal of Science* **286**, 105–126.

Philpotts, A. R., Caroll, M. & Hill, J. M. (1996). Crystal-mush compaction and the origin of pegmatitic segregation sheets in a thick flood-basalt flow in the Mesozoic Hartford Basin, Connecticut. *Journal of Petrology* **37**, 811–836.

Plank, T. (2005). Constraints from thorium/lanthanum on sediment recycling at subduction zones and the evolution of the continents. *Journal of Petrology* **46**, 921–944.

Pollock, J. C. & Hibbard, J. P. (2010). Geochemistry and tectonic significance of the Stony Mountain gabbro, North Carolina: Implications for the Early Paleozoic evolution of Carolinia. *Gondwana Research* **17**, 500–515.

Pollock, J. C., Hibbard, J. P. & Van Staal, C. R. (2012). A paleogeographical review of the peri-Gondwanan realm of the Appalachian orogeny. *Canadian Journal of Earth Sciences* **49**, 259–288.

Puffer, J. H. (1992). Eastern North American flood basalts in the context of the incipient breakup of Pangea. In: Puffer, J. H. & Ragland, P. C. (eds) *Eastern North American Mesozoic Magmatism. Geological Society of America, Special Papers* **268**, 95–119.

Puffer, J. H. (2001). Contrasting HFSE contents of plume sourced and reactivated arc-sourced continental flood basalts. *Geology* **29**, 675–678.

Puffer, J. H. (2003). A reactivated back-arc source for CAMP magma. In: Hames, W. E., McHone, J. G., Renne, P. R. & Ruppel, C. (eds) *The Central Atlantic Magmatic Province: Insights from Fragments of Pangea. Geophysical Monograph, American Geophysical Union* **136**, 151–162.

Puffer, J. H. & Horter, D. L. (1993). Origin of the pegmatitic segregation veins within flood basalts. *Geological Society of America Bulletin* **105**, 738–748.

Puffer, J. H. & Student, J. J. (1992). Volcanic structures, eruptive style, and posteruptive deformation and chemical alteration of the Watchung flood basalts, New Jersey. *Special Paper of the Geological Society of America* **268**, 261–277.

Puffer, J. H., Block, K. A. & Steiner, J. C. (2009). Transmission of flood basalts through a shallow crustal sill and the correlation of sill layers with extrusive flows: the Palisades Intrusive System and the basalts of the Newark Basin, New Jersey, U.S.A. *Journal of Geology* **117**, 139–155.

Renne, P. R., Mundil, R., Balco, G., Min, K. & Ludwig, K. R. (2010). Joint determination of ^{40}K decay constants and ^{40}Ar*/^{40}K for the Fish Canyon sanidine standard, and improved accuracy for ^{40}Ar/^{39}Ar geochronology. *Geochimica et Cosmochimica Acta* **74**, 5349–5367.

Saal, A. E., Runick, R.L., Ravizza, G. E. & Hart, S. R. (1998). Re–Os isotope evidence for the composition, formation and age of the lower continental crust. *Nature* **393**, 58–61.

Sahabi, M., Aslanian, D. & Olivet, J.-L. (2004). A new starting point for the history of the central Atlantic. *Comptes Rendus Géosciences* **336**, 1041–1052.

Salters, V. J. M., Ragland, P. C., Hames, W. E., Milla, K. & Ruppel, C. (2003). Temporal chemical variations within lowermost Jurassic tholeiitic magmas of the Central Atlantic Magmatic Province. In: Hames, W. E., McHone, J. G., Renne, P. R. & Ruppel, C. (eds) *The Central Atlantic Magmatic Province: Insights from Fragments of Pangea. Geophysical Monograph, American Geophysical Union* **136**, 163–177.

Samson, S. D., Coler, D. G. & Speer, J. A. (1995). Geochemical and Nd–Sr–Pb isotopic composition of Alleghanian granites of the southern Appalachians: Origin, tectonic setting, and source characterization. *Earth and Planetary Science Letters* **134**, 359–376.

Schoene, B., Guex, J., Bartolini, A., Schaltegger, U. & Blackburn, T. J. (2010). Correlating the end-Triassic mass extinction and flood basalt volcanism at the 100 ka level. *Geology* **38**, 387–390.

Schultz, K. J., Stewart, D. B., Tucker, R. D., Pollock, J. C. & Ayuso, R. A. (2008). The Ellsworth terrane, coastal Maine: Geochronology, geochemistry, and Nd–Pb isotopic composition—Implications for the rifting of Ganderia. *Geological Society of America Bulletin* **120**, 1134–1158.

Sebai, A., Féraud, G., Bertrand, H. & Hanes, J. (1991). ^{40}Ar/^{39}Ar dating and geochemistry of tholeiitic magmatism related to the early opening of the Central Atlantic rift. *Earth and Planetary Science Letters* **104**, 455–472.

Shirley, D. N. (1987). Differentiation and compaction in the Palisades sill, New Jersey. *Journal of Petrology* **28**, 835–865.

Smoliar, M. I., Walker, R. J. & Morgan, J. W. (1996). Re–Os, isotope constraints on the age of Group IIA, IIIA, IVA, and IVB iron meteorites. *Science* **271**, 1099–1102.

Spera, F. J. & Bohrson, W. A. (2001). Energy-constrained open-system magmatic processes I: general model and energy-constrained assimilation and fractional crystallization (EC-AFC) Formulation. *Journal of Petrology* **42**, 999–1018.

Sun, S. S. & McDonough, W. F. (1989). Chemical and isotopic systematics of oceanic basalts: implication for mantle composition and processes.. In: Saunders, A. D. & Norry, M. J. (eds) *Magmatism in the Ocean Basins. Geological Society, London, Special Publications* **42**, 313–345.

Thomas, W. A. (2004). Genetic relationship of rift-stage crustal structure, terrane accretion, and foreland tectonics along the southern Appalachian–Ouachita orogen. *Journal of Geodynamics* **37**, 549–563.

Thomas, W. A. (2006). Tectonic inheritance at a continental margin. *GSA Today* **16**, 4–11.

Tollo, R. P. & Gottfried, D. (1992). Petrochemistry of Jurassic basalt from eight cores, Newark basin, New Jersey. In: Puffer, J. H. & Ragland, P. C. (eds) *Eastern North American Mesozoic Magmatism. Geological Society of America, Special Papers* **268**, 233–260.

Tomascak, P. B., Brown, M., Solar, G. S., Becker, H. J., Centorbi, T. L. & Tian, J. (2005). Source contributions to Devonian granite magmatism near the Laurentian border, New Hampshire and Western Maine, USA. *Lithos* **80**, 75–99.

Van Staal, C. R., Dewey, J. F., MacNiocaill, C. & McKerrow, W. S. (1998). The Cambrian–Silurian tectonic evolution of the Northern Appalachians and British Caledonides: History of a complex, west and southwest Pacific-type segment of Iapetus. In: Blundell, D. & Scott, A. C. (eds) *Lyell: The Past is the Key to the Present. Geological Society, London, Special Publications* **143**, 199–242.

Van Staal, C. R., Whalen, J. B., Valverde-Vaquero, P., Zagorevski, A. & Rogers, N. (2009). Pre-Carboniferous, episodic accretion-related, orogenesis along the Laurentian margin of the northern Appalachians. In: Murphy, J. B., Keppie, J. D. & Hynes, A. J. (eds) *Ancient Orogens and Modern Analogues. Geological Society, London, Special Publications* **327**, 271–316.

Verati, C., Bertrand, H. & Féraud, G. (2005). The farthest record of the Central Atlantic Magmatic Province into West Africa craton: Precise $^{40}Ar/^{39}Ar$ dating and geochemistry of Taoudenni basin intrusives (northern Mali). *Earth and Planetary Science Letters* **235**, 391–407.

Verati, C., Rapaille, C., Féraud, G., Marzoli, A., Bertrand, H. & Youbi, N. (2007). $^{40}Ar/^{39}Ar$ ages and duration of the Central Atlantic Magmatic Province volcanism in Morocco and Portugal and its relation to the Triassic–Jurassic boundary. *Palaeogeography, Palaeoclimatology, Palaeoecology* **244**, 308–325.

Walker, K. R. (1969). *The Palisades Sill, New Jersey: a Reinvestigation. Geological Society of America, Special Papers* **111**, 1–178.

Webster, T. L., Murphy, J. B. & Gosse, J. C. (2006). Mapping subtle structures with light detection and ranging (LIDAR): flow units and phreatomagmatic rootless cones in the North Mountain Basalt, Nova Scotia. *Canadian Journal of Earth Sciences* **43**, 157–176.

Weigand, P. W. & Ragland, P. C. (1970). Geochemistry of Mesozoic dolerite dykes from eastern North America. *Contributions to Mineralogy and Petrology* **29**, 195–214.

Whalen, J. B., Jenner, G. A., Currie, K. L., Barr, S. M., Longstaffe, F. J. & Hegner, E. (1994). Geochemical and isotopic characteristics of granitoids of the Avalon Zone, southern New Brunswick: possible evidence for repeated delamination events. *Journal of Geology* **102**, 269–282.

White, R. & McKenzie, D. (1989). Magmatism at rift zones: the generation of volcanic continental margins and flood basalts. *Journal of Geophysical Research* **94**, 7685–7729.

White, R. & McKenzie, D. (1995). Mantle plumes and flood basalts. *Journal of Geophysical Research* **100**, 17543–17585.

Widom, E. (1997). Sources of ocean island basalts: a review of the osmium isotope evidence. *Physica A* **244**, 484–496.

Wilson, M. (1997). Thermal evolution of the Central Atlantic passive margins: continental break-up above a Mesozoic superplume. *Journal of Geological Society, London* **154**, 491–495.

Woodhead, J. D., Hergt, J. M., Davidson, J. P. & Eggins, S. M. (2001). Hafnium isotope evidence for 'conservative' element mobility during subduction zone processes. *Earth and Planetary Science Letters* **192**, 331–346.

Woodruff, L. G., Froelich, A. J., Belkin, H. E. & Gottfried, D. (1995). Evolution of tholeiitic diabase sheet systems in the eastern United States: examples from the Culpeper Basin, Virginia–Maryland, and the Gettysburg Basin, Pennsylvania. *Journal of Volcanology and Geothermal Research* **64**, 143–169.

Workman, R. K., Hart, S. R., Jackson, M. G., Regelous, M., Farley, K. A., Blusztajn, J., Kurz, M. D. & Staudigel, H. (2004). Recycled metasomatized lithosphere as the origin of the enriched mantle II (EM2) end-member: evidence from the Samoan volcanic chain. *Geochemistry, Geophysics, Geosystems*, 2003GC000623.

Zartman, R. E. & Doe, B. R. (1981). Plumbotectonics—the model. *Tectonophysics* **75**, 135–162.

Zindler, A. S. R. & Hart, S. (1986). Chemical geodynamics. *Annual Review of Earth and Planetary Sciences* **14**, 493–571.